Optimizing Global LC-MS Lipidomics for Future use in Clinical Diagnostics

Sander Johannes Thorbjørnsen Guttorm

Master Thesis
Analytical Chemistry
60 credit points

Department of Chemistry
Faculty of Mathematics and Natural Sciences

UNIVERSITY OF OSLO

July 2023

Optimizing Global LC-MS Lipidomics for Future use in Clinical Diagnostics

Sander Johannes Thorbjørnsen Guttorm

Master Thesis Analytical Chemistry

60 credit points

Department of Chemistry

Faculty of Mathematics and Natural Sciences

University of Oslo

July 2023

Optimizing Global LC-MS Lipidomics for Future use in Clinical Diagnostics

Sander Johannes Thorbjørnsen Guttorm

Abstract

Global lipidomics offers a deeper understanding of lipid metabolism, lipid signaling, and lipid-related diseases. Lipids poses great analytical challenges due to their diversity in chemical properties. For lipids of clinical relevance, both LogP values and concentration ranges can differ by several orders. For lipidomics to be used as a tool in clinical diagnostics normal variations needs to be mapped.

In this study a global lipidomics UHPLC-MSMS method is presented, utilizing a C30 column for lipid separation. Ion source parameters were optimized for better lipid coverage. With the optimized method, two acquisition methods, Data-Dependent Acquisition and scheduled MSMS was tested and compared. The comparison showed that scheduled MSMS is superior in number of lipids detected. Linearity between number of carbons present in the acyl chains of lipids and retention time were observed. The improved global lipidomics method was evaluated as close as possible to the lipidomics standard initiative (LSI), and proved intra-batch and in-between batch variations to be minimal. The evaluated method was then applied to a simple study focusing on normal variation in the lipidome induced by high-intensity training (HIT). The scheduled MSMS method was able to observe exercise induced changes in the lipidome composition. From this study it was concluded that the method was sufficient for observing normal and abnormal variations in the lipidome. On the basis of this study the method will hence be used in clinical research and diagnostic in the future.

Preface

The presented work was performed at the Department of Medical Biochemistry at Oslo university hospital, Rikshospitalet from January 2021 to July 2023. My supervisors have been Katja B. P. Elgstøen, at Rikshospitalet and Steven R. H. Wilson at the Department of Chemistry, University of Oslo.

I would like to thank Steven and Katja for giving me this amazing master project. It was truly a pleasure deep diving into the unknown territory of lipidomics and the challenges that came with it. I would like to thank Katja for all the supervision, motivation and encouragement she brought into the project, and for giving me the freedom to direct the project the way I wanted to. It was a big pleasure being a part of her research group, and the interest everyone showed in project is something I appreciated a lot. I also want to thank Steven for great supervision, for the scientific discussions, and for your honest feedback.

Elise and Hanne deserve a big thank you as well for all the talks in the office and at the lab. I had so much fun learning from the best of the best regarding metabolomics. I also want to thank Tharsana my fellow master student, for all the fun we had in the lab and for showing me how things work. Thank you Lukáš for helping me understand lipidomics and answering all of my questions.

 I want to give a big thank you to Helge, for the interest and enthusiasm he showed over my results, and for always checking in on me whenever he had the opportunity.

The Bioanalytics group at the Department of Chemistry also deserves a big thank you for being so welcoming and including. Not only by arranging social gatherings, but also during conferences and showing interest in each other's work.

Shoutout to Norsk Selskap for Massespektrometri for financial support, which provided me with the opportunity to attend the Nordic MS Winter meeting 2023.

Lastly, I want to thank my friends, girlfriend and family for all the support and love you gave me during this time. And not to mention the understanding you showed when I was too busy with this project. This could have not been possible without you.

Sander, July 2023

Table of Content

1   Abbreviations

AcCa   Acyl Carnitine

AcCA(16:0)   3-(hecadecanoyloxy)-4-(trimethylaxaniumyl)butanoate

AcCa(18:1)   3-[(9E)-octadec-9-enoyloxy]-4-(trimethylazaniumyl)butanoate

ACN   Acetonitrile

AF   Ammonium Format

CE   Cholesteryl Ester

CE(18:1 (d7)) Cholest-5-en-3b-yl (9Z-octadecenoate (d7))

Cer (d18:1(d7)/15:0)   N-(pentadecanoyl)-sphing-4-enine (d7)

Cer   Ceramide

CoQ10   Coenzyme Q10

CV   Coefficient of Variation

DDA   Data Dependent Acquisition

DG   Diacylglycerol

DG(15:0/18:1 (d7))   1-pentadecanoyl-2-(9Z-octadecenoyl (d7))-sn-glycerol

DIA   Data Independent Acquisition

E   Mass Accuracy

EIC   Extracted Ion Chromatogram

ESI   Electro Spray Ionization

FA   Fatty Acyl

FA(16:0)   Hexadecenoic acid

FA(18:0)   Octadecanoic acid

FWHM	Full Width Half Maximum
FFA	Free Fatty Acid
HPLC	High-Pressure Liquid Chromatography
Hz	Hertz
IPA	2-propanol
kDA	kilodalton
LC	Liquid Chromatography
LPC	Lysophosphatidylcholine
LPC(18:1 (d7))	1-(9Z-octadecenoyl (d7))-2-glycero-3-phosphocholine
LPE(18:1 (d7)))	1-(9Z-octadecenoyl (d7))-2-glycero-3-phosphoethanolamine
m/z	Mass-to-charge ratio
MeOH	Methanol
MG(18:1 (d7))	1-(9Z-octadecenoyl (d7))-glycerol
MRM	Multiple Reaction Monitoring
MS	Mass Spectrometry
NMR	Nuclear Magnetic Resonance
PC	Phosphatidylcholine
PC	Principal Component
PC(15:0/18:1 (d7))	1-pentadecanoyl-2-(9Z-octadecanoyl (d7))-glycero-3-phosphocholine
PCA	Principal Component Analysis
PE	Phosphatidylethanolamine
PE(15:0/18:1(d7))	1-pentadecanoyl-2-(9Z-octadecenoyl (d7))-glycero-3 phosphoethanolamine
PG(15:0/18:1 (d7))	1-pentadecanoyl-2-(9Z-octadecenoyl (d7))-glycero-3-phospho-(1'-sn-glycerol)

2

PI   Phosphatidylinositol

PIS   Product Ion Scan

PI(15:0/18:1 (d7))   1-pentadecanoyl-2-(9Z-octadecenoyl (d7))-glycero-3-phospho-(1'-myo-inositol)

PPT   Protein Precipitation

PS   Phosphatidylserine

PS(15:0/18:1 (d7))   1-pentadecanoyl-2-(9Z-octadecenoyl (d7))-glycero-3-phosphoserine

R   Resolution

RT   Retention Time

SD   Standard Deviation

SM   Sphingomyelin

SM(d18:1/18:1 (d9))   N-(9Z-octadecenoyl (d9))-sphing-4-enine-1-phosphocholine

sn   Stereospecific numbering

SRM   Single Reaction Monitoring

ST(21:4;O5)   17-alpha,21-dihydroxypregn-4-ene-3,11,20-trione

TG   Triacylglycerol

TG(15:0/18:1/15:0 (d7))   1-pentadecanoyl-2(9Z-octadecenoyl)-3-pentadecanoyl (d7)-sn-glycerol

TIC   Total Ion Chromatogram

UHPLC   Ultra-High-Pressure Liquid Chromatography

4

2 Introduction

2.1 Metabolomics and Lipidomics in Clinical Diagnostics

Diagnostics refers to the process of identifying and determining the nature and cause of a particular disease or medical condition. Diagnostic tests may include physical examinations, medical imaging, laboratory tests, and other specialized procedures that help to identify the presence and severity of a disease or condition. The information obtained from these tests is used by healthcare professionals to make treatment decisions and to monitor the natural progression or healing of the disease, as well as the effect of treatment. Diagnostics plays a critical role in healthcare, as accurate and timely diagnosis is essential for effective treatment and management of diseases. Advances in medical technology have led to the development of new and more sophisticated diagnostic tools, which have significantly improved the accuracy and speed of diagnoses, as well as enabling diagnosing new diseases that were previously not known as separate entities [1]. Combining the best diagnostics with the most up-to-date and proven treatments constitutes the hallmarks of evidence-based medicine and is the basis of modern medicine. The more advanced treatment model is called personalized medicine. It is a medical model that takes advantage of individuals' genotypes to tailor the correct strategy and treatment [2]. The diagnostic tools used for personalized medicine are in general global approaches, and genomics is so far the most used and best documented [3]. Global metabolomics and global lipidomics has just recently been introduced to take medicine to the next level of personalization. Metabolomics and lipidomics are explained in greater detail in part 2.2 and 2.3. In personalized medicine, the initial diagnostics and thorough evaluation of the patient's characteristics are more elaborative and costly, but is expected to pay off by more precise and effective treatments with less side effects and more rapid healing and recovery. Figure 1 compares the traditional and the personalized approaches of evidence-based medicine.
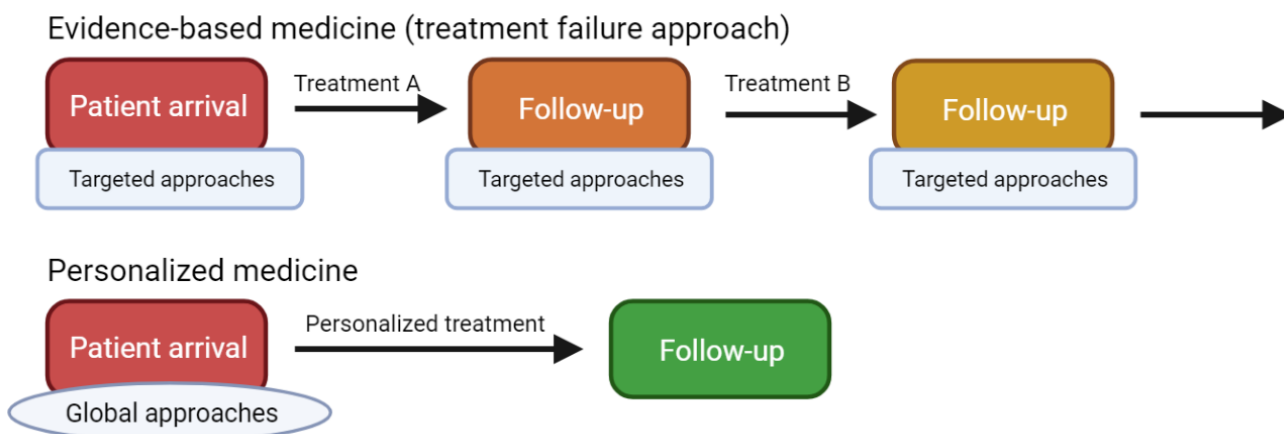
Figure 1: Evidence-based medicine (treatment-failure approach) is compared to the personalized medicine approach. The regular treatment-failure approach requires multiple treatments and follow-up appointments, meaning it is patient, time and health care resource demanding. The personalised medicine approach ideally only requires one treatment and one follow-up appointment. Figure adapted from [1].

Metabolomics and lipidomics are two rapidly growing areas of biomedical research that have the potential to revolutionize clinical diagnostics. Both fields involve the comprehensive analysis of small molecules and lipids, respectively, in biological samples, such as blood, urine, and tissue. Metabolomics aims to identify and quantify all metabolites present in a given biological sample, while lipidomics focuses specifically on the analysis of lipid molecules [4]. Thus, lipidomics is in reality metabolomics optimized for analyzing the most hydrophobic part of the metabolome. The information obtained from these analysis can provide valuable insights into the metabolic state of an individual, and can potentially be used to diagnose and monitor a wide range of diseases [5].

In clinical diagnostics, metabolomics and lipidomics have shown promising results in the early detection of diseases, such as cancer, cardiovascular disease, and metabolic disorders [6]. For example, metabolomic profiling has been used to identify biomarkers for the early detection of prostate cancer [7]. Biomarkers are measurable indicators of health and disease typically used for diagnostics, prediction, prognostics or monitoring of progression and response to treatment. Ideally, biomarkers should be sensitive and specific for the condition it is used, and be easily available for sampling and analysis.

Lipidomic analysis has been shown to be useful in the diagnosis of lipid disorders such as familial hypercholesterolemia [8]. In addition to diagnosis, metabolomics and lipidomics can also be used to monitor disease progression and treatment responses. For example, changes in metabolite or lipid profiles can be used to assess the effectiveness of chemotherapy or other

treatments, and to identify potential side effects [9]. For metabolomics and lipidomics to be used as a tool in clinical diagnostics, normal variations needs to be mapped. Normal variations are caused by factors such as, gender, age, ethnicity, and lifestyle. Exercise is a great example of a factor which cause normal variations in the metabolome and lipidome [10].

Understanding normal variations contributes to personalized medicine approaches. Mapping normal variations can improve the selectivity of metabolomics and lipidomics diagnostics. Individuals have unique metabolomic and lipidomic profiles, by mapping these normal variations the tailored treatment approach can be based on individual's specific baseline. Baselines for metabolomics and lipidomics profiles can determine abnormal patterns indicative of diseases or lifestyle. Without knowledge of the normal variations, it becomes challenging to differentiate abnormalities associated with diseases and those that occur naturally in healthy individuals.

Despite their potential, there are still many challenges to be addressed in the use of metabolomics and lipidomics in clinical diagnostics [5,11]. These include the need for standardized sample collection and preparation methods, as well as the development of robust analytical methods for large-scale studies.

2.2 Metabolites, the Metabolome and Metabolomics

Metabolites are substrates, intermediates, and products from enzymatic reactions [12], and have a molecular mass typically less than 1.5 kDA, Some examples of metabolites are amino acids, carbohydrates, and lipids. The metabolites within a biological system (cells, tissue, organs, biofluid, or organisms) are called the metabolome. The human metabolome is heterogeneous and very complex [13].

Metabolites can be split into two different groups depending on their origin, endogenous and exogenous metabolites. The endogenous metabolites are consumed and/or synthesized within a biological system, while the exogenous metabolites are introduced into a biological system from different external sources like dietary intake, supplements and medications, as well as form the microbiomes of the intestines and other internal or external body surfaces. The metabolites can be further categorized into different biochemical groups based on their

chemical structure, functional groups, and their role in a biological system. Examples of this can be organic acids, lipids, etc [1].

Metabolomics is the study of the metabolome. The metabolome indicates a direct connection between metabolites and their corresponding concentrations to diseases generated by genetic mutation [14], life style, diseases or environmental factors. However, the metabolome can change rapidly depending on diet, physical activity, time of day, age, etc. Furthermore, diseases will alter the metabolome. Different metabolites can be increased or decreased in response to for example exercise or as a consequence of disease, resulting in an altered metabolome compared with the "normal" healthy resting metabolome. The normal metabolome provides a baseline for understanding pathways, biomarker, and how they can be affected by diseases and other circumstances [15]. It is important to note that the normal metabolome isn't static, but rather indicates reference ranges which can vary depending on many factors of daily life for one individual and between individuals. Metabolomics collects data in a form of a snapshot of the metabolome at the time of sampling.

As seen in Figure 2, lipids and lipid-like molecules cover almost 80% of the expected human metabolome [16]. Metabolomics tends to look at the more polar part of the metabolome and only detects a limited proportion of the lipids and lipid-like molecules. The reason for this is the complexity and various problems in lipid analysis, explained in more detail in part 2.3.
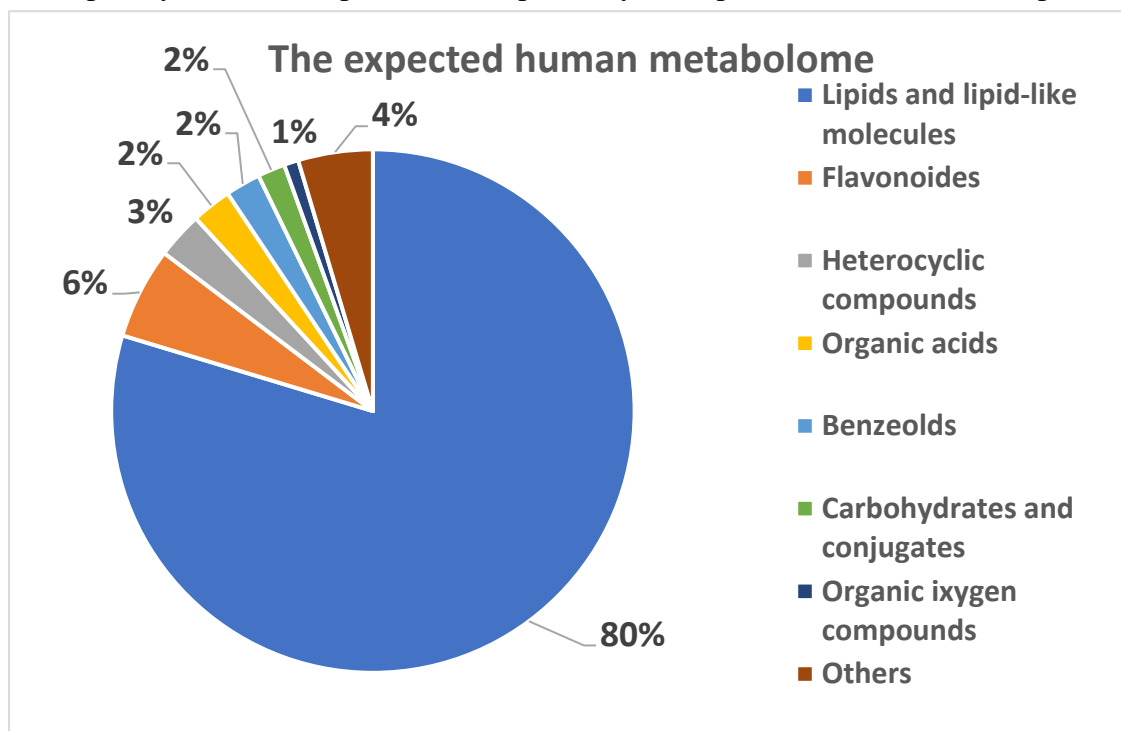

Figure 2: Pie chart of the expected human metabolome. Including organic acids, benzeolds, flavonoids, hetrocyclic compounds and lipid and lipid like molecules. 79.35% of the human metabolome consists of lipids and lipid-like molecules. Reference numbers from [16].

2.3 Lipids, the Lipidome and Lipidomics

The lipidome is the complete lipid profile within a cell, tissue, body fluid or organism, and is a subset of the metabolome [17]. Lipids are a biochemical class of their own because of their hydrophobicity and structural diversity. Lipids correspond to the lipidome the same way metabolites correspond to the metabolome. Similar to the metabolome, the lipidome can indicate a direct connection between endogenous lipids and their corresponding concentration to a disease generated by a genetic mutation or environmental factors [18].

Lipids are synthesized in various cellular compartments within the body, primarily in the endoplasmic reticulum (ER) and, to some extent in the mitochondria. ER contains enzymes involved in the biosynthesis of phospholipids, glycerolipids and sterols. Once synthesized, the lipids need to be transported within the cell and the body. This transportation can happen either by vesicular trafficking or non-vesicular trafficking [19]. For the lipids to be in a biological fluid, such as blood, they have to diffuse or be transported across the cell membrane. After crossing the cell membrane, they can be transported within the blood stream by either binding to serum albumin, chylomicrons, or other lipoproteins [20], or as free unbound lipids, for example, free fatty acids (FFA). The lipidome will differ depending on which bio-matrix that is analyzed. For instance, there are fewer lipids in human urine compared to that in blood [21].

Lipids are involved in many different vital cellular processes and thus are a very important class of biomolecules. Because of their hydrophobicity, lipids' main cellular function is membrane building, because lipid membranes can separate cells from their natural surroundings and subcellular organelles from one another and the cytoplasm within the cell. The second most important function of lipids is energy storage. The energy is incorporated and stored as triacylglycerol in adipose tissue. Adipose tissue is more energy dense than glycogen and it contains almost double the amount of energy compared to an aliquot of carbohydrates [22].

Lipids can be divided into different categories based on their origin, and are defined as; hydrophobic or amphipathic molecules, small molecules that may originate entirely or in part by carbanion-based condensation of ketoacyls and or by carbocation-based condensation of isoprene units [23]. Currently, there are eight main lipid classes, Fatty Acyls (FA), Prenols (PR), Sterols (ST), Glycerophospholipids (GP), Glycerolipids (GL), Sphingolipids (SP), Polyketides (PK), and Saccharolipids (SL) [24], see Figure 3.
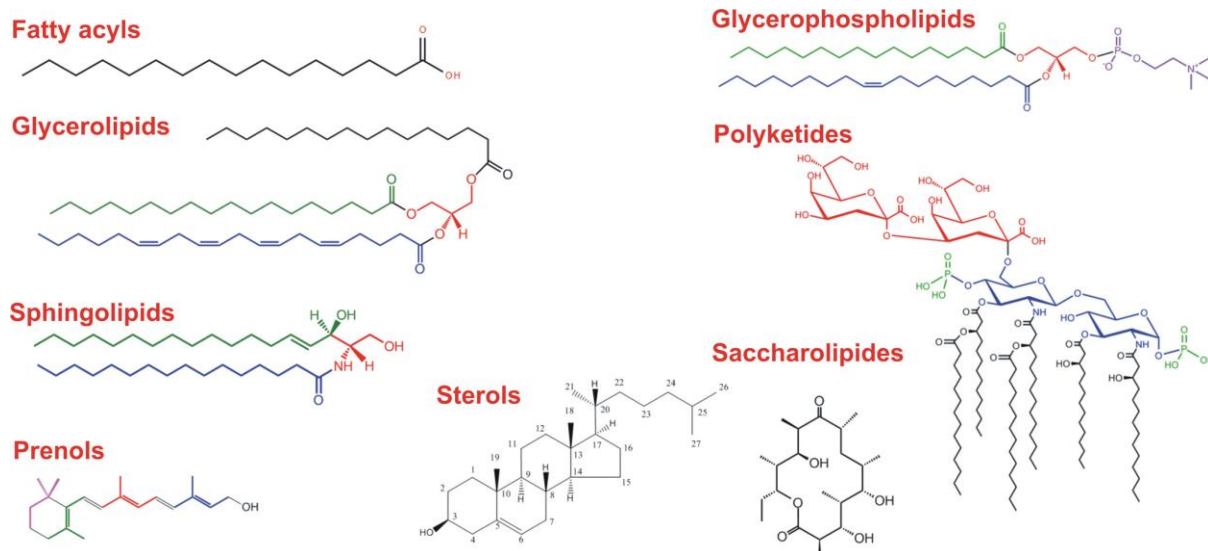
Figure 3: The 8 main lipid categories according to the International Lipids Classification and Nomenclature Committee, with one representative structure shown for each of the 8 main lipid classes, Fatty acyls, Prenols, Sterols, Glycerophospholipids, Glycerolipids, Polyketides, Saccharolipids and Sphingolipids. Figure from [25].

As mentioned above, lipids originate in part or entirely by condensation of two main building blocks, ketoacyl and isoprene groups, see Figure 4 for the structure of ketoacyl and isoprene units. Carbanion condensation of ketoacyl creates six different lipid classes, FA, GP, GL, SP, SL and PK. Carbocation condensation of isoprene groups are used to create the ST and PR. This is one of the reasons why there is a wide range in chemical properties of the different lipid categories.
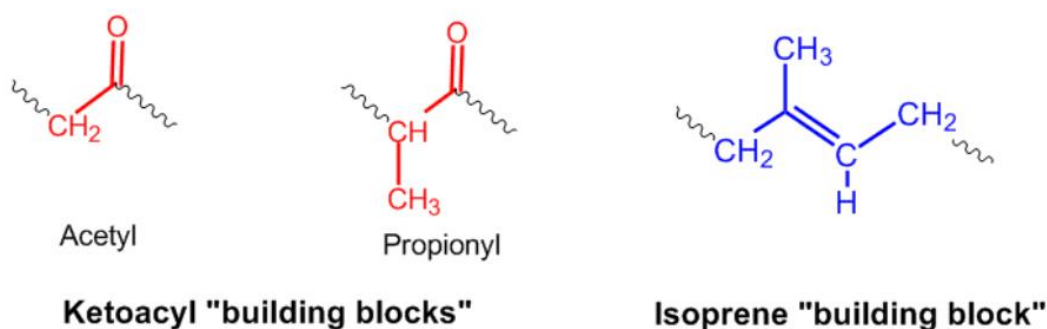
Figure 4: Structure of the ketoacyl and isoprene building blocks used to build lipids[23].

One of the most diverse group of lipids is fatty acyls (FA). The FA structure represents one of the major building blocks in complex lipid structures and is perhaps the most important lipid class. FAs are known for their carbon chains and their acid head group. FAs can be categorized based on the carbon chain composition, if it's straight or branched, saturated or unsaturated just to give some examples [26], see Figure 5.
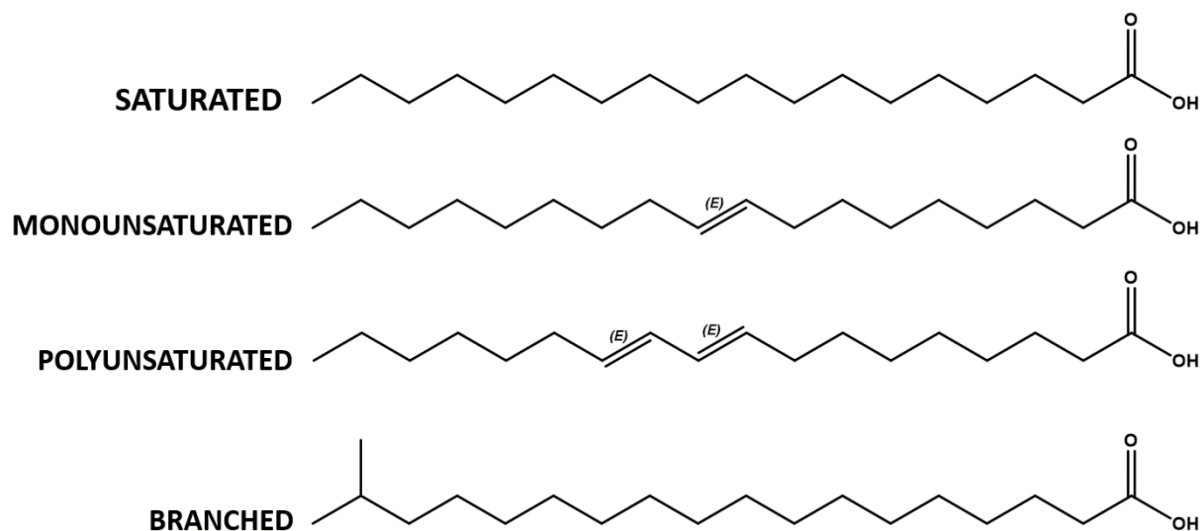
Figure 5: Examples of how the structure of a saturated, monounsaturated, polyunsaturated and branched fatty acid can look like. Saturated fatty acid: Steric acid, monounsaturated: 9(E)-octadecadienoic acid, polyunsaturated: 9(E),11(E)-octadecadienoic acid, branched: 17-methyl-octadecanoic acid.

Fatty acids are not only interesting because of the wide variety of structures, but also their chemical properties. Fatty acids play an important role in membrane structure, lipid function, and lipid signalling. They can also be disease related. It has been found that different types of fatty acids are related to cardiovascular diseases, cancer, and metabolic diseases like type 2 diabetes, to name a few. In type 2 diabetes as an example, the fatty acyl palmitic acid [27] is found in elevated amounts and is converted into more harmful fatty acyl derived lipids. This means that the length of the carbon chain, degree of saturation and position of double bonds has a lot to say with respect to biological and clinical relevance.

Lipid nomenclature has three different categories. The systematic name, the common name, and the shorthand notation. From the systematic name and the common name, it can be a bit difficult to understand the structure of the lipid, while with the shorthand notation the lipid structure is more comprehensible. The lipid shorthand notation consists of the lipid class, the length of the different side chains, and the presence of any double bonds and their location on the side chain. The shorthand notation starts with the lipid class abbreviation for instance TG (triacylglycerol), then the length and position of the different acyl or alkyl chain [28]. The position of the acyl or alkyl chains can be described with stereospecific numbering (*sn*). In case for TG, the *sn-1* position refers to the first carbon atom of the glycerol moiety. The length and degree of saturation is indicated with the parentheses, for example TG(16:1/18:1/18:1), where it is clear visible that the three different alkyl groups have one double bond each. The position of the double bond on the alkyl chains is described with an number, then a Z or E to describe if it is in cis or trans geometry, for example FA(10:1(8Z))

[23]. More common nomenclature is the ω and Δ phrase. The ω describes which carbon from the end methyl group on the alkyl chain where a double bond is present. For Omega-3 fatty acids the double bond is located at carbon 3, counting from the methyl end of the alkyl chain [28]. Δ describes where the double bond is located counting from the functional group of the acyl sidechain. Phosphatidylcholines can also have a "O-", which indicates if the carbon chain is an alkyl ether substituent, or "P-" prefix, which indicates if the carbon chain is an 1Z-alkenyl ether substituent. There can also be a "d" or "t" inserted which refers to 1,3-dihydroxy and 1,3,4-trihydroxy, which only applies to the sphingolipid class [28]. Even though one lipid has one molecular weight corresponding to one molecular formula, it can correspond to multiple lipids.

The large number of lipid isomers, that is, different lipid compounds with the exact same elemental composition, but different structure, makes nomenclature very important. Imprecise and cases of improper lipid annotation limits the biological interpretation [29]. Sphingolipids are known take part in various environmental stress responses [30], and have a powerful function in regulating ion channels [31]. Therefore, identifying the specific sphingolipid causing the regulation of different ion channels can be crucial. This is why it is very important to be precise when identifying different lipids, and use the nomenclature which gives the most structural information. To correctly identify lipids is difficult and time consuming. A problem regarding analyzis of lipids is their big difference in chemical and physical properties.

The different lipid classes can differ in their polarity (LogP) value by several orders [32]. LogP is the partition coefficient of a molecule between a polar (water) and nonpolar (octanol) phase. The variability in polarity makes lipid analysis one of the hardest and most difficult analyzes to carry out. Choice of sample preparation method and instrumentation for analysis will have impact on the lipidomes harvested. There are many different varieties of each method, each with its advantages and disadvantages. For sample preparation, the gold standard for lipid extraction has been Folch, Bligh & Dyer's [33] methods [34]. Lipid extraction giving satisfactory recovery for all the different lipid classes is hard to achieve. A single-phase extraction (protein precipitation) using Isopropanol (IPA) has shown promising results [35] , and at the same time it is safer than the chloroform extraction that Bligh & Dyer proposed [35]. Protein precipitation using acetonitrile is also often used [36], but it has been shown that acetonitrile extraction enhances lipase activity [37], causing unstable lipid extraction yield of glycerolipids.

Lipidomics is a system-based study of all lipids, and their interactions within a biological systems [38], for multianalyte identification and quantification of endogenous and exogenous lipids and their metabolites [39]. This is typically done using a combination of analytical techniques such as chromatography and mass spectrometry (MS), or nuclear magnetic resonance spectroscopy (NMR), explained in part 2.5. Lipidomics is a powerful tool used to discover new biomarkers of health and disease. It has applications in various fields such as medicine, nutrition and biotechnology. As mentioned earlier, almost 80% of the expected human metabolome consists of lipids and lipid-like molecules. Therefore, a lipidomics approach to diagnostics can uncover substantial amount of information [40]. Lipidomics has in recent years experienced an exponential growth because of technical analytical improvements and better databases and software following the increased interest in lipidomics.

2.3.1   Targeted and Global Lipidomics

As with metabolomics, lipidomics is divided into two distinct categories, global lipidomics and targeted lipidomics. The goal in a global lipidomics approach is to maximize the number and diversity of lipids detected. The global approach focuses on the entire lipidome, including a broad range of lipid classes, molecular species, and as many lipidomic features as possible. A global approach gives more understanding of the interactions and correlations between lipids and diseases and generally how lipids function and interact in the body. In targeted lipidomics, however, the goal is to detect certain lipid species and involves a predefined set of lipid species that are selected based on their biological relevance or specific research objectives [41].

A targeted approach requires prior knowledge of the lipid targets and the use of appropriate standards provides accurate quantification, simplifying the data analysis and interpretation of results. Data analysis in global lipidomics is more complex due to the comprehensive nature of the analysis. It involves identification and quantification of a large number of lipid species across various lipid classes. Advanced statistical tools, multivariate analysis, software, databases for identification, and bioinformatics approaches are commonly employed to process and interpret the extensive lipidomics data generated [36]. Furthermore, the quantification is relative and not absolute since it is not possible to have internal standards covering the whole lipidome present in a sample. The extracted information and hypothesis generated following global analysis can then be used to develop targeted lipidomics

approaches. See Figure 6 for comparison of targeted vs global lipidomics. Whereas the targeted approach is set to extract specific analytes of interest, the global approach wants to gather and retain as much information about all metabolites as possible. Thus, that the targeted approach is typically described as hypothesis testing, whereas the global approach is hypothesis generating.
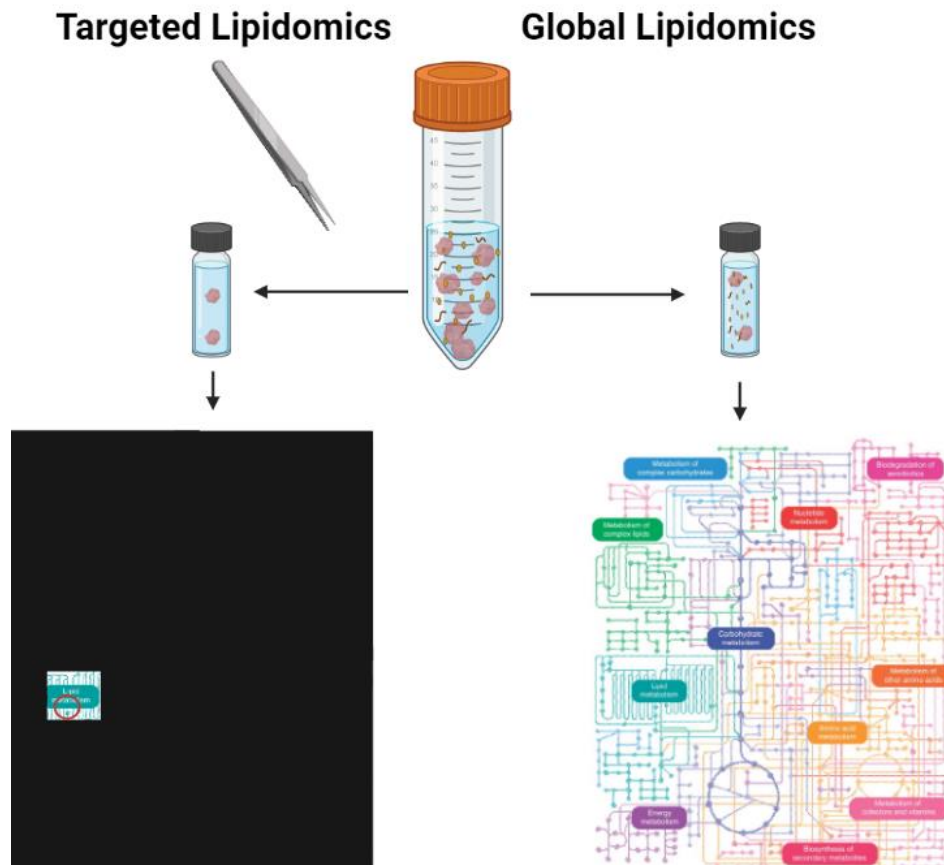
Figure 6: A targeted approach where the sample preparation (imagine tweezers plucking out certain analytes from the sample) is specific so the information extracted from the sample is limited, while the global approach shows a nonspecific sample preparation which will give a broader and more complete insight of the biochemical picture.

Although the global approach grants the ability to find relationships between different lipid classes and species in correlation to diseases, there are some challenges to global lipidomics. These challenges include; data complexity, analytical sensitivity and specificity, lipid annotation and identification, standardization and quality control, lipidome coverage and biological interpretation [42].

2.4 Workflow in Global Lipidomics

The workflow used in global lipidomics is very similar to the one used in global metabolomics. It follows a generic workflow divided into different steps, see Figure 7. The workflow includes study design, data acquisitions including sample preparation and analysis of samples, data processing and statistical analysis, identification, pathway analysis and biological interpretation [36].
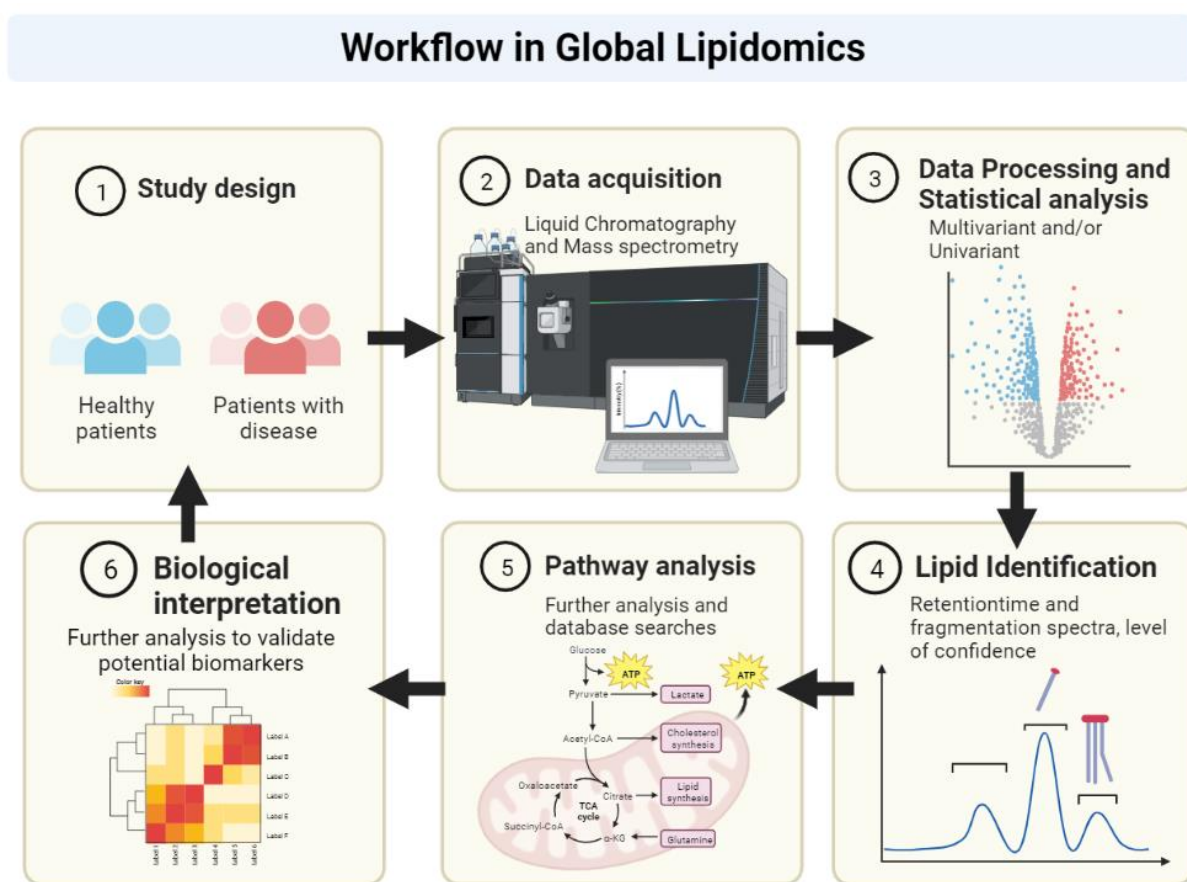
Figure 7: Workflow in Global Lipidomics. Following a full round, hypotheses generated can be used for another round with a new study design or used to establish targeted analysis for hypothesis testing.

Analytical platforms used in global lipidomics will be discussed in the next chapter as well as biological matrices and data acquisitions used for global lipidomics. This way of working is known as hypothesis generating, meaning that the results obtained with a global lipidomics workflow needs to be further tested with a targeted lipidomics approach to verify or disprove the hypothesis.

2.5 Analytical platforms for Global Lipidomics

There are many different analytical platforms for lipidomics, the two most common are Mass Spectrometry (MS) and Nuclear Magnetic Resonance (NMR) [43]. The MS is the most popular due to the high sensitivity, but the NMR platform has gained some popularity. The main reason for this is the stability of the NMR analysis. NMR is considered stable because the resonance frequency called chemical shift, for a certain structure will stay the same if the same magnet size is used. This provides excellent reproducibility. Furthermore, there are no extra steps for sample preparation, and it is possible to do quantitative analysis as well.

The biggest disadvantage with NMR is the low sensitivity and selectivity compared to MS. As seen in Figure 8, the MS can do quantification at lower concentrations than NMR and still detect more metabolites [44]. The disadvantage with MS however is the more troublesome quantitative analysis and lack of reproducibility across different platforms and on the same platform on subsequent runs. Details of MS will follow in the chapter below.
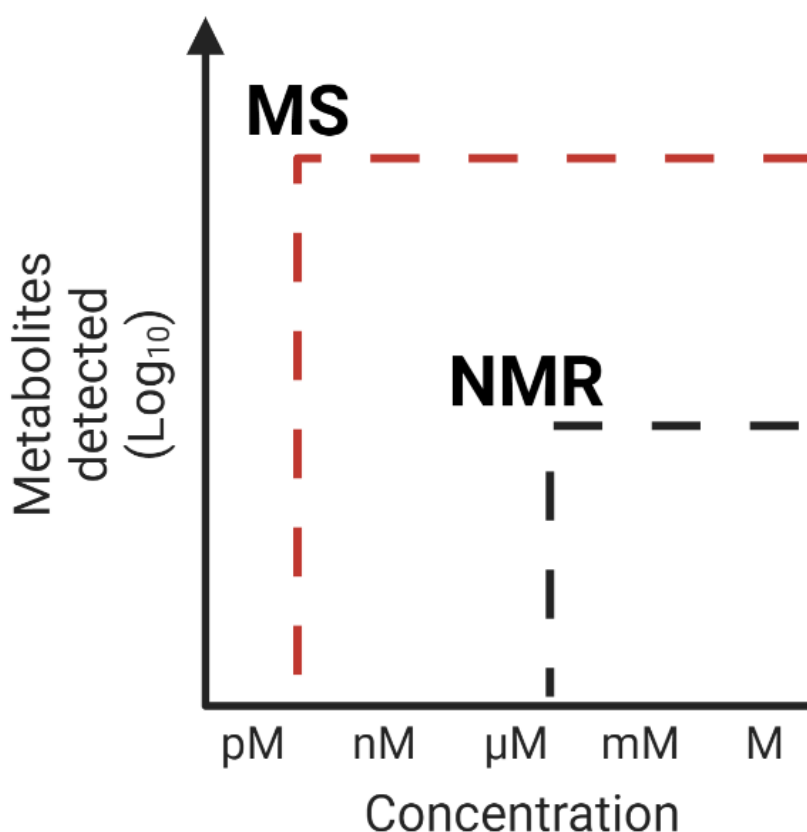
Figure 8: Relative sensitivity of nuclear magnetic resonance (NMR) compared to mass spectrometry (MS). Overall, the MS can detect a higher number of metabolites and at lower concentrations compared to NMR [44]. Figure adapted from [44].

Even though the MS can be problematic due to the lack of reproducibility, it is the most commonly used platform for global lipidomics and metabolomics due to superior sensitivity and large number of lipids and metabolites detected [44]. When an MS spectrum is obtained it can also be run through many different online databases or in-house libraries to verify findings. This is also possible with NMR, but the databases are limited. For lipidomics, just as for metabolomics, the MS is usually coupled to a High-Performance Liquid Chromatography (HPLC) or Gas Chromatography (GC).

2.5.1   Mass Spectrometry

As mentioned earlier the most common technique for lipidomics is HPLC coupled with MS [45]. The MS separates and detects gas phase ions based on their *m/z* value, the mass to charge ratio for a given ion, by using a magnetic or electric field. MS can detect and identify compounds by using different modes, MS1 and MS2. MS1 is obtaining data with a full scan. In full scan intact molecules/ precursor ions are detected and measured, giving intensity and *m/z* value. MS2 detects fragmented ions *m/z* value and intensity, fragmentation happens usually in a collision cell. The MS2 spectra are obtained with tandem MS (MSMS). The MS consist of an ionization source, mass analyzer(s), and detector(s), see Figure 9 for illustration.
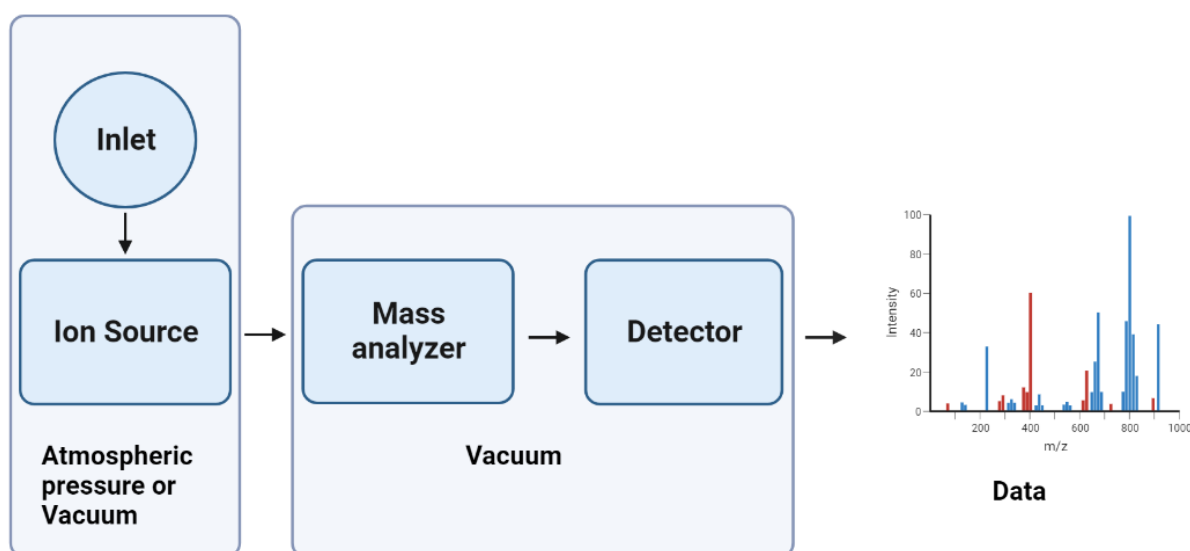
Figure 9: Illustration of the main constituents of a mass spectrometer. Inlet (gas chromatography, liquid chromatography, direct injection) introduces the sample to the ion source. The ion source transfers gas-phase ions to the mass analyzer where the ions are separated. The detector will then generate a signal in response to the incoming ions. The vacuum reduces the chance of collision between the different ions.

The analytes need to be in gas phase ion form to be analyzed by a mass spectrometer, the phase transitioning occurs in the ion source. The ion source can use different methods for

transferring ions into gas phase. Atmospheric Pressure Ionization (API) is one method that includes Electro Spray Ionization (ESI), Atmospheric Pressure Chemical Ionization (APCI), and Atmospheric Pressure Photoionization (APPI). When choosing the ionization method, the size and polarity of the target analyte needs to be considered.

APPI can ionize non-polar compounds with low molecular weight, while ESI can ionize a lager molecular weight field. ESI cannot ionize very non-polar compounds. ESI and APPI are both considered soft ionization techniques, due to low fragmentation when ionizing the sample, making them more suitable for lipidomics. ESI is more commonly used in lipidomics due to its versatility and high compatibility with HPLC [46]. See Figure 10 for the correlation between different polarities and molecular weight for the different API sources.
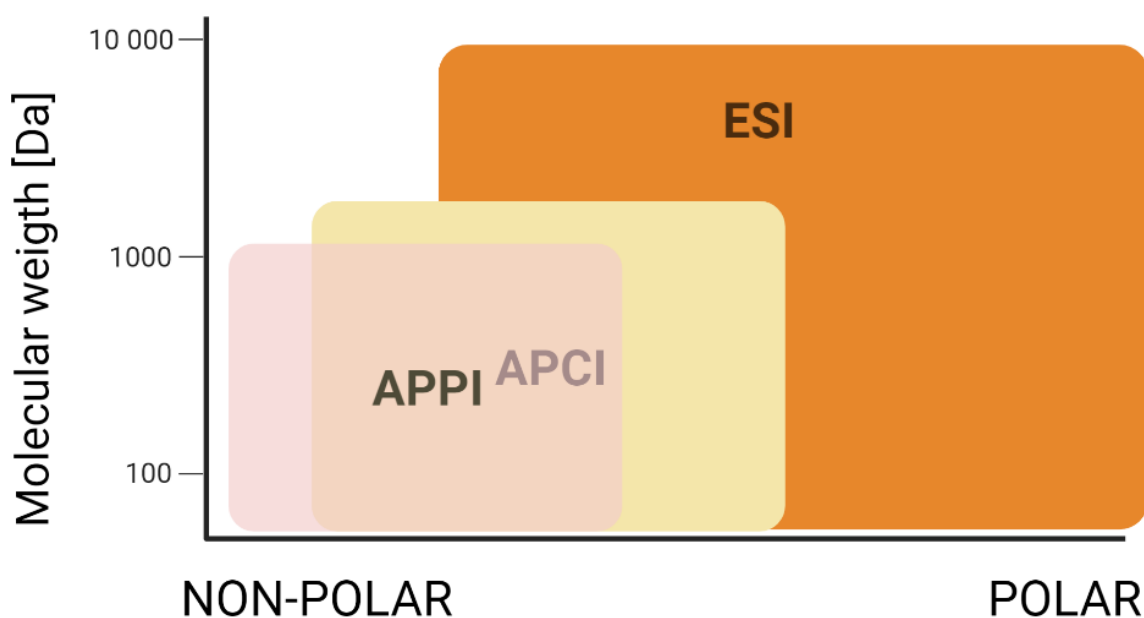
Figure 10: Coverage of polarity and molecular weight for different atmospheric pressure ion sources. Atmospheric Pressure Photoionization (APPI), Atmospheric Pressure Chemical Ionization (APCI) and Electrospray Ionization (ESI). Figure adapted from [47].

ESI uses electricity to create a spray which aid the ions from aqueous phase to gas phase. The phase change happens in different steps. First the sample is introduced to a spray capillary applied with a high voltage. This voltage can either be positive or negative, hence positive and negative ionization mode. The applied voltage creates a Taylor cone, a cone formation of the analyte solution at the end of the capillary. From this Taylor cone a jet is created using a coaxial nebulizing gas (N2) which aids in directing the droplets. The jet brakes into small charged droplets, the solvent in the droplets evaporates resulting in increased charge density, until the repulsion created by electrostatic energy is higher than the surface tension, resulting in ions "breaking out" of the droplet. This is known as Coulombic explosion. The charged

ions will then enter the mass spectrometer due to the vacuum established inside the MS [47]. See Figure 11 for how positive ions are created with ESI.

Electrospray ionization (ESI)
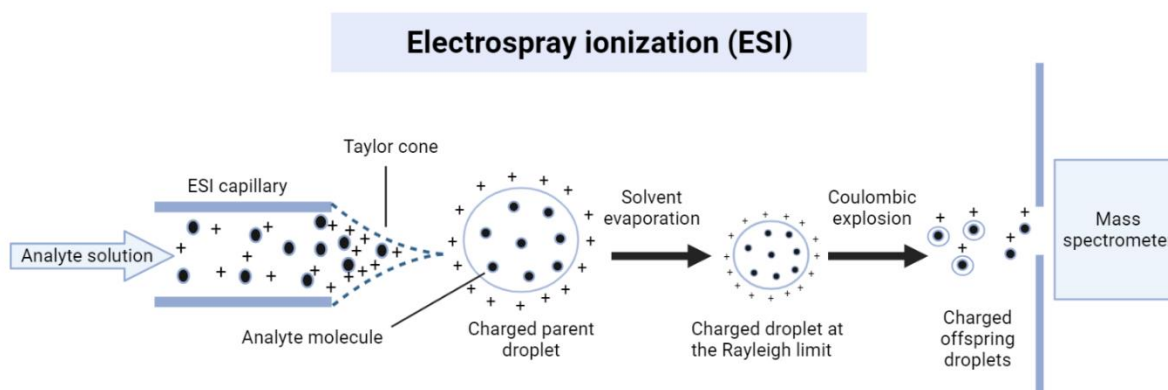
Figure 11: Illustration of how electrospray ionization (ESI) works. The solution containing the analyte enters the ESI capillary. The capillary is charged which results in the creation of a Taylor cone, from the Taylor cone a jet is created using a coaxial flow of nebulizing gas. The solvent surrounding the ions evaporate until the ions "break out" of the droplet due to coulombic explosion. The single ions then enters the mass spectrometer.

The resulting ions and adducts created by ESI can either be positive or negative with the form $[M+nH]^{n+}$ or $[M-nH]^{n-}$. Where M is the monoisotopic mass of the compound, n is the number of adducts donated or accepted, and H is the mass of the proton. In some cases, other adducts are formed in addition to proton adducts, for example, it is possible to have adducts with the addition of ammonium, sodium, carboxylic acid group, and more.

The mass analyzer separates the ionized compounds based on the *m/z* value and sends them to the detector where they are detected. The performance of the mass analyzer is determined by scan speed, sensitivity, mass accuracy, and mass resolution [47]. Scan speed is the speed at which the entire *m/z*-range is scanned, given in hertz (Hz). Sensitivity is the change in intensity per change in concentration of an analyte. The sensitivity correlates to the signal-to-noise ratio (SNR), as the SNR increases as higher sensitivity is obtained. Mass accuracy (E) is the difference between the measured *m/z* signal and the exact *m/z* signal. Mass resolution (R) is the minimal separation needed between two peaks, resolution is calculated with the formula R = M/ΔM. M is mass of the second peak and ΔM is resolving power, given in full width half maximum (FWHM) [47]. High mass resolution makes it possible to separate ions with almost identical *m/z* values, high mass accuracy allows for a more accurate detection of ions and their corresponding *m/z* value.

There are many different mass analyzers. The most common are quadrupole, ion trap, time of flight (ToF), and orbitrap. The highest resolution obtained is not the same for all mass analyzers. Quadrupoles are known for low resolution, but have no requirement for very high

vacuum, are simple to use and are considered to be very robust. In contrast, the ion trap and Time of Flight (ToF) are known for their very high resolution. Another mass analyzer known for its high resolution and high mass accuracy is the orbitrap, see Figure 12. Hybrid instruments consisting of multiple mass analyzers are often used in lipidomics. The hybrid instruments used the most in global lipidomics includes an orbitrap mass analyzer, see Figure 12.
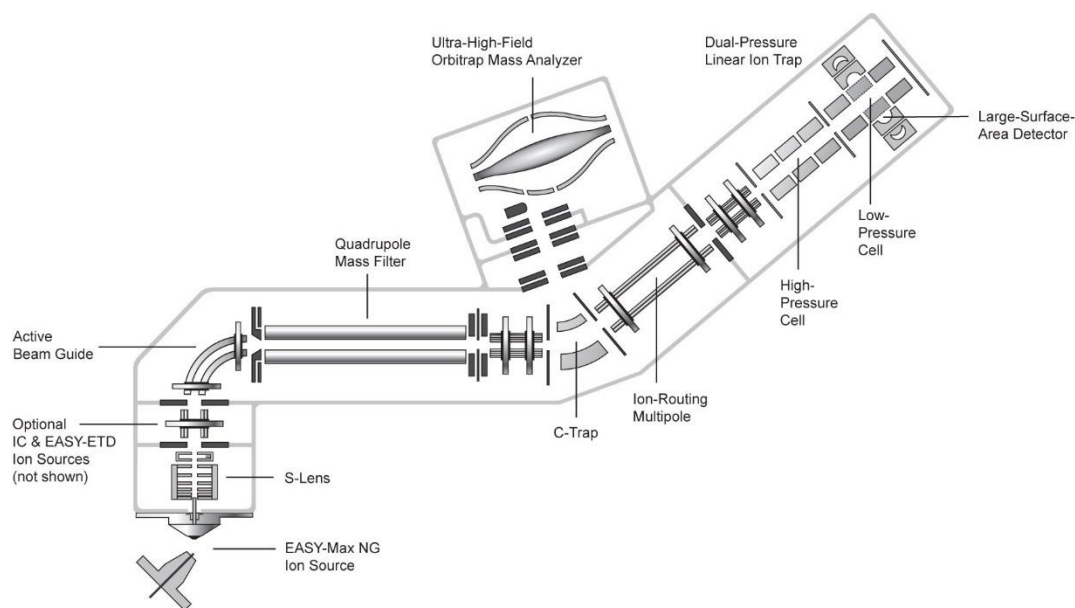
Figure 12: Illustration of Fusion Orbitrap Tribrid mass spectrometer (MS). The ions will enter from the ion source, the ions will be bent in a 90 degree bend to the quadrupole mass filter. The filtered ions enter the c-trap which direct them to the orbitrap mass analyzer or the dual-pressure linear ion trap. Figure from Thermo Fischer scientific.

Ions created by the electro spray ionization source enter a beam guide before entering the quadrupole mass filter. The quadrupole directs a selected range of *m/z* values to the c-trap. The c-trap will further direct the ions towards the orbitrap mass analyzer or the dual-pressure linear ion trap, depending if MS1 or MS2 is used. When MS2 spectra are obtained the ions will be directed from the c-trap to the dual-pressure linear ion trap. The ion trap works as a collision cell and fragment ions. The fragmented ions will be sent to the orbitrap for detection through the c-trap. An orbitrap works by trapping the ions, applying radial excitation and Fourier transformation to create a signal. The ions are introduced into the Orbitrap, where they are trapped by an electrostatic field created by a set of electrodes. The electrodes are arranged in a cylindrical shape, with the central electrode being a metal rod. Radial excitation is when a voltage is applied to the central electrode, causing the ions to oscillate in a radial motion around the central electrode. As the ions oscillate, they generate an image current that is detected by the outer electrodes. The image current is then processed using a Fourier

transform algorithm to obtain a mass spectrum. The mass spectrum provides information on the mass-to-charge ratio (*m/z*) of the ions present in the sample [44].

Even though mass spectrometry has shown to be an excellent tool for lipidomics, it requires some sort of separation of the sample components *in time*. Lipids can have tenfold of isomers, with high difference in concentration for the different lipid species. If all analytes entered the MS at the same time the MS spectra would be very complex, it would be affected by ion suppression in the ion source, and in general very hard to interpretate. To avoid this problem, chromatography is commonly be used. Chromatography is a technique for separating different compounds in a sample by passing the sample in solution through different matrixes/ mediums which causes the different components to move at different rates. In lipidomics the two most commonly used techniques are, HPLC and GC coupled to a MS. HPLC is usually chosen over GC in regards to lipidomics. This is because lipids are in general not volatile and the GC can only analyze volatile compounds, whereas HPLC can deal with any soluble compound regardless of its volatility. See part 2.5.2 for more details about HPLC and separation of lipids.

2.5.2   Liquid Chromatography

High-Pressure Liquid Chromatography coupled to a mass spectrometer (HPLC-MS) is the most commonly used analytical technique when it comes to lipidomics. It is a well-known approach for both routine analysis and research due to its sensitivity and selectivity. See Figure 13 for schematic representation of a HPLC-MS.
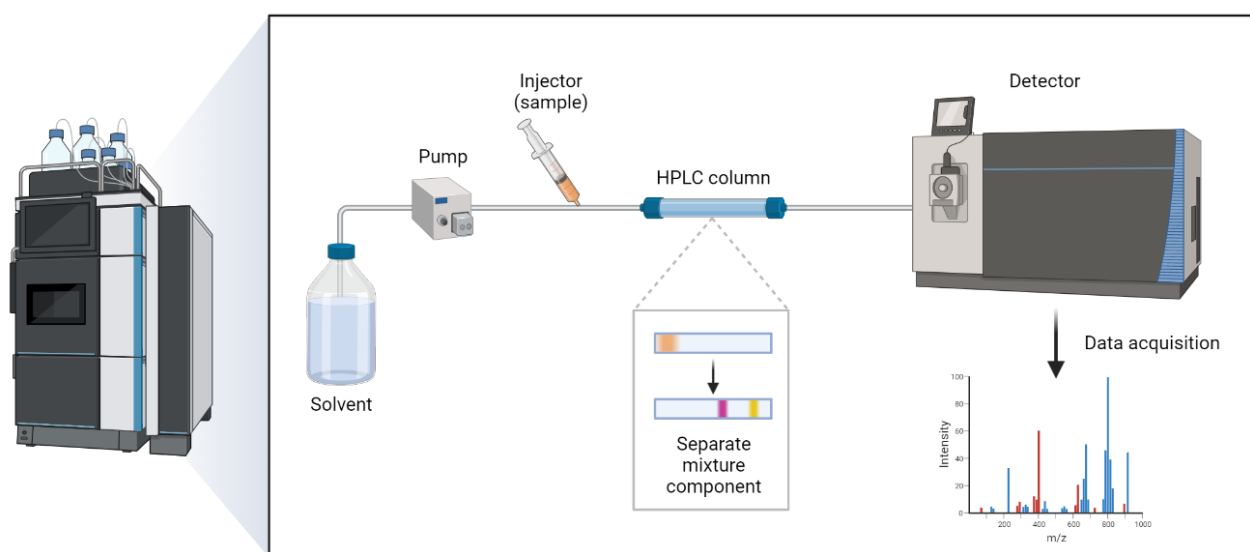
Figure 13: Illustration of a high-pressure liquid chromatography coupled to a mass spectrometer (HPLC-MS), with solvent which is the mobile phase, and the pump which pumps the mobile phase and sample to the MS. The injector introduces the sample to the column where the different compounds comprising the sample are separated before they reach the MS which generates an MS spectrum.

HPLC uses a mobile phase and a stationary phase to separate analytes from each other. The function of the mobile phase is to transfer the sample from the beginning of the system to the detector (MS). The chromatographic columns function is to separate the analytes based on interaction between the stationary phase and the analyte, and interaction between the analyte and the mobile phase [48]. If the analyte has a higher affinity for the mobile phase, it will elute faster and have less interaction with the stationary phase and the opposite when the affinity is higher for the stationary phase.

The mobile phase and stationary phase are highly customizable. New stationary phases and columns are developed continuously to suit different needs. For lipidomics, the two main separation principles used are, reverse phase (RP) and hydrophilic interaction liquid chromatography (HILIC). HILIC will separate the lipids based on the "head" groups, meaning that it will separate the different lipids and lipid classes primarily based on the polar part of the lipid. RP, however, will separate the lipids mainly based on the "tail" group, based on the hydrophobicity of the fatty acyl chains. RP separation allows for a class and intra-class separation based on both saturation and length of the carbon chain, creating intra-class and class separation based on chemical properties [42]. See Figure 14 for an illustration of RP separation, where the lipids will group together on the stationary phase due to hydrophobic effects, which is driven by entropy. This is because of the high hydrophilicity of mobile phase which causes the lipids to have a higher affinity for the stationary phase than the mobile phase. When the eluent strength of the mobile phase increases the entropy in the system increases as well. The increased concentration of hydrophobic mobile phase will

cause the lipids to have a higher affinity for the mobile phase, and thus release the lipids from the column.
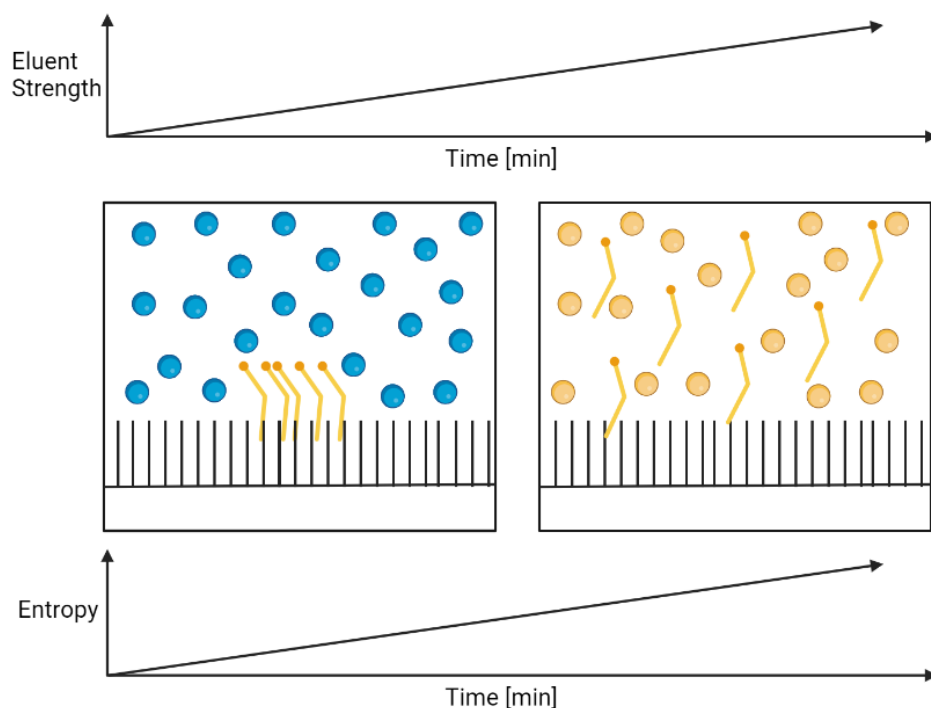
Figure 14: Illustration of how the separation in reversed phase chromatography happens. When the eluent strength is low the entropy inside the column is low (high concentration of hydrophilic mobile phase), causing the lipids to be grouped together on the stationary phase. When the eluent strength increases the entropy increases as well (high concentration of hydrophobic mobile phase). The higher entropy and increased concentration of hydrophobic mobile phase will release the lipids from the stationary phase of the column.

RP is the most used separation principal in lipidomics, and the stationary phase composition is usually either C8, C18, or less commonly C30 [49], bound to a silica base. The particle size can also vary depending on the column. For instance, Ultra High-Pressure Liquid Chromatography (UHPLC) columns have particle size <2 µm while a regular HPLC column uses particle sizes between 3 and 5 um. Smaller particle size allows a faster analysis and improves sensitivity and resolution. The disadvantage of using smaller particle sizes is that it creates higher pressure and reduces column life time.

The use of C18 and C30 stationary phases are a bit debated in the lipidomics field. The C30 stationary phase will have greater lipid separation due to the longer stationary phase chains, thereby causing more interaction with the different lipid acyl sidechains. While this is an advantage, it also has its downsides. Due to stronger retention, longer analysis time is needed and the risk of retention being too strong is present [50–53]. See Figure 15 for comparison of separation of lipid species with C18 and C30 stationary phase.

23
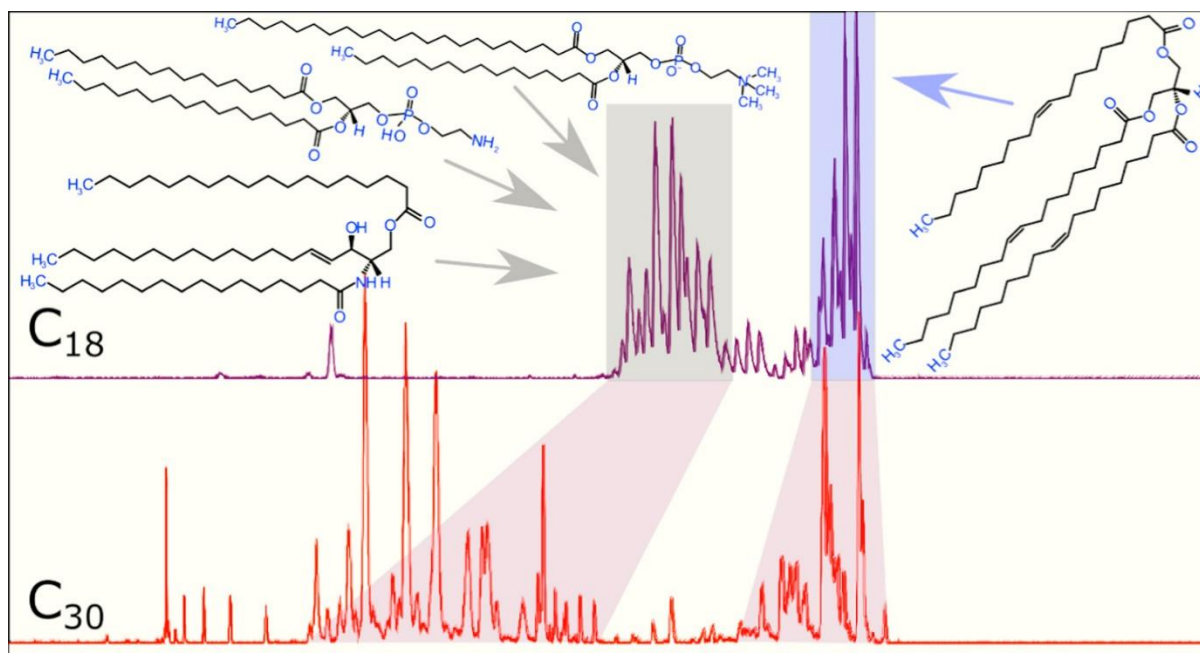
Figure 15: Illustration of C18 stationary phase separation of lipids compared to C30 stationary phase separation. As seen in the illustration the separation is better with the C30 stationary phase than the C18 stationary phase. Fetched from Jankevics 2021.

Chromatographic separation of lipids before they enter the mass spectrometer aids the identification process of the different lipid species present in a sample. To correctly identify lipid species, different data acquisition methods acquiring fragmentation spectra through tandem MS can be used.

2.5.3   Data Acquisition for lipid identification

For lipids to be properly identified, fragmentation spectra obtained with tandem MS is needed. Tandem MS is possible when the MS instrument has two or more mass analyzers. Tandem MS operates with three different methods, precursor ion scan, product ion scan, and natural loss scan. The most used in lipidomics is product ion scan (PIS), where one or multiple precursor ions are selected and product ions originating from the precursor ions are scanned. PIS can be done in two ways, user-defined product ion scan and instrument-defined product ion scan. Targeted lipidomics uses user-defined product ion scan. Other experiments used are selected reaction monitoring (SRM), multiple reaction monitoring (MRM), or parallel reaction monitoring (PRM). PRM can only be done if the third mass analyzer is an orbitrap. In global lipidomics the precursor ion is instrument defined. Data-dependent

acquisition (DDA) and data-independent acquisition (DIA) are examples of instrument defined product ion scans. See Figure 16 for comparison of SRM and DDA.
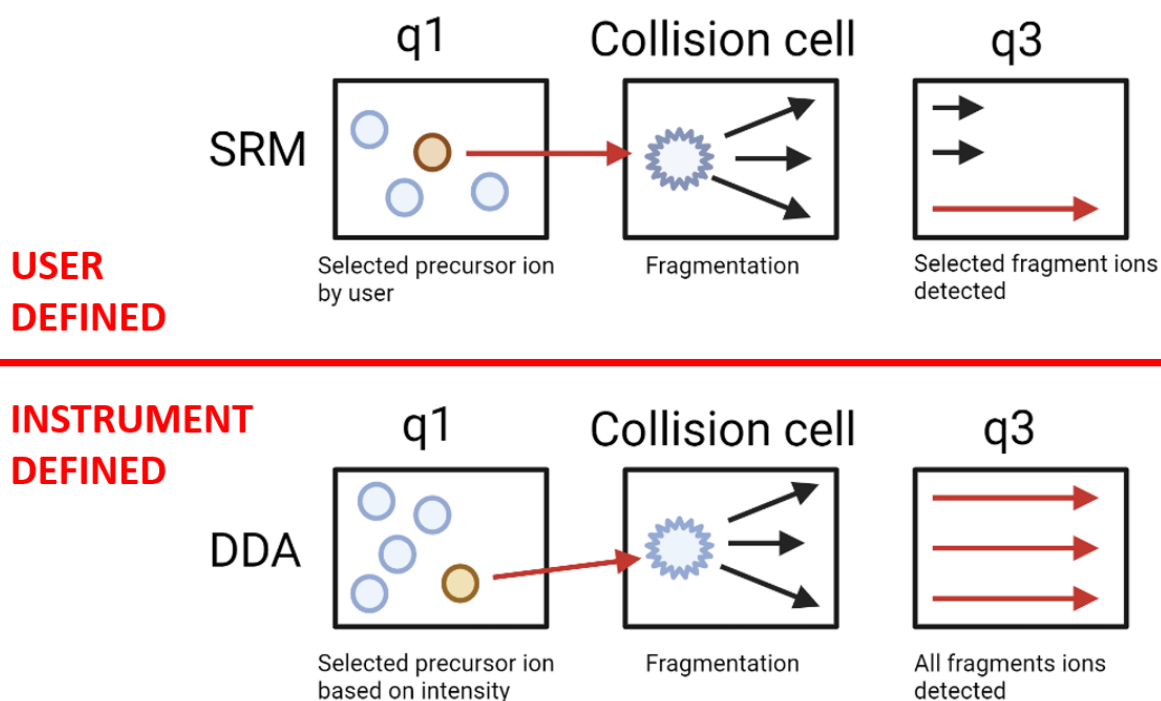
Figure 16: Comparison of selected reaction monitoring (SRM) and data-dependent acquisition (DDA). Whereas the SRM has selected precursor and fragment ions by the user, in the DDA approach the instrument chooses the precursor ion based on intensity. In DDA all fragment ions are detected, in contrast to SRM where pre-selected fragment ions are detected, and other fragment ions are excluded.

DDA is the most common methods of acquiring data in global lipidomics. In DDA a full scan will be conducted in MS1, with one constant precursor isolation window for the whole analysis, as opposed to the many small windows in DIA. Selected precursor ions with the highest intensity will be sent to fragmentation, see Figure 17. This is also known as DDA Top N, where N is the number of ions sent to fragmentation, usually, it is 3, 5 or 10, depending on the threshold used. DDA is the dominating method used for global lipidomics, and the selectivity is based on ion intensity [54].
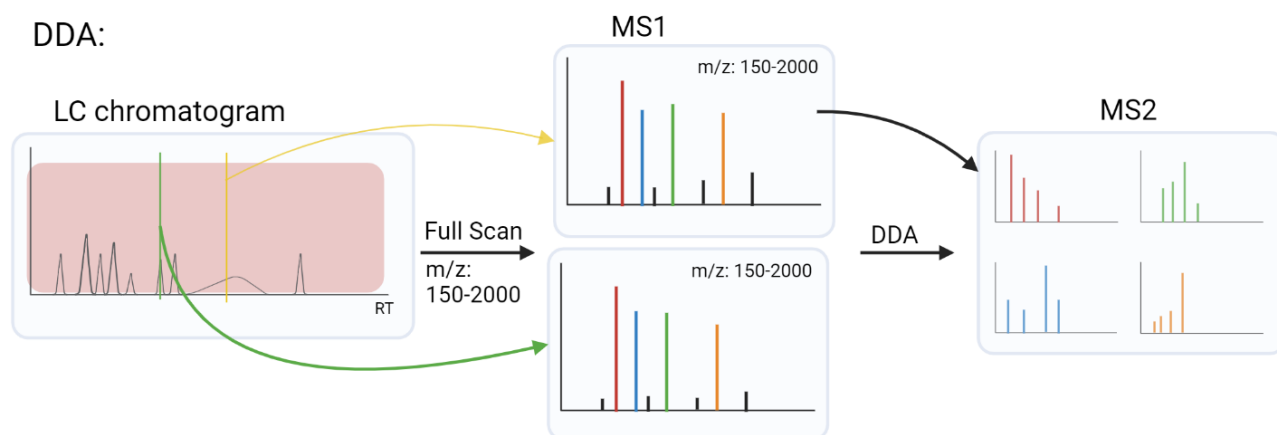
Figure 17: Illustration of how regular data dependent acquisition (DDA) works, precursor isolation window is constant during the whole run. The ions with the highest intensity are chosen to be fragmented by the instrument.

The advantage of DDA contra DIA is the removal of background noise. The problem with DDA is that it loses a lot of signals to remove the background noise. To counter this inclusion and exclusion lists are made to either add or remove ions to the Top N that are sent to fragmentation. Another problem with the DDA is that the mass window is fixed for the whole experiment, meaning that in some cases it can remove ions thar are interesting [55].

2.5.4 Scheduled MSMS for Global Lipidomics

As mentioned earlier, the disadvantage with DDA is the constant mass window throughout the experiment, resulting in lipids not being detected because they have precursor ions outside the chosen range. Inclusion lists can be used to include certain precursor ions of interest. Since the analytes are separated beforehand with HPLC, retention time can be used to improve the DDA method. With separation of the different lipid classes, and known retention times, multiple DDA experiments can be applied in one MSMS experiment. This is because the elution profile of the lipid classes is based on lipid class and composition of the aliphatic chains. One constant *m/z* window throughout the whole analysis is therefore, not optimal, see Figure 18 for an illustration of scheduled MSMS.
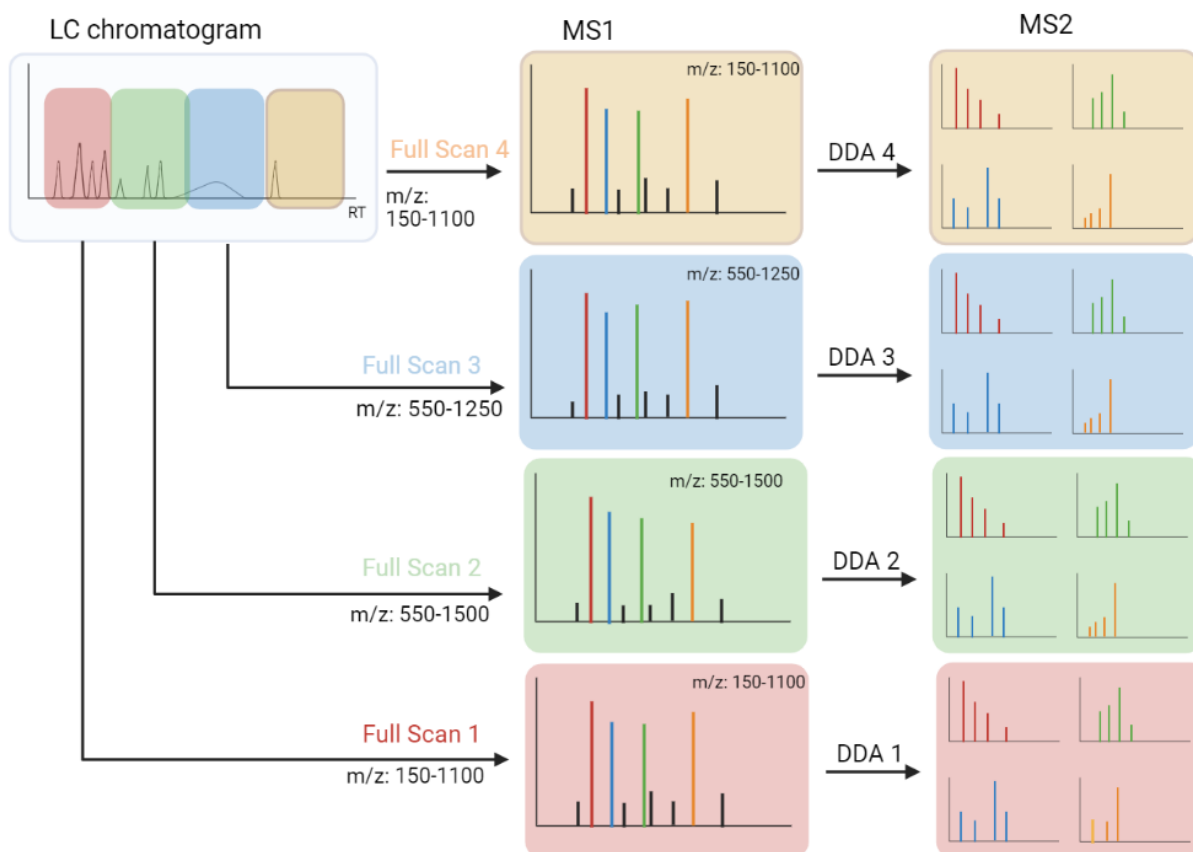
Figure 18: Illustration of how scheduled MSMS works with different m/z windows given during different time intervals, which can lead to more compounds detected. Starting with a full scan in a certain mass range, then the ions for fragmentation are selected by the DDA. After x minutes the m/z range will change from range 1 used in full scan 1 to range 2 used in full scan 2.

Scheduled MSMS works very similar to DDA, but with multiple precursor isolation windows. In Figure 18 there are four different precursor ion isolation windows. First a full scan is conducted, then the different precursor ion isolation windows select which ions will be sent to fragmentation based on intensity, as in DDA. The use of different *m/z* windows will gather more data compared to using one constant *m/z* window, Jankevics 2021.

The reason why more data can be collected is because with a smaller *m/z* range, the time it takes to scan the selected range is less than with regular DDA, where a wider mass range is chosen. The shorter cycle time gives the instrument time to do "extra" cycles per analysis compared to regular DDA. For example, if the analysis is 10 minutes, cycle time for DDA is 3 seconds, giving a maximum number of 200 cycles. If the cycle time is reduced to 2 seconds because of the narrower *m/z* window, the maximum number of cycles will be 300, which is a 50 percent increase, resulting in increased sensitivity.

Another big advantaged with the scheduled MSMS approach is the reduced need for instrument time. Jankevics 2021 compared the scheduled MSMS approach to regular DDA, and found that a total of 5 different experiments using DDA covering different *m/z* ranges was needed to reach the same amount of lipids detected with only one analysis when using the scheduled MSMS approach. The big disadvantage of the scheduled MSMS approach is the need for very reproducible chromatographic retention time to ensure that all lipid species fall within their expected precursor isolation window. Variations in the chromatographic retention times can come from the analytical method being used, but also the samples being analyzed. Matrix effects occurs in biological samples and can affect ionization and retention time to analytes of interest [56].

2.6   Biological Matrixes for Lipidomics

Even though lipids can be found in all biological matrixes, some biological matrixes are more suited for lipidomics than others. Take blood and urine as two examples. Urine is one of the human biological matrices where fewest lipids are present. This is due to the different roles lipids has in the body (mentioned in chapter 2.2) and the body wants to keep the lipids and not excrete them. However, that does not mean that there is no lipidomics information to collect from urine. Some diseases, one mentioned in chapter 2.2 can be detected by the lipid species found in urine. There are different types of blood, capillary blood and venous blood, based on from where the blood sample is taken. One study showed that there are significantly lower concentrations of lipids and lipoproteins in capillary blood compared with venous blood [57].

A blood sample can typically be categorized as, plasma, serum or whole blood. Whole blood contains everything found in blood, whereas plasma is the fluid fraction without the cells and the platelet that can be collected when coagulation is prevented by an anticoagulants. Serum is the liquid which remains when the whole blood has clotted, removing the cells, platelets and the coagulation factor. In theory the removal of blood cells and platelets lowers the total lipid concentration and might even remove some lipid species which is present in the membranes and interior of whole blood cells and platelets [58].

Tissue and cells are other biological matrices which contain high lipid concentrations. For tissue, the lipid concentration is very high. A challenge when analysing tissue is that the lipid extraction process can be tricky and recovery can be low. Tissue samples are also more

difficult to get from patients, since they usually require invasive procedures and often demand a hospital visit and specialized equipment [36]. Urine is the easiest biological matrix to collect, since it is something the body excretes naturally. A blood sample is invasive, however minimally so, and usually demand a visit to a doctor, laboratory or a hospital. There are, however, different blood sampling methods which are considered more or less non-invasive and does not require the presence of medical personnel e.g. Dried Blood Spots.

2.7   Dried Blood Spot – Sampling made easy and inexpensive

Dried Blood Spot (DBS) is a well-known sampling method used to collect blood samples from newborns [59]. DBS sampling requires only a few drops of blood which are spotted onto the DBS filter card and left to dry, see Figure 19. The DBS card can then be sent by mail to hospitals or other laboratories for analysis. The method is non-invasive and it can be done virtually anywhere. For analysis, the blood spots are punched out, and analytes are extracted from the paper punch with different methods depending on the target of the analysis.
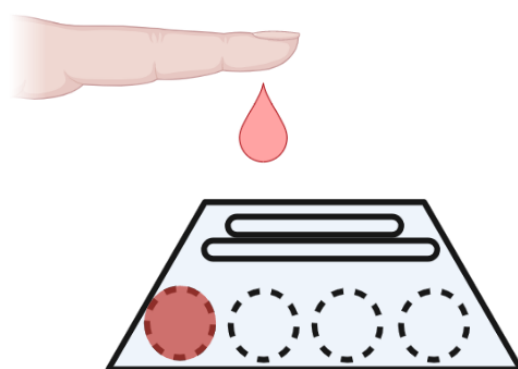
Figure 19: Illustration of Dried Blood Spot, a drop of blood from the fingertip is spotted onto the DBS filter card.

The advantage of DBS is its cheap and easy handling. Many developing countries send DBS cards to other countries for either new-born screening or other targeted analysis [60]. It is not only helpful for developing countries but also for individual patients that do not have easy access to blood sampling facilities. Collecting liquid blood samples are a demanding process. Therefore, the option for patients to be able to collect samples themselves at home can be very beneficial and favourable. The reason why DBS cards can be sent with postal services is due to their stability. The most common technique for analysing DBS cards is HPLC [61].

DBS works typically by dropping blood from a finger puncture onto a filter card. The card can hold approximately 50 µL of blood per marked circle (when the diameter is 1.2 cm). For

analysis, the disk punched out of the card is typically 3.2 mm in diameter, corresponding to 2.5 – 5 µL of blood. Thus, it is possible to get multiple samples from one blood sample, enabling several different types of analyses and repeated analysis if needed. The filter cards are made of non-cellulose and cellulose matrix with different pore sizes or thickness.

A problem that can occur when using DBS cards in global lipidomics, is oxidation, moisture accumulation and lipid degradation due to hydrolysis that can lead to problems with the identification of the different lipid species. Some lipid species are more prone to oxidation than others. In theory, lipids containing polyunsaturated fatty acids can oxidize, which include cholesteryl esters, sphingomyelins, phosphatidylcholines, glycerolipids and phosphoethanolamines [62]. Researches have reported that less than 5 % of the original lipids present in a dried blood spot are oxidized, and concluded that DBS can be used to obtain information about the global lipidome [62]. To get the most accurate results from DBS samples analyzed with global lipidomics, measurements for quality assurance and system reliability needs to be in place.

2.8 Quality Assurance and System Suitability in Global Lipidomics

Perhaps the biggest issue with omics (both lipidomics and metabolomics, and general omics techniques) is to capture as much data from a sample as possible, while maintaining high quality data and reproducibility. To check the quality of the performance of the analytical platform pooled quality controls (PQC) can be used. PQC are a mixture of small aliquots from each sample, see Figure 20 for illustration of how PQC is made. The function of the PQC is to represent the matrix and the metabolite/ lipid composition of each sample. PQC is analyzed multiple times during a sequence. The quality of the samples and the assessment of the analytical variance created by the method or instrumentation throughout the analysis can thus be monitored.
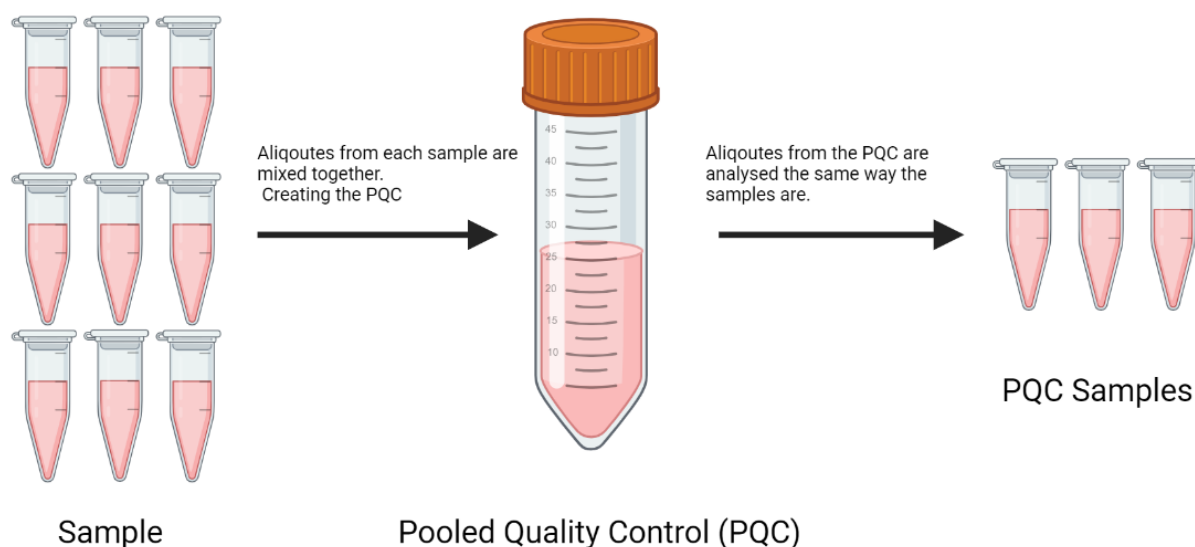
Figure 20: Preparation of Pooled Quality Control (PQC) made by combining small aliquots from each sample. The PQC are then analyzed in the same way the samples are, and are repeatedly analyzed throughout the sequence. Figure adapted from Broadhurst et al (2018) [63].

The PQC is analyzed multiple times during an analytical sample sequence. The result obtained are typically easily compared using principal component analysis (PCA) [63]. If the PQC samples are tightly grouped, the analytical analysis is of high quality. With PQC it is also possible to evaluate the precision of each lipid detected, but only if the lipid is present in the PQC.

Another function the PQC has is the possibility of signal alignment. As mentioned above, the PQC consist of small aliquots of each sample, and the PQC is analyzed multiple times throughout a sample sequence. Therefore, the signal intensity and retention time should be the same for all specific metabolites present in the PQC for each PQC injection. However, this is seldom the case due to drift throughout the analytical analysis. Specialist software recognizes the change in the PQC of each measured *m/z* value throughout the analytical analysis, and corrects the signal intensity of each *m/z* value in each sample corresponding to the change in PQC signal in the same time segment. See Figure 21 for signal correction done with PQC. Using certain software the signal alignment can be done on single lipid species. This is an advantage since some lipids will have a linear or non-linear change in signal strength, whereas other lipid species have little to no drift in signal strength.
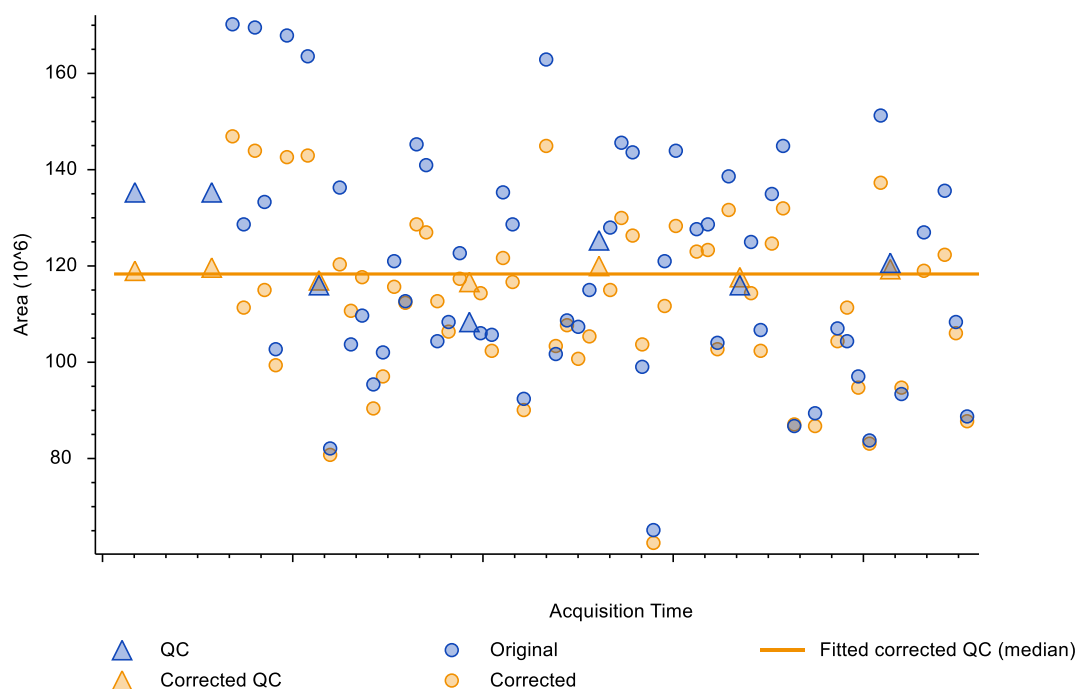
Figure 21: Example of how pooled quality control correction works. The samples (circles) will be corrected in relation to fitted corrected median of the pooled quality controls (triangles). X-axis is acquisition time, and Y-axis is area (a.u). Blue represents uncorrected signal intensity and yellow represents corrected signal intensity.

When a LC-MS method is implemented, a way to ensure the quality of separation and detection is to use system suitability tests (SST) [64]. System suitability is a set of tests that are performed to verify that the chromatographic and mass spectrometry system is working correctly and is capable of producing reliable and accurate results. System suitability tests can include assessing the mass accuracy, resolution, retention time, peak shape, and sensitivity of the analytical method [64]. By performing system suitability tests regularly, any changes in the analytical system can be detected early, and corrective actions can be taken before they impact the results of the experimental samples.

Both PQC and SSTs are essential for lipidomics studies to ensure that the data obtained are accurate and reliable, and that the results can be reproduced in different laboratories or by different analysts. The use of PQC and system suitability tests can help to identify any issues with the analytical method and to improve the quality of the lipidomics data generated. When following a global lipidomics workflow, the next step after the signal alignment process is identification of the different lipid species present in the samples.

2.9 Identification and Level of Confidence in Global Lipidomics

After the experimental data has been collected and the quality of the data assessed, the identification process begins. When doing global lipidomics, hundreds of different lipid species can be present in one sample. Identification of the different lipid species can thus be challenging. The identification process involves the use of various techniques and criteria to accurately and confidently identify lipid species. Lipid species are identified based on their retention time, *m/z* signal, and fragmentation pattern [53]. This involves comparing the experimental spectra with reference databases or in-house libraries of mass spectra for known lipid species. The identification is divided into different levels, known as levels of confidence, see Figure 22.
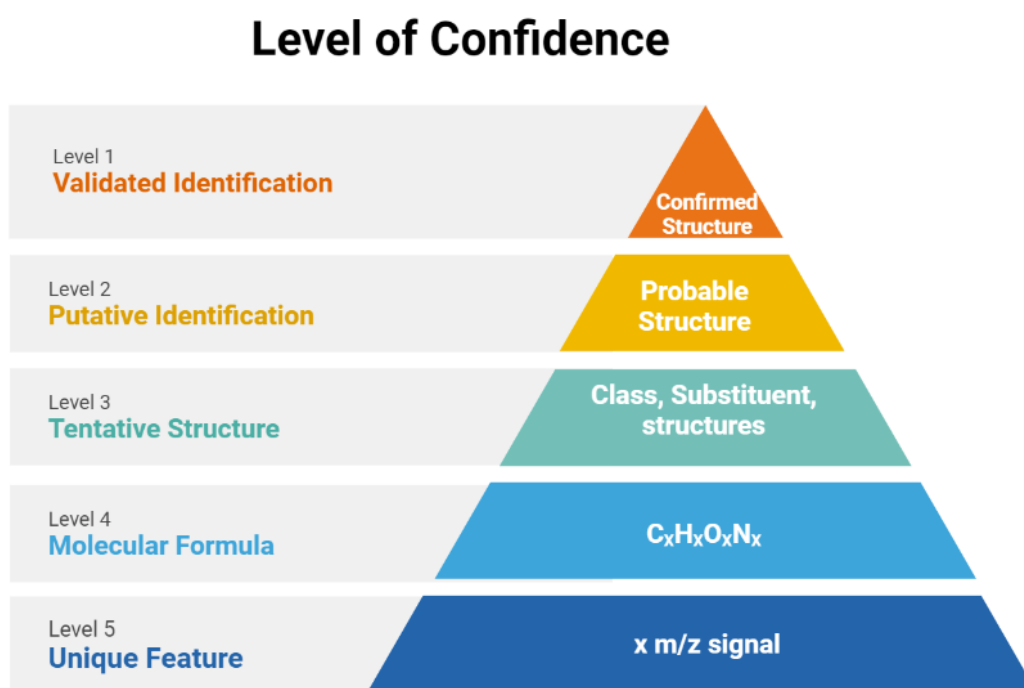
Figure 22: Level of Confidence triangle. Confidence in identification of a metabolite/ lipid is divided into 5 different levels, ranging from the lowest level 5, where only a unique feature (m/z) is observed, up to the highest level 1 where the identification is validated. Adapted from [5].

The different levels describe how confident the identification of a lipid is when preforming global lipidomics. The lowest level of confidence (level 5) is when an *m/z* signal with a certain mass accuracy is detected. The reason of why this is the lowest level is because an *m/z* signal is not necessarily specific for one lipid species, many lipid species can give the same *m/z* signal, due to isomers. The level of confidence increases with the amount of additional

information [65], up to level 1 (the highest level of confidence), when an analytical standard (reference standard) is analyzed with identical analytical conditions, and gives the exact same retention time and fragmentation pattern.

Identification and level of confidence in lipidomics rely on the use of robust analytical methods, high-quality data analysis and appropriate validation to ensure the accuracy and reliability of the results. Lipidomics Standard Initiative (LSI) was therefore started to create guidelines for the major lipidomics workflows, including sample preparation, lipid identification, and validation and evaluation guidelines for lipidomics methods. The guidelines aim to track methodological progress and improve the data quality obtained in the field of lipidomics [66].

2.10   Aim of Study

The aim of this project was to establish, optimize and evaluate a global lipidomics HPLC-MSMS method, originated from Jankevics 2021. The method was set up on a Vanquish Horizon UHPLC system coupled to a Fusion Orbitrap Tribrid mass spectrometer from Thermo Fisher Scientific. The method utilizes a C30 stationary phase column and scheduled MSMS for data acquisition. A key question would be if the scheduled MSMS acquisition method would outcompete previous recordings, thus two different data acquisition methods was tested and compared, DDA and Scheduled MSMS. The study includes an optimization part aiming for optimizing the lipid coverage of the LC-MSMS lipidomics method. The method were optimized using analytical standards and human serum. The study includes an evaluation part, aiming to ensure stable performance, plus accurate and reliable results, following the lipidomics standard initiative (LSI) guidelines.

For the method to be applicable to clinical diagnostic it must be able to observe normal variations in the lipidome. The optimized and evaluated method were then be applied to a simpler study focusing on normal variations in the lipidome induced by high intensity training (HIT). A research question would be if the scheduled MSMS acquisition method were able to detect exercise induced changes in the lipidome, and if the observed changes in the lipidome were connected to energy metabolism (consumption and restitution) or to other functions of lipids and their biological pathways and networks.

3 Experimental

3.1 Small Equipment

The pipettes used was Fisherbrand[TM] Elite[TM] adjustable-volume pipettes from Fisher Scientific (Waltham, MA, USA). Thermomixer Comfort from Eppendorf (Hamburg, Germany). For LC analysis, Snap-top vial, Snap Ring Cap and 0.1 mL Micro-Insert, from Matriks AS (Oslo, Norway). Analytical weight AG 245 from Mettler-Toledo (Columbus, OH, USA). For sample preparation Fresco[TM] Microcentrifuge from Thermo Fisher Scientific (Waltham, MA, USA)

3.2 Chemicals

3.2.1 Solvents

The solvents used are listed in Table 1, with abbreviation, purity, manufacturer, and place of origin. Type 1 water with a resistivity of 18.2 MΩ•cm at 25 °C was provided from a Milli-Q-Purification system. The system used a quantum cartridge, and a 0.2 µm pore filter membrane from Merck (Darmstadt, Germany). Type 1 water was the only water used in this thesis.

Table 1: List of Solvent used in this project with their names, abbreviations, purity, manufacturer and place of origin.

Name	Abbreviation	Purity	Manufacturer	Place of origin
Methanol	MeOH	LC-MS grade	Rathburn Chemicals Lrd	Walkerburn, Scotland
Isopropanol	IPA	LC-MS grade	Merck KGaA	Dramstadt, Germany
Acetonitrile	ACN	LC-MS grade	Rathburn Chemicals Lrd	Walkerburn, Scotland
Formic Acid	FA	98-100%	Merck KGaA	Darmstadt, Germany

3.2.2   Reagents

Ammonium formate (NH_4HCO_2, abbreviation: AF) was from Sigma-Aldrich Chemistry (Steinheim, Germany). The EquiSPLASH™ LIPIDOMIX® quantitative isotopically labelled

internal standard and LightSPLASH™ LIPIDOMIX® quantitative mass spectrometry primary standard was both obtained from Avanti® Polar lipids Inc, (Alabaster, AL, USA). Cortisone, decanoate, coenzyme Q10 analytical standards used were from Sigma-Aldrich Chemistry (Steinheim, Germany).

3.3 Solutions

3.3.1 Mobile Phases

Mobile phases used in the project are shown in Table 2. All mobile phases were kept at approximately 20ºC. Freshly made mobile phases were prepared before each experiment or when it was needed.

Table 2: List of Mobile phase compositions used in global lipidomics method.

	Mobile phase A	*Mobile phase B*
Lipidomics	Acetonitrile (60%) + 20mM AF	Isopropanol (85.5%) + Acetonitrile (9.5%) + 20 mM AF

3.3.2 System Suitability Test Solutions

System Suitability Test solution for the lipidomics platform consisted of the following compounds with concentrations shown in Table 3.

Table 3: Shows the different lipid standards used in the lipidomics system suitability test solution. Including name, concentration, adduct found in positive ionization mode and negative ionization mode.

Name	*Concentration (µM)*	*Adduct in positive ionization*	*Adduct in negative ionization*
FA 10:0 (Decanoic Acid)	90.8	n/a	[M-H]-
DG (15:0/18:1 (d7))	3.1	[M+Na]+	[M-H]-
LPC (18:1 (d7))	4.8	[M+H]+	[M-HCOO]-
ST (21:4;O5) (Cortisone)	43.4	[M+H]+	[M-H]-
Coenzyme Q10	18.1	[M+H]+	[M-H]-
SM (d18:1/18:1 (d9))	3.4	[M+H]+	[M-HCOO]-

3.3.3 Calibration Solution

For calibration of Fusion Orbitrap Tribrid, Pierce FlexMix Calibration solution obtained from Thermo Fisher Scientific (Waltham, MA, USA) (stored in RT) was used.

3.3.4 Equisplash lipidomics standard solution

The EquiSPLASH™ LIPIDOMIX® quantitative isotopically labelled internal standard and was diluted with 10 mL MeOH, and stored at -20 °C. Hence the concentrations shown in Table 4. The EquiSPLASH™ LIPIDOMIX® is referred to as Equisplash lipidomics standard.

Table 4: EquiSPLASH™ LIPIDOMIX® quantitative isotopically labelled internal standard compounds with systematic name, abbreviation and concentrations, molecular formula and Log P value.

Name	Abbreviation	Concentration [μM]	Formula	Log P value
1-pentadecanoyl-2-(9Z-octadecenoyl (d7))-glycero-3-phospho-(1'-myo-inositol)	PI (15:0/18:1 (d7))	11.8	$C_{42}H_{72}O_{13}PD_7$	9.8
1-pentadecanoyl-2-(9Z-octadecenoyl)-3-pentadecanoyl (d7)-sn-glyserol	TG (15:0/18:1 (d7)/15:0)	12.3	$C_{51}H_{89}O_6D_7$	21.0
1-pentadecanoyl-2-(9Z-octadecenoyl (d7))-glycero-3-phosphoserine	PS (15:0/18:1 (d7))	12.9	$C_{39}H_{67}NO_{10}PD_7$	9.5
1-pentadecanoyl-2-(9Z-octadecenoyl (d7))-glycero-3-phospho-(1'-sn-glycerol)	PG (15:0/18:1 (d7))	13.1	$C_{39}H_{68}O_{10}PD_7$	11.8
1-pentadecanoyl-2-(9Z-octadecanoyl (d7))-glycero-3-phosphocholine	PC (15:0/18:1 (d7))	13.3	$C_{41}H_{71}NO_8PD_7$	13.1
N-(9Z-octadecenoyl (d9))-sphing-4-enine-1-phosphocholine	SM (d18:1/18:1 (d9))	13.5	$C_{39}H_{61}D_9N_2O_6PD_9$	12.4

1-pentadecanoyl-2-(9Z-octadecenoyl (d7))-glycero-3-phosphoethanolamine	PE (15:0/18:1 (d7))	14.1	$C_{38}H_{67}NO_8PD_7$	9.9
Cholest-5-en-3b-yl (9Z-octadecenoate (d7))	ChE (18:1 (d7))	15.2	$C_{45}H_{71}O_2D_7$	16.6
1-pentadecanoyl-2-(9Z-octadecenoyl (d7))-sn-glycerol	DG (15:0/18:1 (d7))	17.0	$C_{36}H_{61}O_5D_7$	13.7
N-(pentadecanoyl)-sphing-4-enine (d7)	Cer (d18:1 (d7)/15:0)	18.8	$C_{33}H_{58}NO_3D_7$	12.3
1-(9Z-octadecenoyl (d7))-2-glycero-3-phosphocholine	LPC (18:1 (d7))	18.9	$C_{26}H_{45}NO_7PD_7$	5.7
1-(9Z-octadecenoyl (d7))-2-glycero-3-phosphoethanolamine	LPE (18:1 (d7))	20.5	$C_{23}H_{39}NO_7PD_7$	2.5
1-(9Z-octadecenoyl (d7))-glycerol	MG (18:1 (d7))	27.5	$C_{21}H_{33}O_4D_7$	6.5

3.4 Sample Preparation
3.4.1 Sample Preparation of Human Serum

Venous blood from a healthy voluntary were collected in a Vacuette® Tube 4 mL Z Serum Sep Clot Activator, obtained from Greiner Bio-One (Kremsmünster, Austria). To 50 µL of serum, 150 µL of cold (4 °C) isopropanol (IPA) was added and vortexed for approximately 20 seconds. The sample was centrifuged (20 minutes, 20 000-g, 4°C), 150 µL of the supernatant was taken out and placed in HPLC vials with insert glass and cap. See Figure 23 for illustration of sample preparation.
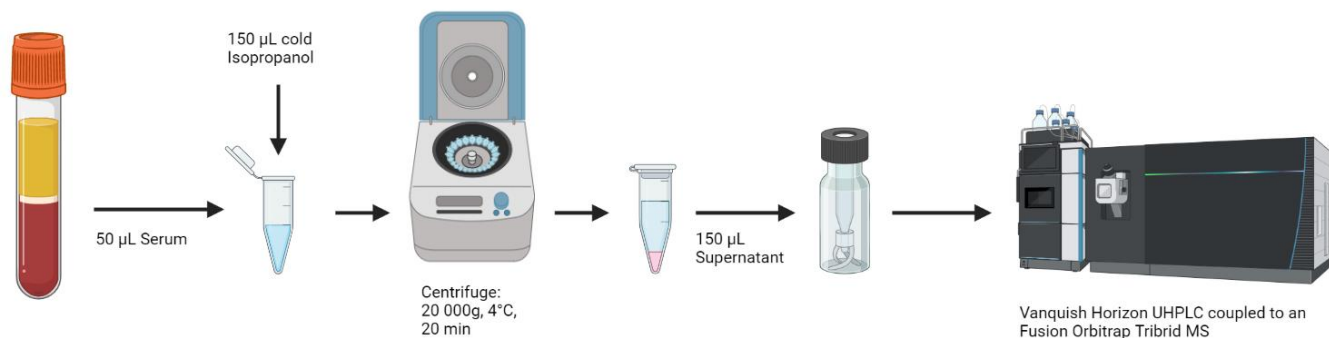
Figure 23: Illustration of sample preparation of human serum. To serum, cold isopropanol was added, then the sample was centrifuged and the supernatant was transferred to a HPLC vial for analysis.

3.4.2 Sample Preparation of Dried Blood Spots and preparation of PQC's.

To Whatman 903 Protein Saver Cards, obtained from Sigma-Aldrich Chemistry (Steinheim, Germany), one drop of capillary blood was dripped in each of the marked circle, and left to dry in RT for at least 4 hours. After drying one punch was taken from the centre of the blood spot with a manual puncher. The punch was then placed into individual Eppendorf tubes (1.5 mL), and 100 µL of IPA was added to each tube. The tubes were then mixed for 45 minutes at 45º at 700 rpm using a Thermomixer Comfort. A PQC was made by transferring 10 µL aliquots from each tube into a separate Eppendorf tube, and mixed thoroughly. Aliquots from the PQC was transferred into HPLC-vial with insert glass and cap. The remaining aliquots in each Eppendorf tube (from the samples) was transferred into separate HPLC-vials with insert glass and cap. See Figure 24 for illustration of the sample preparation.
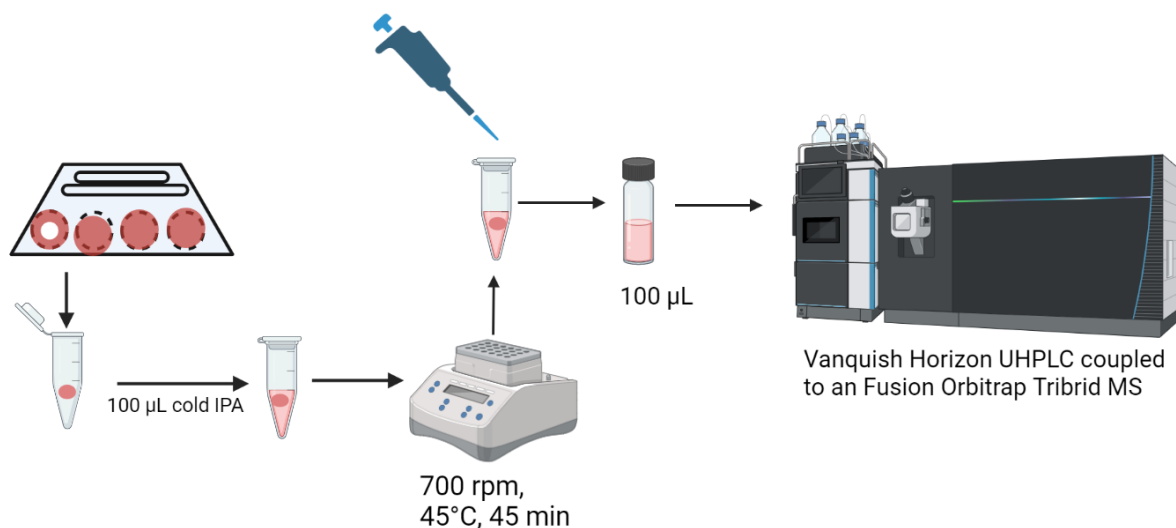
Figure 24: Sample preparation of dried blood spot cards. A center punch was taken from the DBS sample. To the punch cold IPA was added. The sample was then thermomixed, and the supernatant was transferred to a HPLC-vial for analysis.

3.4.3 Preparation of System Suitability Test for Lipidomics

One aliquot of Equisplash lipidomics standard (concentrations listed in 3.3.4) was used for the preparation of the system suitability test. To this standard 1 aliquot of each cortisone, decanoate and coenzyme Q10 standard was added. The mixture was then whirl mixed to get a homogeneous solution and transferred to an HPLC-vial. See section 4.1.5 for the development and testing of the lipidomics system suitability test. Concentrations are listed in Table 14.

3.5 Liquid Chromatography Mass Spectrometry Instrumentation and Settings

LC instrumentation used for global lipidomics was a Vanquish Horizon UHPLC binary system pump, column compartment H, and autosampler, from Thermo Fisher Scientific (Waltham, MA, USA). The MS used was a Fusion Orbitrap Tribrid from Thermo Fisher Scientific (Waltham, MA, USA). The ionization source was electrospray where samples were analyzed in both positive and negative ionization mode. The column used was a Accucore C30 column (150 mm x 2.1 mm, particle size 2.6 µm, carbon load 5%; Thermo Fisher

Scientific, MA, USA). The LC settings used are shown in Table 5. The 30 minutes assay gradient is shown in

Table 6 and Figure 25. The initial LC-MS method was adapted from Jankevics 2021.

Table 5: The liquid Chromatography settings used in this project.

Parameters	Settings
Mobile Phase A	See Table 2
Mobile Phase B	See Table 2
Gradient	See Figure 25 and Table 6
Injection volume	2 µL
Column Temperature	55°C
Flow rate	0.400 mL/min
Analysis Time	30 min
Re-equilibration time	10 min

Table 6: The gradient with time (min) and mobile phase B (%) composition, used in the global lipidomics method. Mobile phase B is defined in Table 2.

Time (min)	Mobile phase B(%)
0	20
2.5	20
2.6	55
12	60
12.1	80
19	90
21	100
23	100
23.1	20
30	20
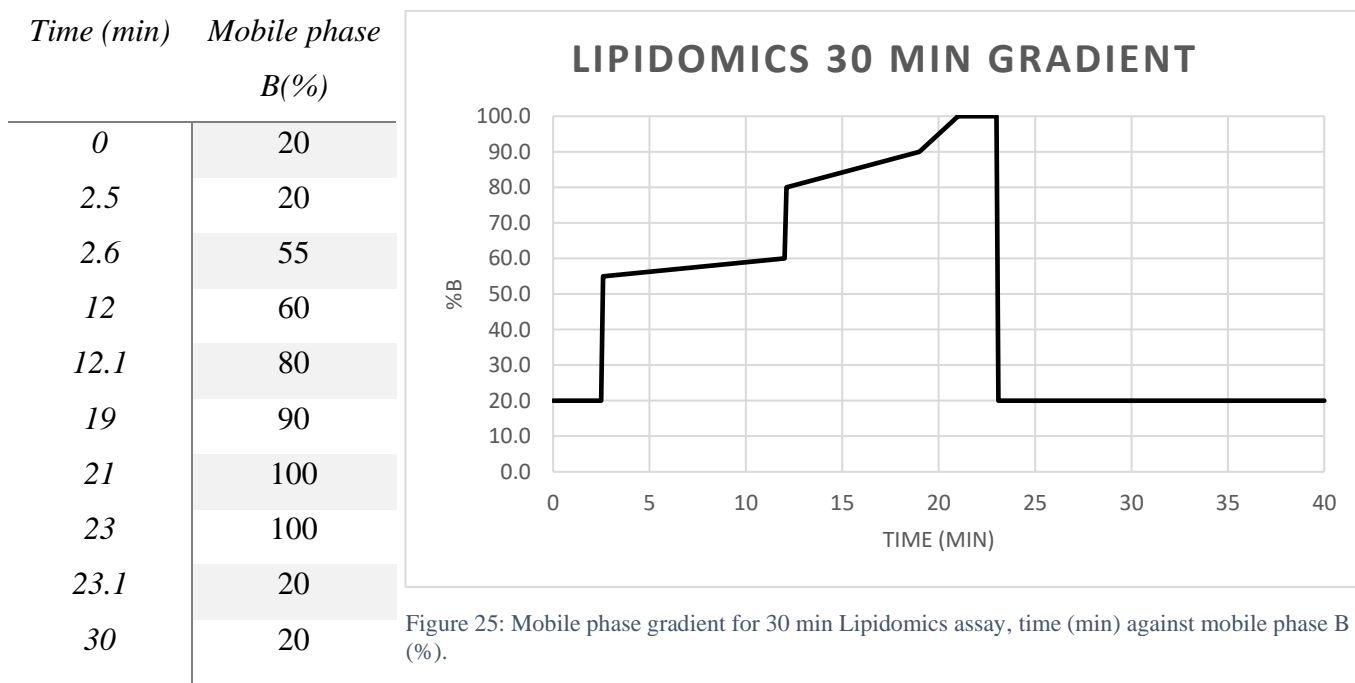
Figure 25: Mobile phase gradient for 30 min Lipidomics assay, time (min) against mobile phase B (%).

The settings for Fusion Orbitrap Tribrid MS is shown in Table 7.

Parameter	Setting
Scan Type	Full MS
	Data Dependent Acquisition (DDA), Top 5
	Scheduled MSMS
Scan Range	150-1500 *m/z*
Polarity	Positive and Negative
Resolution	Full MS: 120 000
	DDA, top 5: 30 000
	DDA, Top 10: 30 000
	Scheduled MSMS Top 5: 30 000
	Scheduled MSMS Top 10: 30 000
Micro scans	1
Lock masses	Off
Automatic gain control target value	FullMS: Standard
	DDA, Top 5: 5e5
	Scheduled MSMS Top 5: 5e5
	DDA, Top 10: 5e4
	Scheduled MSMS Top 10: 5e4
Maximum injection time (ms)	Auto
Stepped normalized collision energy	20, 40, 100
Analysis time (min)	30
Re-equilibration time (min)	10 min

The settings for the optimized ESI parameters are shown in Table 8.

Table 8: The settings for the optimized electro spray ionization source used in this project.

Parameter	Settings
Electrospray Voltage (kV)	POS: 3.6 NEG: 2.8
Sheat gas (N_2) flow rate (a.u)	40
Auxiliary gas (N_2) flow rate (a.u)	10
Sweep gas (N_2) flow rate (a.u)	2
S-Lens RF Level	60

Ion Transfer Tube Temperature (°C)	350
Vaporize temperature (°C)	400
Electrospray needle position	1.2

3.6 Computer Software

Xcalibur (version 4.3, Thermo Fisher Scientific) was used to control the LC-MS parameters and acquire data. For calibration of the Fusion Orbitrap Tribrid mass spectrometer Tune (version 3.3) was used. For calibration in positive and negative ionization MODE to be approved, total ion count (TIC) variation needed to be under 10% relative standard deviation, measured TIC over 10^6 ions/sec, base peak intensity of calibration solution over 10^5, mass accuracy under 3 ppm for external calibration and under 1 ppm for internal calibration. Calibration solution is mentioned in part 3.3.3.

Compound Discoverer (version 3.3, Thermo Fisher Scientific) was used for data processing, statistical analyzes, and in-house and online data base searches (using mzVault, mzCloud, ChemSpider, LipidBlast, and Metabolika). The data processing included signal alignment, quality control correction, and compound detection. The statistical analyzes calculated the statistical significance using ANOVA and Tukey honest significance test post-hoc. Cut-off for statistical significance was p-value under 0.05, and log 2 fold change over 1 and under -1.

LipidSearch (version 5.1.6, Thermo Fisher Scientific) was used for accurate lipid identification and signal alignment. LipidSearch contains >1.5 million lipid ions and their corresponding predicted fragmentation ions. Signal alignment aligns extracted ion chromatographic peak within a retention time window. Mass accuracy under 5 ppm for precursor ions, and under 8 ppm for product ions were used. Signal to noise ratio threshold was set to 3 and retention time correction tolerance was 0.5 minutes.

FreeStyle (version 1.8, Thermo Fisher Scientific) was used to extract ion chromatograms, observe peak areas, and observe fragmentation spectra. Extracted ions needed to have a mass accuracy <5 ppm, and peak areas above 10^4.

Excel 2016 was used for calculating coefficient of variation, standard deviations, effect size and conducting sign tests. These calculations were applied to peak areas obtained from LipidSearch.

4 Results and Discussion

4.1 Optimization of Lipidomics LC-MSMS Method
4.1.1 Lipids selected to represent the lipidome

Lipids selected to represent the lipidome came from four different lipid classes, phospholipids, sterol lipids, glycerophospholipids and sphingolipids. The 13 lipid standards, their structure, concentration, molecular formula and Log P value can be seen in Table 4, section 3.3.4. These different lipids were chosen because they represent different lipid classes, and Log P values, with varied molecular weight. The non-deuterated version of the lipids species used were expected to be found in whole blood.

4.1.2 Optimizing the ion source parameters for increased lipid class coverage

The optimization process started with testing the different ion source parameters. The optimized ion source values are found in Table 8, part 3.5. The different parameters optimized was electrospray voltage (in both positive and negative ionization mode), sheat gas flow rate, auxiliary gas flow rate, sweep gas flow-rate, S-lens RF level, capillary temperature, auxiliary gas heater temperature and electrospray needle position. The original method parameters published by Jankevics 2021 is listed in Table 9.

Table 9: ESI parameters published by Jankevics 2021: electro spray voltage, sheat gas, auxiliary gas, sweep gas, S-Lens RF level, ion transfer tube temperature, vaporization temperature, and electrospray needle position.

Parameter	Settings
Electrospray Voltage (kV)	POS: 3.2 NEG: 2.7
Sheat gas (N_2) flow rate (a.u)	48
Auxiliary gas (N_2) flow rate (a.u)	15
Sweep gas (N_2) flow rate (a.u)	0
S-Lens RF Level	60
Ion Transfer Tube Temperature (°C)	350
Vaporize temperature (°C)	400
Electrospray needle position	Not included in the article

When using the settings listed in Table 9, 12 out of the 13 lipid standards included in the Equisplash lipidomics standard mixture were detected. Criteria used for detecting compounds was mass accuracy of ±5 ppm from exact mass of the molecular ion, and peak area greater than 10^4 a.u.

The lipid not found using the initial settings was Cholest-5-en-3b-yl (9Z-octadecenoate (d7)), (ChE (18:1 (d7))). Increasing the electrospray voltage in both positive and negative ionization mode from 3.2 kV and 2.7 kV to 3.6 kV and 2.8 kV, respectively, was tested to see if it had any effect on molecular ionization and detection. This resulted in all 13 lipid species being detected. Gas flow rates (Sheat gas, auxiliary gas, and sweep gas) was optimized for increasing the signal intensity for the 13 lipid standards. S-lens RF level, capillary temperature, and auxiliary gas heater temperature was also tested, but these parameters were not altered from the original method settings. These new settings were therefore chosen to be the ion source values applied to the optimized method, and no in-source fragmentation was observed. See Figure 26 for comparison of the peaks of CE (18:1 (d7)) with the original ion source values and the optimized ion source values. With the original ion source values it was not possible to detect a chromatographic peak for the cholesteryl ester, meaning that the ionization process was not working as efficient as it did with the optimized settings.
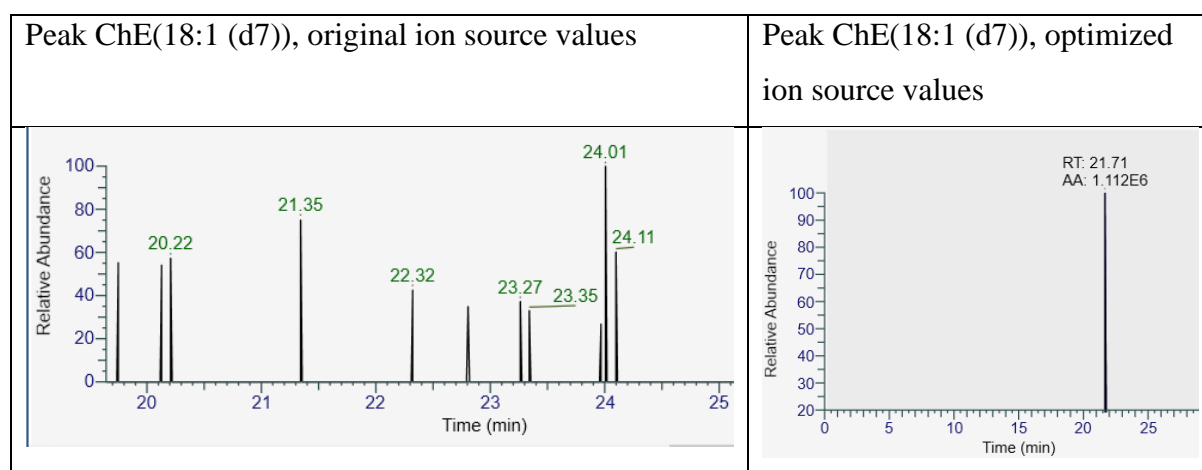
Figure 26: Extracted ion chromatograms for ChE(18:1(d7)) with the original ion source parameters to the left, and the optimized ion source parameters to the right.

In lipidomics the main goal is to detect as many lipid species as possible. Not being able to detect, one of the chosen standards of one of the lipid classes is therefore not wanted. The areas obtained with the optimized method were above the criteria which was set for detection of compounds for all the chosen lipids. A problem with ESI-MS detection of cholesteryl esters in general is that it is a neutral lipid class with few polar groups in the structure. See Figure 27 for structure of ChE(18:1 (d7)).

46
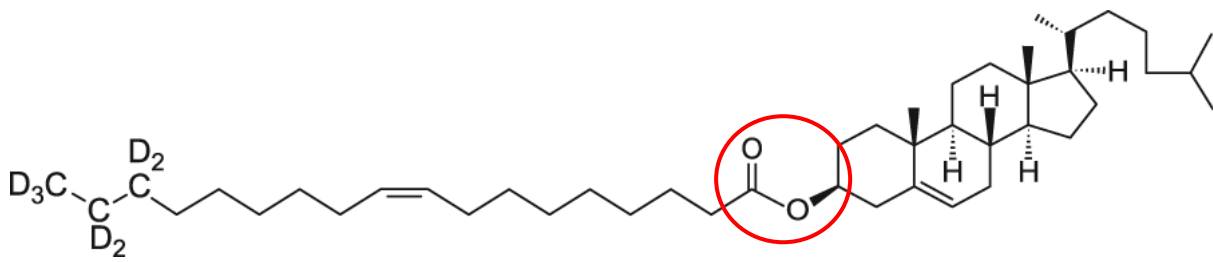
Figure 27: Molecular structure of ChE(18:1(d7)), with the ester group marked with the red circle.

See Figure 28 for extracted ion chromatograms (EIC) of the 13 lipids in the Equisplash lipidomics standard mixture. Both LPC(18:1(d7)) and LPE(18:1(d7)) create double peaks, because the acyl chain can be present in *sn1* or *sn2* position, creating 2 isomers. PG(15:0/18:1(d7)) has the biggest peak tailing. The reason for this can be the interaction between PG hydroxyl group and silanol groups on the stationary phase. PG is also not the easiest compound to ionize in positive ionization mode due to its functional glycerol group.
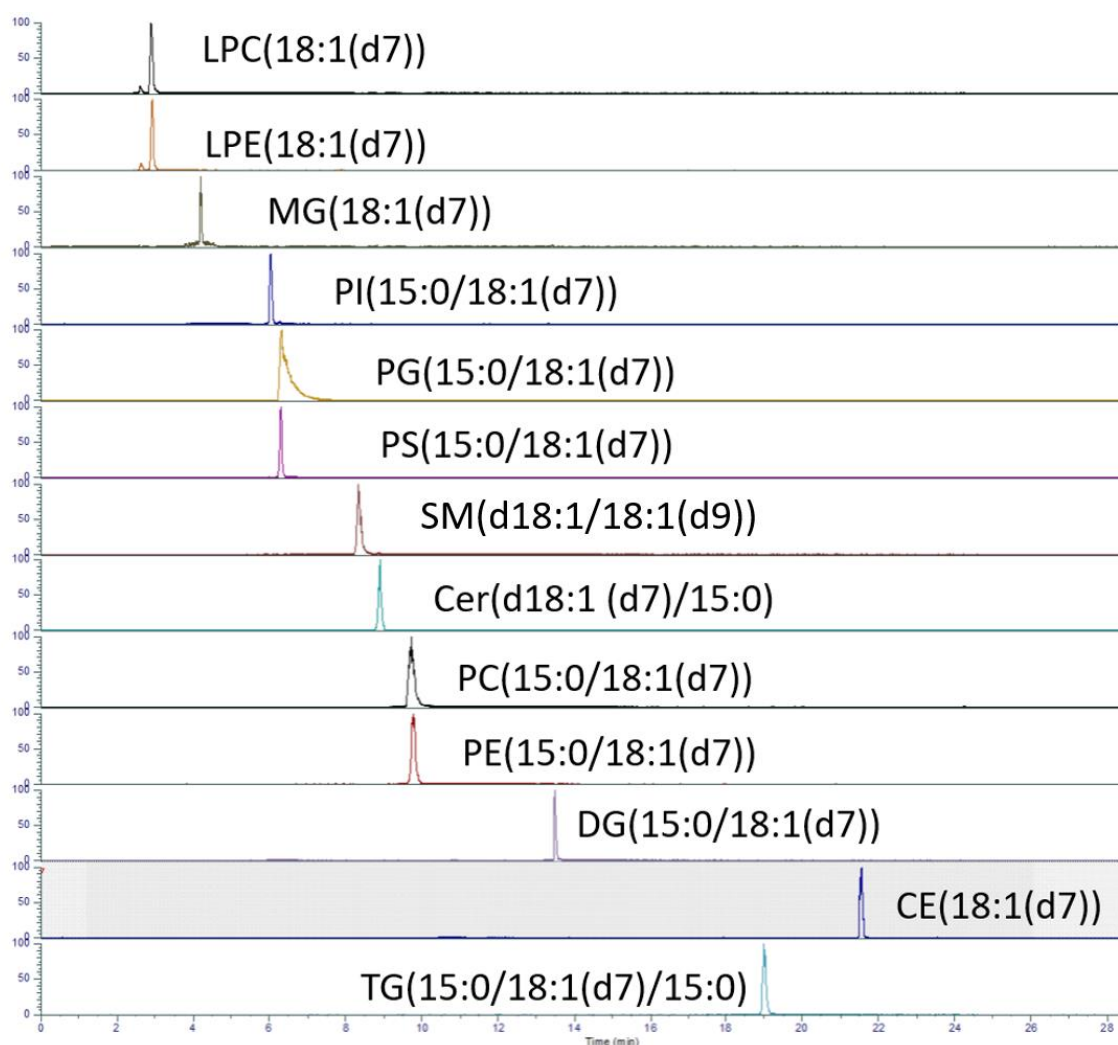
Figure 28: Extracted ion chromatograms for the lipids in Equisplash lipidomics standard mixture in positive ionization mode. X-axis shows retention time in minutes, y-axis is relative intensity.

After the ion source parameters were optimized, the position of the ESI needle was tested to obtain highest possible intensity and signal stability. The ESI ion source needle position can be altered in different directions including, the distance from the sweep cone, and the angle between the spray cone and sweep cone. The distance of the ESI needle can vary from position 1 (very close to sweep cone) to position 3, which were further away from the sweep cone. When placing the needle in position 1, the intensity of the spray displayed high variance. While in position 2 and 3 the intensities were low compared to what was obtained in position 1. Different position in-between position 1 and 2 were, i.e. 1.1, 1.2, 1.3, etc. Position 1.2 gave the highest intensity and greatest stability and was therefore chosen for the optimized method. The stability was observed as relative standard deviation of the total ion current, which was < 5%.

4.1.3 Linear correlation between chromatographic separation and sidechain composition for lipid classes.

The next step in the optimization process was to find the elution time frames for the different lipid species created by the LC gradient. This was first done with the Equisplash lipidomics standard mixture, and then with human serum to cover more lipid classes and to give a realistic matrix, for the diagnostic purpose of the method. Retention times for the lipid standards was checked against the endogenous lipids found in serum to see if the retention time was matrix dependent, the retention time for the 13 lipid standards was not matrix dependent. Equisplash lipidomics standard was injected multiple times across a time period of one month. This was done to check for instrumental variation which can cause drift in the retention time. If the analytical performance of the instrumentation and method was not stable it could have a drastic effect on the amount and quality of data collected with the data acquisition method. This is discussed later in the evaluation part. For the Equisplash lipidomics standard the retention time drift was observed for all the 13 lipids, and is presented in chapter 4.2.

Human serum from a healthy volunteer was used to establish broader range of the elution time frames, covering more lipid classes and including more lipid species inside different lipid classes. The sample preparation of serum is described in part 3.4.1. To identify the different lipid species LipidSearch v5.1 was used. LipidSearch uses fragmentation spectra to identify and grade the level of confidence in lipid identification. After the identification process of lipids in human serum the elution time frames were created. To evaluate the elution time frame further, it was compared to the data obtained by Jankevics 2021. The resulting elution time frames are shown in Figure 29.
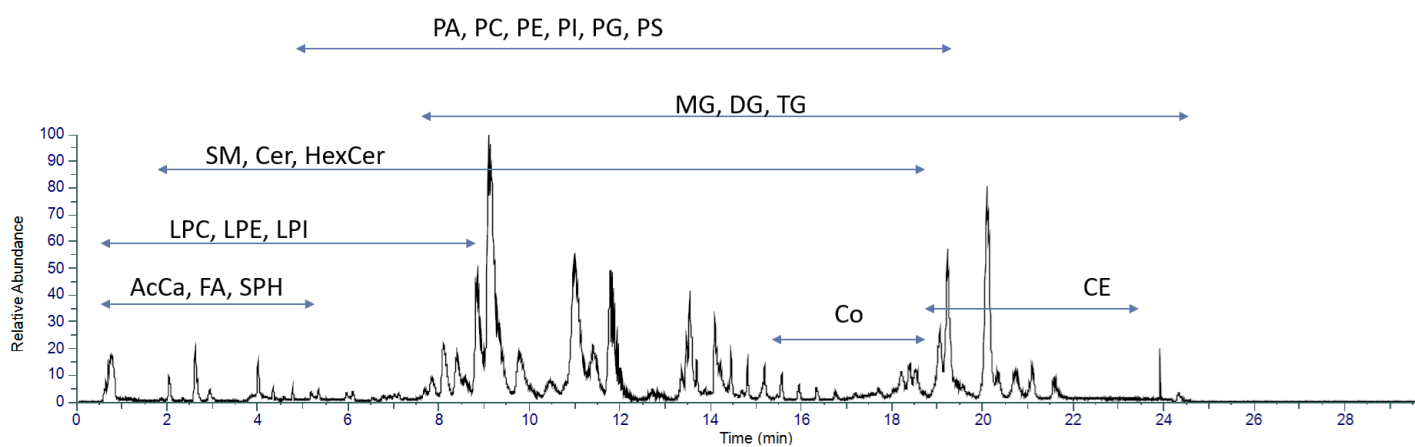
Figure 29: Elution of lipid species in Human Serum based on LipidMAPS annotations (FA=fatty acids, LPC=lysophosphocholine, LPE=lysophosphatidylethanolamine, LPI=lysosphosphatidylinositol, Cer=Ceramide, PC=phosphatidylcholine, PE=phosphatidylethanolamine, PS=phosphatidylserine, PI=phosphatidylinositol, PG=phosphatidylglycerol, SM=sphingomyelin, DG=diacylglycerol, TG=triacylglycerol, Co=Coenzyme, CE=cholestrylester, SPH= sphingosine, AcCa= acyl carnitine).

As seen in Figure 29, the chosen C30 column and gradient were able to partially separate different lipid classes chromatographically based on their chemical properties. The elution window widths can shift depending on the length of the lipids non-polar chain. The retention time and separation between different lipid classes are not only explained by the number of carbons present on the acyl chains of the lipid, but also the chemical properties. A linear relationship was observed between number of carbons in the sidechains and retention time within lipid classes. This finding confirmed that reverse phase columns can separate lipids not only based on class, but also on intra-class variations. Retention time within a lipid class correlated with the number of carbons present on the side chain of the lipid, as well as the number of double bonds and their position(s) on the non-polar side chain. The linearity was first calculated for fully saturated triacylglycerol (TG, without double bonds) detected in the human serum samples. See Figure 30 for relationship between number of carbons in the side chain of fully saturated TG and retention time observed. The retention time increased approximately by 30 seconds for each carbon added to one of the sidechains. For unsaturated lipids, the relationship between structure and retention time increases in complexity by double bond position and orientation.
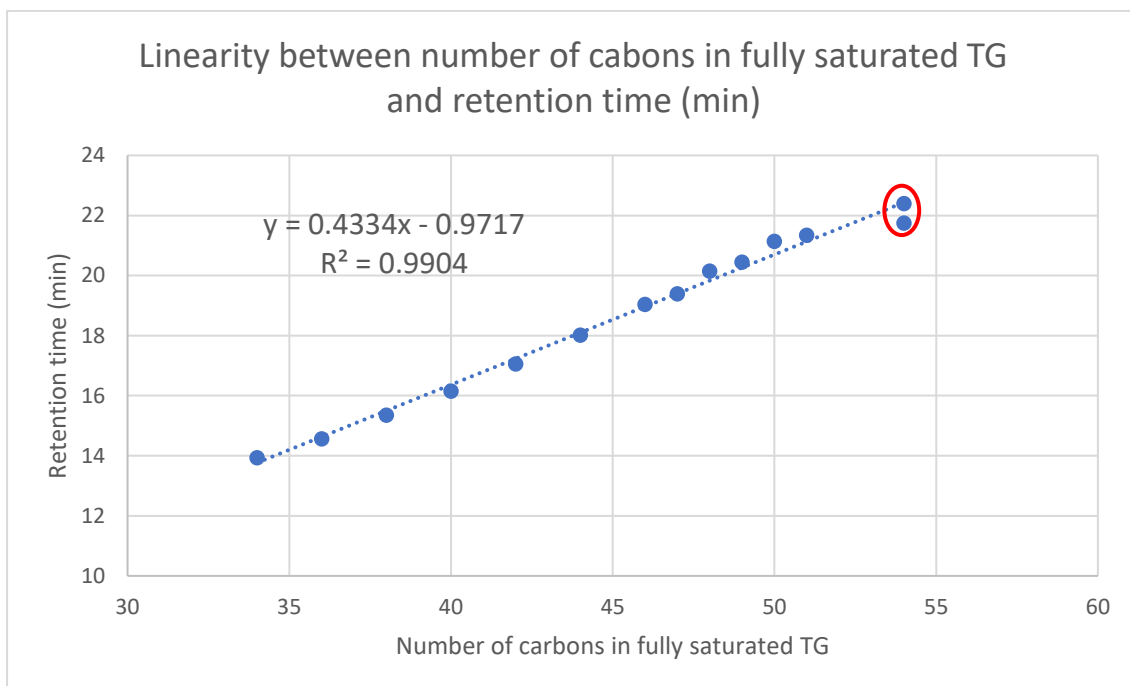
Figure 30: Retention time (min) as a function of number of carbons on the nonpolar side chains in fully saturated triacylglycerol (TG).

As an example, there are two-points (marked in red) representing fully saturated triacylglycerols with 54 carbons in Figure 30. Having the same number of carbons and double bonds (none) one should expect them to have the same retention time. However, due

50

to the structure of TG which has three carbon sidechains which can alter in chain length, these two points are two lipid isomers. This demonstrates that the method is capable of separating lipids isomers based on sidechain length in lipid classes with multiple sidechains, as seen in Table 10.

Table 10: Table showing comparison of retention time for TG(18:0/16:0/20:0) and TG(18:0/18:0/18:0).

Lipid class	Number of carbons	Amount of double bonds	Mean Retention time (min)	Sidechain composition
TG	54	0	21.75	18:0/16:0/20:0
TG	54	0	22.40	18:0/18:0/18:0

The linear correlation between retention time and number of carbons in the non-polar side chain was not only seen in TG, but also in phosphatidylcholine (PC). Thus, retention time can also be used as an indicator to identify unknown lipids, or to check if lipids have been correctly identified.
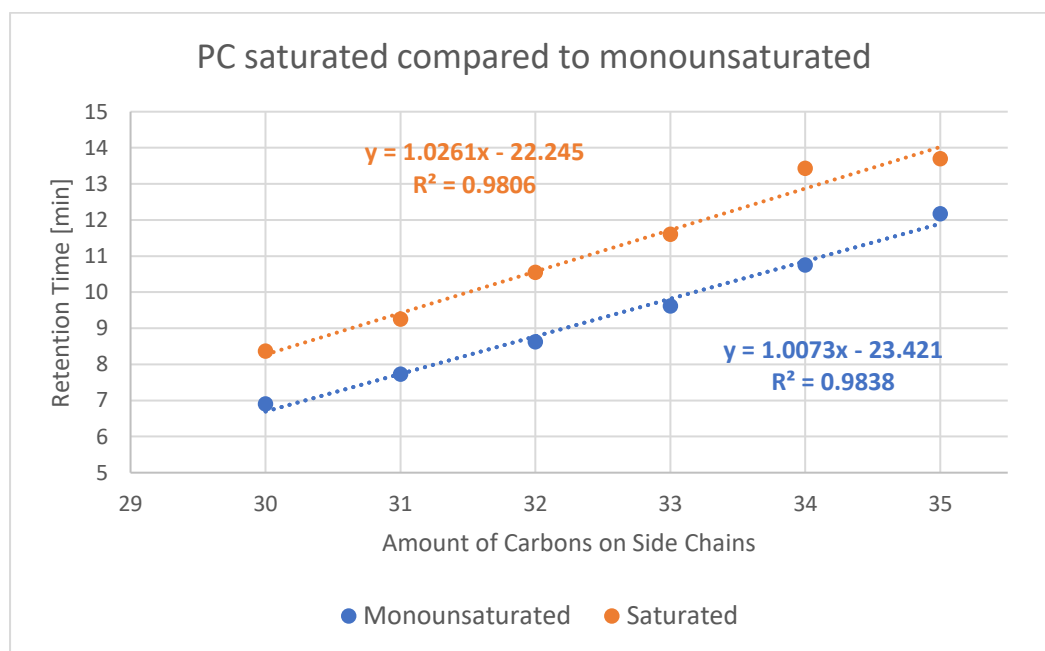
Figure 31: Correlation between retention time (min) and number of carbons for saturated and unsaturated phosphatidylcholine (PC).

As seen in the Figure 31, there is a linear relationship between retention time and the number of carbons for monounsaturated and saturated phosphatidylcholine. The addition of one double bond to a carbon side chain of a phosphatidylcholine will decrease the retention time with approximately 1.5 minutes using the presented method.

This ability to assist in the annotation of unknowns, based on retention time, is a huge advantage in lipidomics compared to metabolomics.

4.1.4 Peak Capacity for describing the performance of the gradient separation

Gradient elution refers to the gradual shift of elution strength of the mobile phase during the chromatographic separation, whiles in isocratic elution the mobile phase composition remains the same throughout the chromatographic run. Peak capacity is a term commonly used in gradient elution chromatography to describe the quality of the chromatographic separation, and is defined as the number of peaks which can be separated within a retention time window [67]. Peak capacity is analogue to the term plate number used in isocratic chromatography. The following equation 1 is used for calculating plate number.

$$Equation\ 1: \quad N = 16\left(\frac{tr}{w}\right)^2$$

When calculating plate number (N), a premise is that the retention factor k is constant. This holds true when running an isocratic elution. In gradient elution, the retention factor k is not constant, and therefore the peaks "develop" differently along the column, see equation 2.

$$Equation\ 2: \quad Pc = 1 + \frac{t_f - t_0}{w_{AVG}}$$

In this formula $t_f - t_0$ is the length of the retention window, last eluting peak minus first eluting peak, and w_{avg} is the average peak width at baseline. Mean peak capacity was calculated by doing multiple injections of human serum on the LC-MS platform during a 4-week period and was found to be 221 (range 206 to 243).

4.1.5   Comparing Scheduled MSMS and Data-Dependent Acquisition for global lipidomics

In global lipidomics the most used MSMS acquisition method is Data-Dependent Acquisition (DDA). For proteomics, however, the most popular acquisition method is Data-Independent Acquisition (DIA). The reason why DIA is more used in proteomics is because the retention time of proteins correlates to their *m/z* in the mass spectrometer [68]. In contrast, the lack of

correlation between chromatographic retention time and *m/z* in metabolomics and lipidomics makes DIA less useful, and DDA a better option. Another reason for why DIA is less useful in global lipidomics, is because it is continuously acquiring MS2 spectrums, without requiring the detection of a precursor ion in MS1. Granting no connection between precursor and product ions, which works well for proteomics, but not lipidomics.

As mentioned in the introduction chapter, DDA has its advantages and disadvantages, advantages being the ability to filter out background noise and the correlation between the parent ion and product ion(s) [55]. Whereas the disadvantage is that in the process of eliminating noise and unwanted signals, ions of interest can be eliminated as well. This can be countered by using inclusion lists and/or dynamic exclusion lists. Inclusion list will tell the MS to fragment given *m/z* values in specific retention time windows. When using dynamic exclusion lists multiple *m/z* signals can be excluded from the MS1 scan for a certain amount of time, giving place for ions with lower intensities to be sent to fragmentation [69]. By doing this, the DDA will include more *m/z* signals for detection. The use of dynamic exclusion list when preforming global lipidomics may be a problem because of the many lipid isomers that elute closely in time from the column. By excluding one specific *m/z* value in MS1, multiple isomers with the same *m/z* value will also be excluded. As the goal in global lipidomics is to identify as many lipids as possible, dynamic exclusion is not typically applied as specific lipid isomers can have significant biological relevance compared to isomers of the same lipid. Consequentially dynamic exclusion was not applied to the acquisition methods presented in this thesis.

An alternative, and better option was tested by Jankevics 2021 [70]. Jankevics et al proved by using scheduled MSMS double the amount of lipid species as regular DDA was detected. In the present work, several tests were conducted to compare the two different data collection methods (DDA vs scheduled MSMS) to evaluate the effect on lipidome coverage (see chapter 2.5.3 and 2.5.4 for description of how the different data collection methods work). The precursor isolation windows used in the scheduled MSMS acquisition were chosen according to when the different lipid classes elute from the column.

As for sample preparation of human serum for the global lipidomics analyzis, protein precipitation with isopropanol, was used, see figure in chapter 3.4.3 (Jankevics 2021). Three technical replicates from the same serum sample were made and analyzed with DDA and scheduled MSMS, with N top 5 and 10 in both positive and negative ionization mode, over a

span of one month. See Table 11 for a comparison of the four different data acquisition methods tested in positive and negative ionization mode.

Table 11: A comparison of the four different data acquisition methods tested in positive and negative ionization mode. The table shows amount of lipids found with each data acquisition method and it's respecive ionisation, identified by LipidSearch.

METHOD	POS	NEG
DDA TOP 5	472	283
SCHEDULED MSMS TOP 5	1091	291
DDA TOP 10	1191	303
SCHEDULED MSMS TOP 10	1247	1172

As seen in Table 11, the scheduled MSMS data collection method was able to identify substantially more lipids than the DDA method in both positive and negative ionization mode. The Scheduled MSMS method was able to detect more than double the amount of lipid species than the DDA when using top 5. For top 10 the Scheduled MSMS method was also able to detect a higher amount of lipid species than the DDA Top 10 method, both in positive and especially in negative ionization mode. These results correspond to the results presented by Jankevics 2021, although they only tested using N Top 5. There was a striking difference in amount of lipid species detected in negative ionization mode utilizing Scheduled MSMS Top 5 and Top 10. The reason for the difference in effect of analysis mode in positive and negative ionization mode is caused by the chemical properties different lipid classes. Triacylglycerols as an example will not be detected in negative ionization mode, and as seen in Table 12, they are one of the most abundant classes found in human serum.

Table 12: Number of different lipids found in different classes when analyzing human serum with the DDA Top 5 and Scheduled MSMS Top 5 data Acquisition methods, in positive ionization, using LipidSearch.

LIPID CLASS	DDA TOP 5 POS	SCHEDULED MSMS TOP 5 POS
DG	13	33
CHE	9	11
PC	245	387
TG	205	309
SM	72	107
LPC	46	54
ACCA	10	12
PG	13	10
PE	20	41
CER	17	26

As seen in Table 12 and Table 13, the Scheduled MSMS data acquisition can in general detect more lipid species in almost all classes, except for phosphatidylglycerol (PG) when applying positively charged ionization.

Table 13: Number of different lipids found in different classes when analyzing human serum with the DDA Top 5 and Scheduled MSMS Top 5 data Acquisition methods, in negative ionization.

LIPID CLASS	DDA TOP 5 NEG	SCHEDULED MSMS TOP 5 NEG
LPE	7	7
PS	1	1
LPI	2	3
CER	12	12
PC	108	118
PE	31	30
PI	16	15
SM	36	35
LPC	21	21

When using negative ionization mode, the two data acquisition methods gave very similar results using N Top 5. The lipid class SM, PC, TG, Cer, LPC and AcCa contains lipids used as biomarkers for different diseases [71]. Therefore, the scheduled MSMS approach will be a

better option when it comes to the use of global lipidomics in clinical diagnostics, and was chosen as the data acquisition method.

4.1.6　System Suitability Test development for quality assuring LC-MS method before analysis

For the description of system suitability test see section 2.8. For the development of a system suitability test (SST), the SST was put together to obtain certain criteria; to cover as many of the 8 main lipid classes as possible, to cover the elution time frame, and the analytes chosen should give high signal. The SST helps to ensure high quality of separation and detection, as if the acceptance criteria of the SST are met (m/z error of 5 ppm compared to the exact mass, retention time CV < 2%, and peak area CV < 20%) the lipidomics platform is considered ready for analysis of samples.

Due to the lack of lipid standards covering the saccharolipid and polyketide classes, these classes were not included in the development of the SST. For further work they should be included. The following 6 classes were evaluated: fatty acyls (FA), prenols (PR), sterols (ST), glycerophospholipids (GP), glycerolipids (GL) and sphingolipids (SL). They are also the classes observed to be most abundant in human blood (see Table 12). See Table 14 for name, abbreviation, concentration, mean retention time and adduct(s) for the lipid species chosen to represent the different main classes.

Table 14: The name, abbreviation, lipid class, retention time and concentration for the lipids used in the system suitability test.

Name→	Cortisone	Decanoate	1-(9Z-octadecenoyl (d7))-2-glycero-3-phosphocholine	N-(9Z-octadecenoyl (d9))-sphing-4-enine-1-phosphocholine	1-pentadecanoyl-2-(9Z-octadecenoyl (d7))-sn-glycerol	Coenzyme Q10
Abbreviation	ST(21:4;O5)	FA(10:0)	LPC(18:1(d7))	SM(18:1(d9))	DG(15:0/18:1 (d7))	CoQ10
Lipid class	Sterol lipid	Fatty Acyl	Glycerophospholipid	Sphingolipid	Glycerolipid	Prenol Lipid

Mean Retention time [min]	0.87	1.33	2.87	8.41	13.60	17.61
Concentration [μM]	43.4	90.8	4.75	3.38	3.08	18.1
Adduct	$[M+H]^+$ and $[M-H]^-$	$[M-H]^-$	$[M+H]^+$ and $[M-HCOO]^-$	$[M+H]^+$ and $[M-HCOO]^-$	$[M+Na]^+$ and $[M-H]^-$	$[M+H]^+$ and $[M-H]^-$

As seen in Table 14 FA(10:0) was only detected using negative ionization mode. This is because it is difficult to add a proton to a carboxylic group which inherently wants to donate away a proton. When the carboxylic group releases the proton, it gets a negative charge $[O^-]$ and the corresponding adduct is therefore $[M-H]^-$. In general, lipidomics works best in positive ionization mode, but as seen for the fatty acyls, some lipid classes can only be detected using negative ionization [72].Lipids are natural substances found in all living organisms and involved in many biological functions. Imbalances in the lipid metabolism are linked to various diseases such as obesity, diabetes, or cardiovascular disease. Lipids comprise thousands of chemically distinct species making them a challenge to analyze because of their great structural diversity [69]. This was done to quality assure the analysis in both positive and negative ionization mode before analyzing samples.

The first lipid eluted at 0.86 minutes and the one eluted after 17.60 minutes, covering 70% of the gradient (total 24 min). See Figure 32 for extracted ion chromatogram (EIC) of the lipidomics SST in positive ionization mode. As can be seen in Figure 29, page 49, the lipids in human serum elute from the column between 0-23 min, due to the re-equilibration starting at 23 minutes. Hence the SST chromatographic separation timeframe coverage this was considered satisfactory.
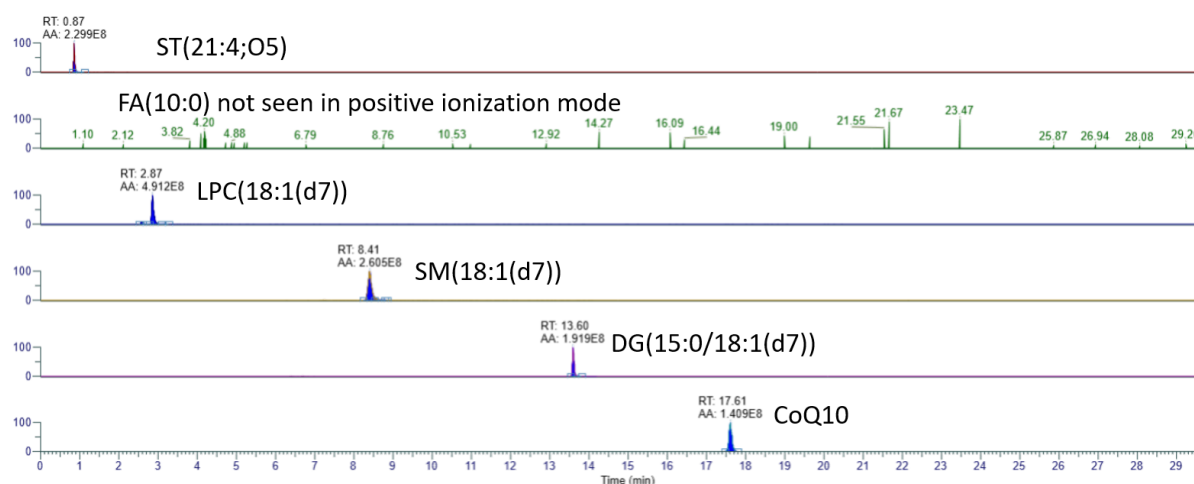
Figure 32: Extracted ion chromatograms (EIC) of lipid standards included in the lipidomics system suitability test (SST), with retention time [min] and peak area [a.u]. Mass accuracy ± 5 ppm.

Summary part 4.1: By optimizing ion source parameters, all the selected lipids were detected, compared to the initial method which detected 12 out of 13 lipids. The LC method was able to separate lipids based on class, and sidechain composition, and a linear relationship was observed between number of carbons and same amount of double bonds for retention time in triacylglycerols and phosphatidylcholines. The mean peak capacity was calculated to be 221. Scheduled MSMS proved to detect more lipid species than Data-Dependent Acquisition, in both positive and negative ionization mode using N top 5 and 10, and was therefore chosen as the acquisition method to be used further in this project. A system suitability test was developed for verifying the LC-MS lipidomics method performance before analysis of samples.

4.2   Evaluation of the Lipidomics LC-MSMS Method

As the optimization of the global lipidomics LC-MSMS method was satisfactory, the optimized method needed to be evaluated. To assure high quality data it is necessary to evaluate lipidomic methods – evaluation should include the following processes [66]:

- Sample carry over.
- Repeatability within batch and reproducibility between batches.
- Repeatability and accuracy for lipid species should be evaluated analyzing the samples subjected to analysis; either pooled samples or selected individual samples at different concentration levels.

Repeatability describes to what extent the same results can be obtained in repeated analyzes using the exact same conditions. Repeatability is often presented as either relative standard deviation in percent (RSD%) or coefficient of variance in percent (CV%). Both describe the dispersion in a data set, and are calculated using equation 3, σ is standard deviation and μ is the mean.

$$Equation\ 3:\quad CV(\%) = 100 * \frac{\sigma}{\mu}$$

4.2.1 Equisplash Lipidomics standard mixture showed great repeatability and reproducibility

Multiple injections of the Equispash lipidomics standard mixture over a period of 4 weeks was used to evaluate the reproducibility and repeatability, testing intra-batch and in-between batch variations for retention time. For testing reproducibility n equals 4 with 3 injections each time. As seen in Table 15 the coefficient of variance (CV) was < 0.7% for all lipid species testing the reproducibility of the retention time.

Table 15: The reproducibility retention time in minutes and coefficient of variance (CV) in percentage for the different lipids chosen to represent the lipidome.

NAME	RETENTION TIME [MIN]	CV [%] REPRODUCIBILITY
LPC (18:1 (D7))	2.92	0.3
LPE (18:1 (D7))	2.93	0.6
MG (18:1 (D7))	4.20	0.2
PI (15:0/18:1 (D7))	6.02	0.2
PG (15:0/18:1 (D7))	6.27	0.1
PS (15:0/18:1 (D7))	6.40	0.2
SM (D18:1/18:1 (D9))	8.35	0.2
CER (D18:1 (D7)/15:0)	8.84	0.3
PC (15:0/18:1 (D7))	9.71	0.3

PE (15:0/18:1 (D7))	9.71	0.7
DG (15:0/18:1 (D7))	13.43	0.2
TG (15:0/18:1 (D7)/15:0)	18.15	0.1
CE (18:1 (D7))	21.45	0.3

This was a satisfactory indicator of the reproducibility between batches for the standard solution of lipids. But as mentioned above in chapter 4.2, as a criterion, the reproducibility should ideally be determined using real biological samples with relevant biological matrixes instead of standard mixtures.

4.2.2 Human Serum to evaluate the reproducibility and repeatability of the Lipidomics method.

Three biological replicates from one serum sample from a healthy volunteer were made and analyzed over a span of 4 weeks. For testing reproducibility n equals 4 with 3 injections each time. The sample preparation used is described in chapter 3.4.3. Selected lipid species in the serum samples were chosen as markers to compare retention times within and between batches.

The lipid species chosen to evaluate the reproducibility in human serum were from the triacylglycerol and phosphatidylcholine classes. Triacylglycerol and phosphatidylcholine were chosen since they were some of the most abundant lipid species detected in human serum (see Table 12). The different triacylglycerols and phosphatidylcholines, their sidechain composition, calculated CV in percentages for reproducibility can be found in Table 16. Retention times can be found in appendix part 7.2. As seen in the table below, highest CV is 1 %, demonstrating very high reproducibility considering this being biological samples and not analytical standards. Biological matrixes are inherently complex and prone to cause ion suppression and retention time shifts [56].

Table 16: List of the different triacylglycerols (TG) and phosphatidylcholines (PC), their sidechain composition, and CV in percentages when measured in human serum samples over a 4-week time period.

TG	CV (%) RT	PC	CV (%) RT

4:0/16:0/16:0	0.4	**28:0**	0.3
6:0/16:0/16:0	1.0	**30:0**	0.3
10:0/14:0/16:0	0.6	**31:0**	0.3
14:0/12:0/16:0	0.7	**32:0**	0.3
14:0/14:0/16:0	0.8	**33:0**	0.2
14:0/16:0/16:0	0.8	**34:0**	0.5
15:0/16:0/16:0	0.8	**30:1**	0.2
14:0/16:0/18:0	0.8	**32:1**	0.4
15:0/16:0/18:0	0.8	**33:1**	0.4
16:0/16:0/18:0	0.7	**34:1**	0.2
16:0/17:0/18:0	0.7	**35:1**	0.6
16:0/18:0/18:0	0.6	**36:1**	0.4
16:0/18:0/20:0	0.7	**37:1**	0.2
		38:1	0.3

For testing the repeatability, one serum sample from a healthy volunteer was injected 10 times in a row. The sample preparation used is described in chapter 3.4.3. From the 10 injection certain lipid species were chosen to evaluate the repeatability, the species chosen was triacylglycerol (TG), phosphatidylcholine (PC) and lyso-phosphatidylcholine (LPC). For calculated CV in percentage see Table 17. Retention times can be found in appendix part 7.2. As seen in Table 17 highest CV is 0.8%, demonstrating high repeatability of retention times for the selected lipid species within one batch.

Table 17: Lipid species chosen to evaluate retention time repeatability as CV in percentage. The selected lipid species was lyso-phosphatidylcholine (LPC), phosphateidylcholine (PC) and triacylglycerol (TG). N equal 10 injections.

LIPID SPECIES	CV(%)
LPC(16:0)	0.8
LPC(18:0)	0.3
PC(30:0)	0.7

PC(32:0)	0.6
PC(33:0)	0.4
PC(34:0)	0.4
TG(46:0)	0.7
TG(48:0)	0.3
TG(50:0)	0.4
TG(52:0)	0.6

Sample carry over was tested by injecting the Equisplash lipidomics mixture before serum samples. None of the deuterated lipid species was detected in any of the human serum samples indicating no carry over. Criteria for detection was, mass accuracy of ±5 ppm from exact mass of the molecular ion, and peak area higher than 10^4 a.u.

To summarize part 4.2: The method was tested according to the Lipidomics Standard Initiative (LSI). Repeatability and reproducibility of retention time between batches and in-between batches was satisfactory for both lipid standards and human serum. No sample carry over was observed. For the future linear dynamic range, limit of detection and stability of the samples should be tested.

The developed lipidomics method is planned for implementation in a clinical setting, thus, evaluation of the methods ability in capturing changes in the lipidome in biological material taken during processes expecting to cause metabolic changes was the next goal. High-intensity training was chosen as a suited intervention.

4.3 High-intensity training as a cause for normal variations in the Lipidome

Hard physical activity like strength or endurance exercise cause profound metabolic changes both during and after the ordeal. The lipidome is initially affected in two different ways; the energy demanding pathways and the catabolic pathways [10]. In the aftermath, regenerative and anabolic processes take over. Whereas the catabolic pathways such as fatty acid oxidation and glycolysis are favoured over anabolic pathways, like fatty acid synthesis. These changes in the lipidome induced by exercise can be observed in different bio fluids.

As mentioned previously, one of the main roles of lipids is energy storage. During physical activity, as well as during resting metabolism, the body uses energy. Lipids are mobilized to assist carbohydrates in creating energy for the body to use, resulting in more lipid circulating in the blood stream. Fatty acids, triglycerides, and acylcarnitines are some of the most known lipids to be utilized during the need of energy [73]. This is because triacylglycerols are broken down to fatty acids, which are transported into the mitochondria bound to carnitine as acylcarnitines . During exercise the body can mobilize phospholipids from the cell membranes for energy production. Since lipids play such an important role in energy production and cell membrane structure, the lipidome will be immediately affected by exercising. Exercising can also affect the production of lipid signalling molecules, such as sphingolipids. These lipid mediators play a role in inflammation, immune response, and muscle adaptation to exercise.

In short, the lipidome will be affected by high intensity exercise. The lipid profile will be altered in different ways, changing the distribution of certain lipid species as discussed above. It is important to note that the specific effects on the lipidome may vary depending on factors such type, intensity and duration of exercise, individual fitness levels, dietary factors, and other physiological variables. Testing the lipidomics platform to see if changes to the lipidome can be observed on lipid species level is in summary an adequate way of assessing the performance of the method, and if the method is able to observe normal variations induced by exercise.

For this project nine volunteers participated in a high intensity exercise session. Four of the participants were selected as the control group, and five participants conducted the exercise. All nine individuals had the same controlled diet, and took DBS samples at the same time

over a three-day period. The exercise consisted of a 9 min 40 sec high intensity training (HIT) program; 30 seconds intensive exercise, 20 seconds break, with four different exercises in cycle, repeated three times, for a total of 9 minutes and 40 seconds. In total 13 dried blood spot (DBS) cards were collected from each participant from the exercise group, and 9 from each participant in the control group. See Figure 33 for a timeline of when DBS cards were collected.
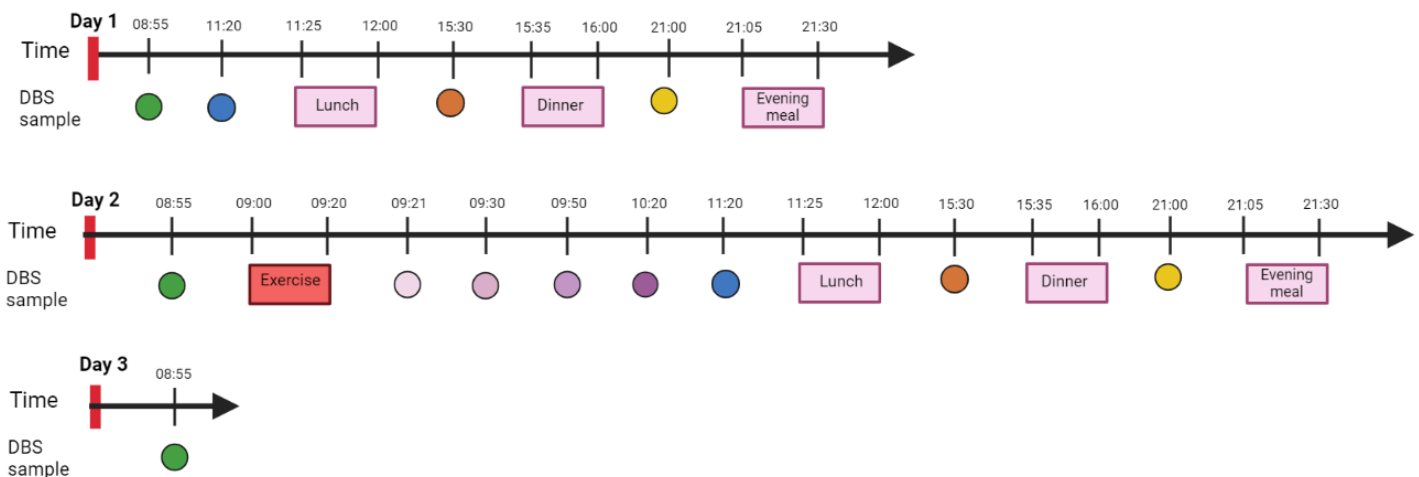
Figure 33: Timeline for when dried blood spot samples were taken on day 1, 2, 3, relative to meals and exercise. The same colours represent the same time points of the day. Green samples were taken after overnight fasting, blue and purple samples were still fasting, orange and yellow were not fasting, but with equal diet for all participants. In total 9 DBS samples were taken while fasting for the exercise group, the control group had 5 DBS samples taken while fasting. Figure created by Maria Nguyen and Nurtene Dernjani.

On day 1, four DBS samples was collected. The first morning sample was taken after fasting for 12 hours. This applied to all the morning samples. The fasting continued to lunch when a new sample was collected before the participant ate their meal. Then a sample was collected before dinner and before evening meal. The sampling scheduled changed on day 2, with more samples collected right after and at certain time points after the HIT workout was carried out. The control group did not take these samples. More details about the controlled diet, sampling requirements and additional information can be found in appendix section 7.3. The samples were prepared according to the sample preparation protocol in part 3.4.2. Hematocrit was not determined for the DBS samples included in this study.

4.3.1 Detection of exercise-induced changes in the Lipidome

Compound Discoverer (version 3.3) was used to perform principal component analysis (PCA) for visualizing the differences between the lipidome of the different DBS samples. In Figure 34, the PCA plot obtained for samples analyzed in positive ionization mode is shown.

One point in the PCA plot represents one sample, including all identified and unidentified lipid found in that one sample. The bigger the distance between two samples in a PCA plot the bigger the variation in lipid composition for those two samples. Principal component (PC) is a vector where the biggest variation between all samples were observed. The biggest PC, PC 1 (representing 12.0% of the variation in positive ionization and 23.2 % in negative ionization) is presented on the x-axis, and PC 2 (7.8% in positive ionization and 8.8% in negative variation) which is the PC where the second most variation is observed, is presented along the y-axis. See Figure 26 for PCA-plot of all samples analyzed in positive ionization mode.
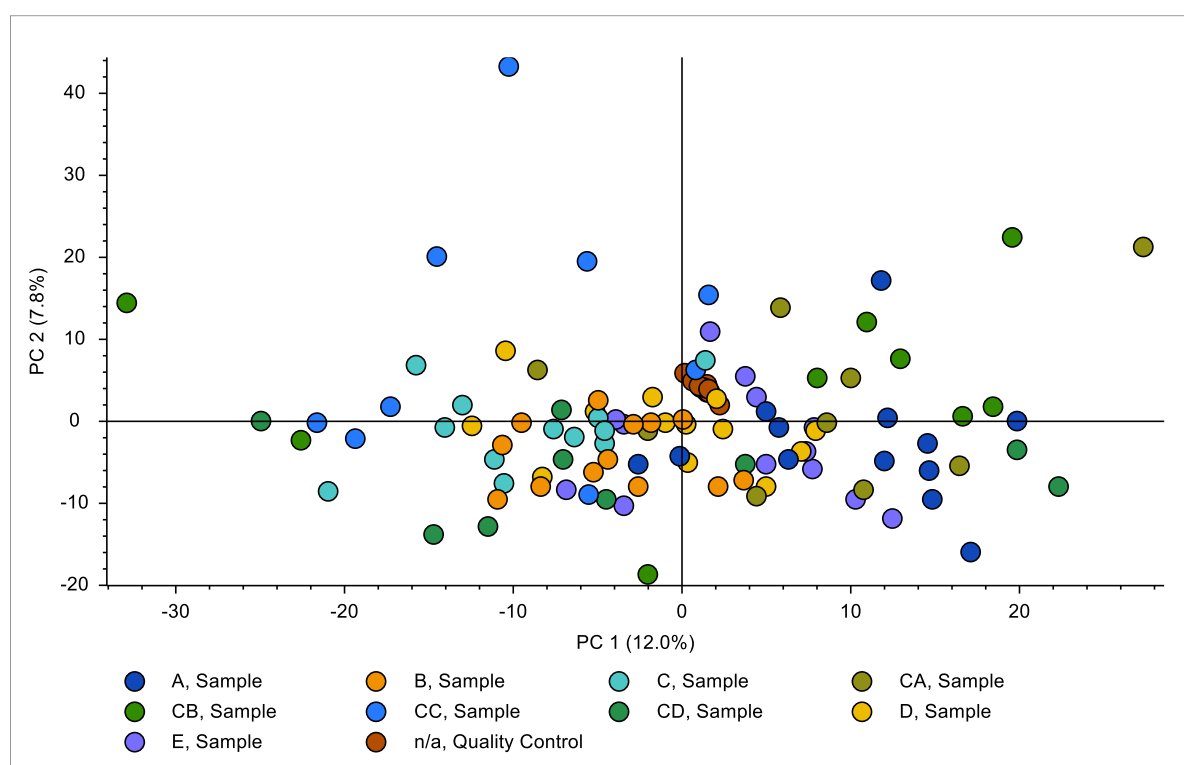
Figure 34: PCA plot of all DBS samples obtained from the participants analyzed in positive ionization mode. A, B, C, D, E, are the participants which conducted the high intensity exercise and CA, CB, CC and CD are the control group. PQC marked as Quality Control.

As seen in the PCA plot above for positive ionization, there was no clear clustering of the participants lipidomes, but they are relatively close to each other in the PCA plot. In general, for lipidomics and metabolomics studies, the biggest differences are found between participants due to biological variations. However, in this PCA plot the different lipidomes overlaps. The pooled quality controls (PQC) are nicely clustered together. The PQC is the same sample injected multiple times throughout the sample sequence, so the different PQC injections should clustered together. This illustrates that there is little instrumental drift throughout the batch. Some samples overlapped from different participants, the overlapping

samples were not taken at the same time points. The overall impression was that the distribution in the PCA plot displays random variation and no obvious systematic trends or clustering except for some clustering of samples from each individual. This could point towards a string individual lipidome signature. For the PCA plot of the sample analyzed in negative ionization mode see Figure 35.
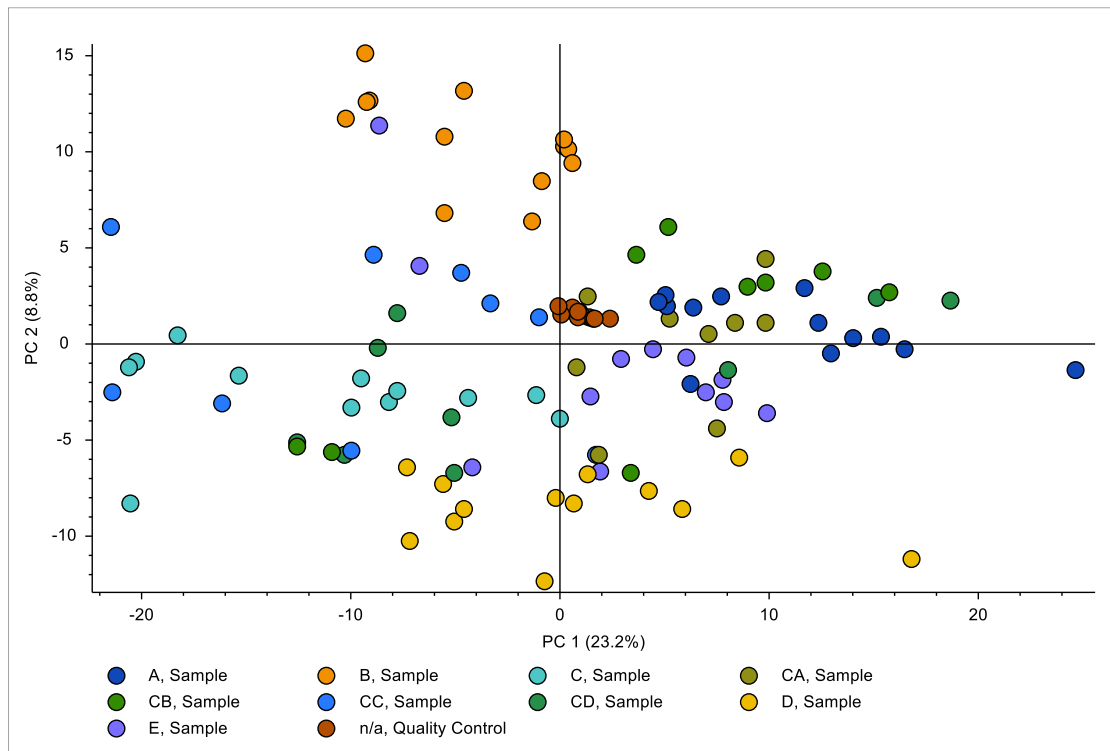
Figure 35: PCA plot of all DBS samples obtained from the participants analyzed in negative ionization mode. A, B, C, D, E were the ones conducting the high intensity exercise, CA, CB, CC and CD were the control group. PQCs marked as Quality Control.

Compared with Figure 34 (positive ionization mode), this PCA plot shows somewhat more clustering of the different participant lipidomes. The grouping of the participants was clearer in negative ionization mode, due to fewer lipids being detected leading to less variation inflicting the principal component analysis. However, there was no clear clustering of the participants who conducted the exercise and the control group. Taken together, each individual was more like him/herself even though a lot of precautions were taken to reduce variation caused by diet, and sampling time. However, the genetic differences and differences related to gender, age etc still remain. It was expected to find that the samples taken after exercise could have displayed global changes that were readily visible in the PCA-plot compared to the samples taken right before exercise. This was, however, not the case.

To visualize the differences in relative lipid abundance between samples taken before exercising and right after exercising, volcano plots were used. In a volcano plot the x-axis

66

represents the difference in relative abundance between the two time points as fold change (log2 fold change). The input data are the m/z values from the mass spectrometer (level 5 of confidence in identification, called "features"). The y-axis shows the negative logarithm of the p-value, meaning that the more significant (lower p-value) data points will be found in the top of the plot. Features with small differences in abundance will therefore lay close to the intersection of the x- and y-axis, in the lower middle of the plot. Features located in areas marked with green and red have a big difference in relative abundance and will be highly significant, with log fold change higher than 1 or lower than -1 and a p-value lower than 0.05. Figure 36 shows volcano plot for comparing samples taken immediately before and after exercise. Data points featured in the red area are higher before exercising and data points present in the green area are higher after exercising.
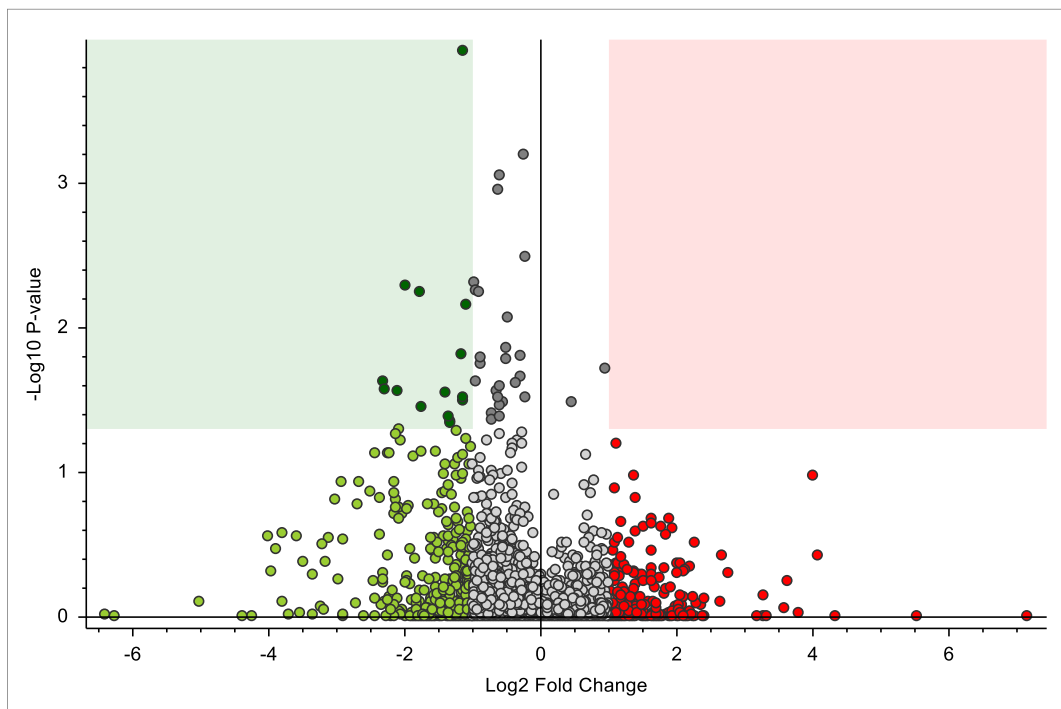
Figure 36: Volcano plot comparing samples taken right before and 1 minute after high intensity exercise analyzed with positive ionization mode. The X-axis shows the log 2 fold change, and the y-axis shows the -log(p-value). Data points featured in the red area are higher before exercising and data points present in green area are higher after exercising.

As seen in Figure 36 multiple features were found to be significantly higher immediately after exercise compared to before exercising. Features found in the green area were diacylglycerols, triacylglycerols, ceramides, and sphingolipids, which were lipid species significantly elevated after exercise compared to before exercising. The significant altered features will be discussed later.

4.3.2 Lipids associated with energy production and consumption influenced by high intensity training

Lipids associated with energy production and consumption were found to be significantly affected by exercise. The lipids which were found to be affected were triacylglycerol, diacylglycerol, fatty acids, and acyl carnitines. During exercise (and fasting due to low sugar levels), triacylglycerol will be mobilized from fatty tissues and reduced to diacylglycerol to release fatty acids into circulation [73,74]. Diacylglycerol can be further reduced to monoacylglycerol to release even more fatty acids into circulation. This process is known as lipolysis, and is caused by a group of enzymes called lipases. The circulating fatty acids will then be activated by conversion to acyl-CoA. Acyl-CoA is then converted to acyl carnitines by the enzyme CTP1. The acyl carnitines can then be transferred into the matrix of the mitochondria with the help of translocase protein. Acyl carnitines are then cleaved to create carnitine and acyl CoA by the enzyme CTP2. Acyl-CoA will then undergo beta-oxidation to ultimately create acetyl-CoA, which will enter in the citric acid cycle[75]. See Figure 37, for the breakdown of TG to MG and the release of FA.

Figure 37: Illustrative representation of lipolysis. Triacylglycerols are hydrolysed to release fatty acids and create diacylglycerols. Diacylglycerols are further metabolised to create fatty acids and monoacylglycerols, which can be further metabolised to glycerol and fatty acids [74].

During exercise, as well as fasting, TGs within adipocytes (fat cells) and muscle cells are hydrolysed to DGs and MGs liberating free fatty acids to be consumed within the cell or transferred to blood for transport to muscle cells and other cells in need of energy [74]. To some extent, TGs are also liberated to blood for transport to tissues in need of energy. The challenge is how to analyze changes in blood to monitor intracellular processes of muscle cells, adipocytes and other cells. Therefore, as a speculation, when exercising TG, DG, and MG will increase as a result lipolysis. Acylcarnitines (AcCa), on the other hand will decrease, since they will be used for energy production and are therefore consumed. One way of observing lipolysis is by observing the change in free fatty acids for example, FA(16:0) and

FA(18:0) levels over time [76]. Increasing amounts of the two fatty acids show ongoing lipolysis. See Figure 38 for FA(16:0) and FA(18:0) levels were influenced by exercise.
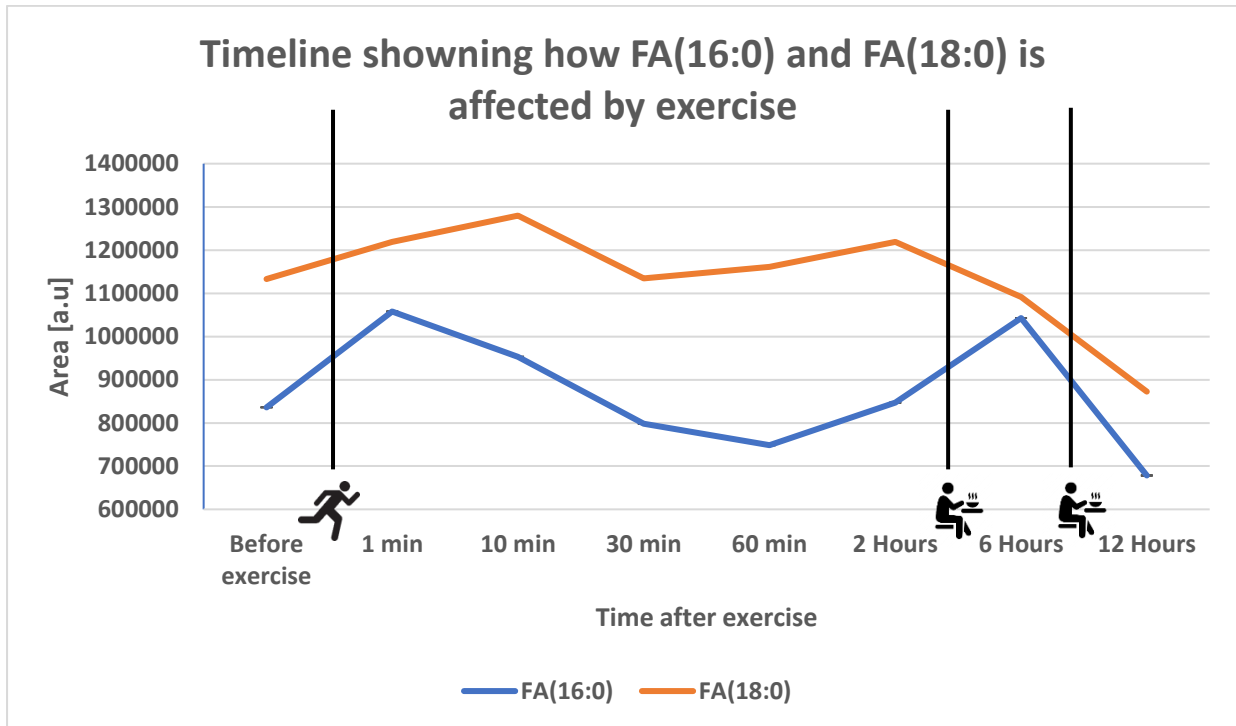
Figure 38: Timeline showing how the extracted peak area of FA(16:0) and FA(18:0) were affected as a result of high intensity exercise and having two meals. Standard deviation, and measured area for each sample is shown in part 7.3 in appendix. Level 1 of confidence.

As seen in Figure 38, both FA(16:0) and FA(18:0) peak areas were higher right after exercise compared to before exercising, meaning that lipolysis was ongoing during the exercise, liberating FA into circulation for transport to muscle cells and other tissues in need of energy. 30 minutes after exercise the levels of FA(16:0) and FA(18:0) have decreased showing that lipolysis has slowed down compared to immediately after exercising. Now the excess fatty acids were converted back into storable lipids, such as triacylglycerols [77]. This is to avoid lipotoxicity, lipotoxicity is a metabolic syndrome caused by increased levels of circulating fatty acids, causing failure in storing the excess fatty acids. FA(16:0) decreases faster than FA(18:0), but both fatty acids used 30 minutes to reach baseline level after exercising. Only FA(16:0) seemed to be influenced by the meal consumed between the 2 and 6-hour sample. FA(16:0), also known as palmitic acid, is found in foods containing unsaturated fats, such as butter, but it is also found in eggs and avocado, which explains the increased amount after lunch, see diet plan in appendix section 7.3, with a lunch containing eggs and avocado.

To show increased lipid mobilization and the consumption of activated FA(16:0), FA(18:0), DG(18:1/18:1), DG(16:0/18:1), AcCa(18:1), and AcCa(16:0), areas were plotted as a graph

over time. See Figure 39 for how acylcarnitines, diacylglycerols areas are affected as a result of exercise.
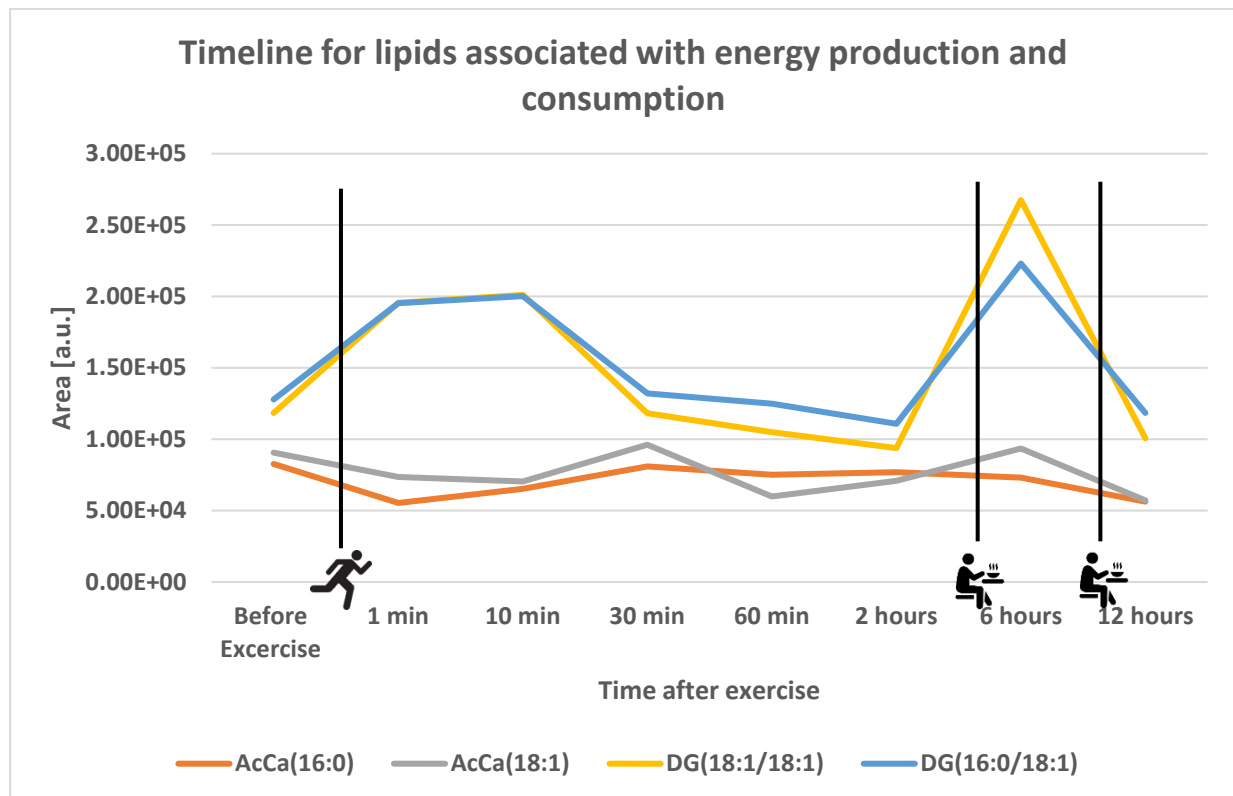
Figure 39: Timeline for how AcCa(16:0), AcCa(18:0), DG(16:0/18:1), and DG(18:1/18:1) levels were affected as a result of high intensity exercise. Standard deviations each time point, and areas found in each sample is shown in table X in appendix. Level 2 of confidence.

As seen in Figure 39, immediately after exercise DG(18:1/18:1), and DG(16:0/18:1) increased significantly ($p<0.05$), while AcCa(18:1) and AcCa(16:0) decreased significantly ($p<0.05$). For calculated standard deviations at each time point see appendix part 7.3. Since acyl carnitines are the fully activated fatty acids they will be consumed to produce energy, and are therefore reduced [75,78]. Acyl carnitines can be used as markers for complete fatty acid oxidation. Depleted levels of acyl carnitines show the consumption of activated fatty acids to produce energy, and that the consumption is faster than the production. Increased levels of acyl carnitine in plasma, on the other hand, are known markers for cardiovascular diseases [7].

The two DG species increased significantly ($p<0.05$) right after exercise proving further that lipolysis were ongoing during and right after exercise. The corresponding triacylglycerol TG(16:0/18:1/18:1), hydrolysed to create DG(18:1/18:1) and DG(16:0/18:1), depending if the lipase responsible for the hydrolysis of TG(16:0/18:1/18:1) is non *sn* specific, or *sn* 1,3 specific. TG(16:0/18:1/18:1) did not increase significantly, and stayed more or less at the

70

same level immediately after exercising, see Figure 40. This complies with the fact that TG get hydrolysed to DG and MG inside the cells instead of being secreted to the blood like FA [79].TG and DG levels increased significantly from the 2-hour mark to the 6-hour mark, as expected following a meal containing lipids. Other DG species which were found to increase significantly right after exercise were DG(17:1/17:1), DG(18:0/18:0), and DG(18:0/16:0).
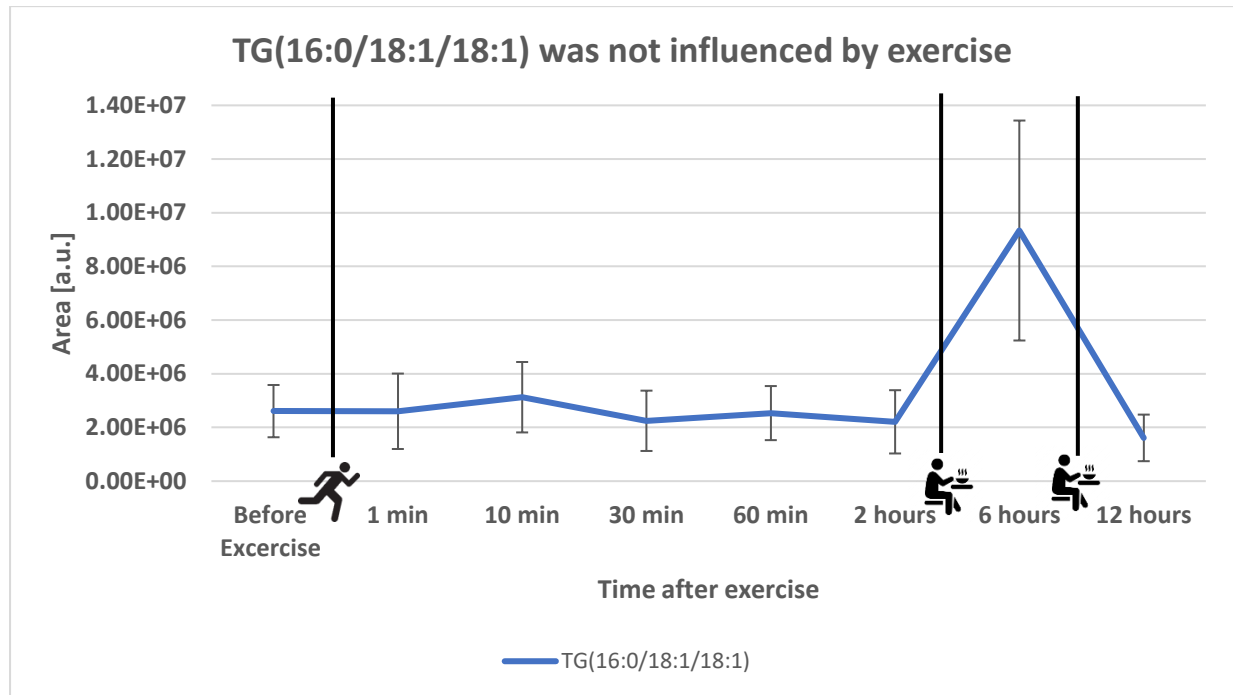
Figure 40: Timeline of how TG(16:0/18:1/18:1) was influenced by high intensity exercise. Including standard deviations in a.u. Level 2 of confidence.

4.3.3 Lipids associated with inflammation affected by high intensity training

Multiple lipid species in the phospholipid and sphingolipid classes were found to be affected by exercise. Among these phosphatidylcholine (PC), ceramide (Cer), and sphingomyelin (SM) were most affected. SM and Cer are known markers for inflammation [80,81]. An induced inflammation response can be expected because exercising can cause muscle damage [82]. The degree of inflammation is dependent on intensity and duration of exercise, individual fitness levels, dietary factors, and other physiological variables. Inflammation is a normal and beneficial response to training, and necessary for e.g. muscular hypertrophy and increased muscular strength [82]. See Figure 41 for SM(d18:1/16:0) alterations as a results of high intensity exercise session.
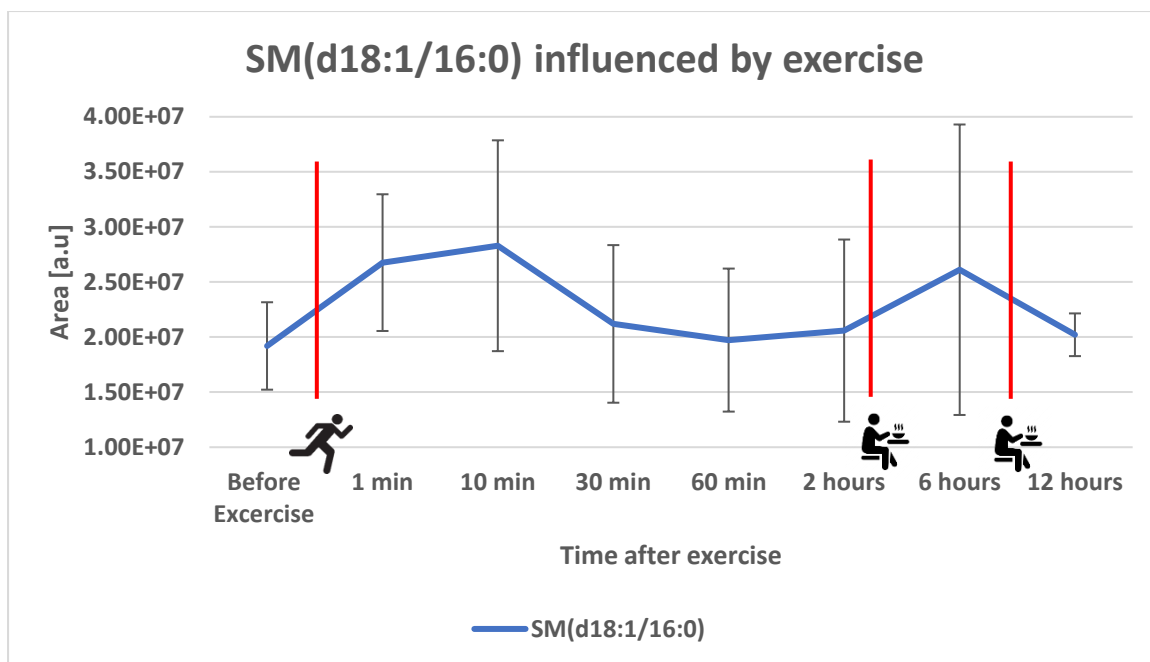
Figure 41: Timeline of how SM(d18:1/16:0) areas are influenced as a result of high intensity exercise. Average peak area for the 5 participants conducting the high intensity exercise. Including standard deviations in a.u for each timepoint. Level 2 of confidence.

As seen in Figure 41, the peak areas for SM(d18:1/16:0) increases significantly ($p<0.05$) right after exercise, suggesting that inflammation was triggered as a response to the ongoing exercise. The SM(d18:1/16:0) peak area reached baseline (starting point before exercising) 1 hour after conducting the exercise. Diet-induced change was also observed for SM(d18:1/16:0), seen between the 2-hour and 6-hour mark after exercising, after a meal. SM(d18:1/16:0) is expected to be found in chicken [83], the increase in average peak area can be explained by the eggs consumed during the lunch
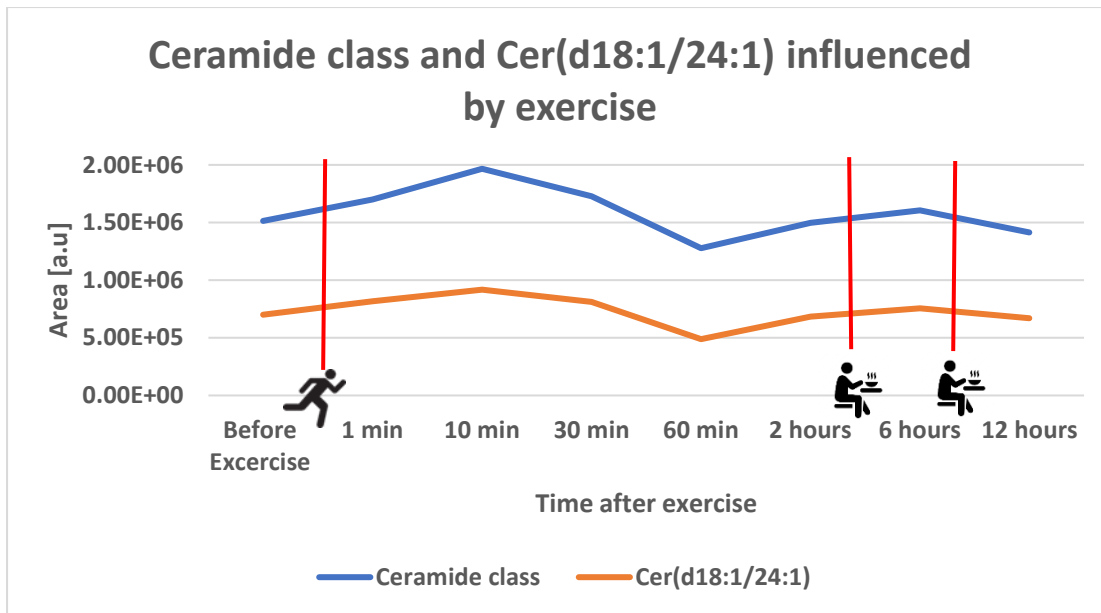
Figure 42: Timeline for how ceramide as a class was influenced by exercise, and how Cer(18:1/24:1) peak areas altered as a result of exercise. Standard deviations can be found in table x and y in appendix. Level 2 of confidence.

As mentioned previously ceramides are also recognised as markers off inflammation. Higher levels of ceramide lipids were therefore expected as a result of exercising, see Figure 42 for how the ceramide class and Cer(d18:1/24:1) was affected by exercising. The ceramide lipid class and Cer(18:1/24:1) also show an increase in area after the exercise. Both increases in peak area were significant ($p < 0.05$), but there was a bigger impact on the whole ceramide class. Cer(d18:1/24:1) has also emerged as a potential prognostic marker for cardiovascular diseases [84]. The sample collection time points in this study do not reveal how high intensity exercise affect the Cer(d18:1/24:1) levels in the long term.
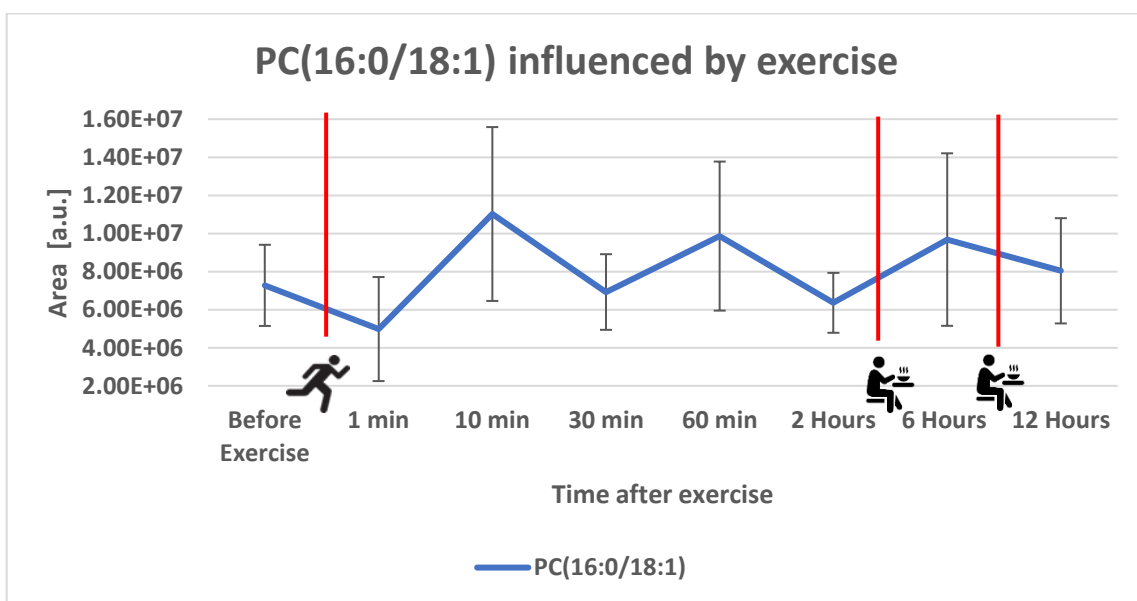
Figure 43: Timeline of how PC(16:0/18:1) average peak areas were affected as a result of high intensity exercising. Including standard deviations in a.u. Level 2 of confidence.

As shown in Figure 43, the peak areas off PC(16:0/18:1) decreased right after exercise, then increased significantly ($p < 0.05$) 10 minutes after exercise before returning to baseline level 30 minutes after exercise. Phosphatidylcholine is one of the main phospholipids in cell membranes. They can also be used to create choline and acetylcholine [85], which are important neurotransmitter in general, but also when it comes to muscle contraction [86]. Therefore, there are many possible reasons for this trend, but too little is known of how and which roles this specific lipid species, PC(16:0/18:1), has in the body to draw any conclusions.

4.3.4 Unidentified lipid influenced by high intensity training

Additionally, to the observed influences a session of HIT exercise had on known lipid classes, an unidentified lipid was found to be significantly ($p < 0.05$) affected by exercise, see Figure 44. There was a big difference between the average peak area before and right after exercising, there was no overlap between the standard deviations for the two time points. The increase in peak area after exercising applied for all individuals conducting the exercise. The unknown lipid returned to baseline level 1 hour after exercise, and it was not influenced by the meal consumed after the 2-hour sample.
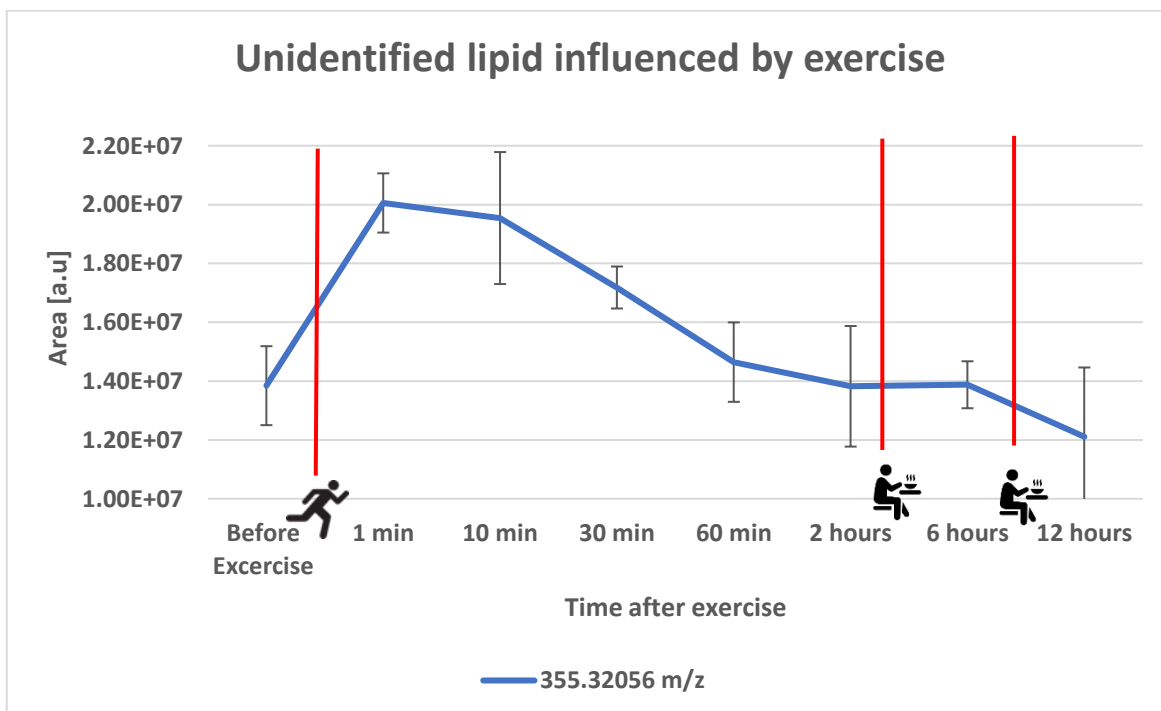
Figure 44: Timeline for the average peak area of the unidentified lipid with m/z value 355.32056 was affected by high intensity exercise, in negative ionization mode. Including standard deviations in a.u.

The unidentified lipid had a *m/z* signal 355.32056, which is suggested to be the [M-H]⁻
adduct. Calculated molecular weight was 356.32766 g/mol, and suggested molecular formula
is $C_{22}H_{44}O_3$. The retention time for the unidentified lipid was 4.280 min. See Figure 45 for
MS1 spectrum. Fragmentation spectrum for the unknown compound can be found in Figure
46.
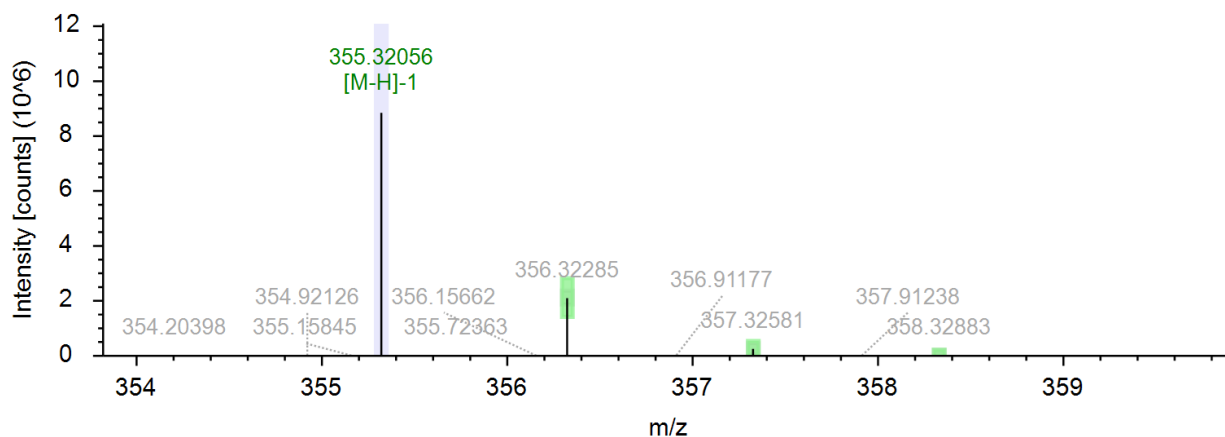
Figure 45: MS1 spectrum for the unknown compound, 355.32056 m/z [M-H]⁻ adduct, calculated molecular weight was
356.32766 g/mol.
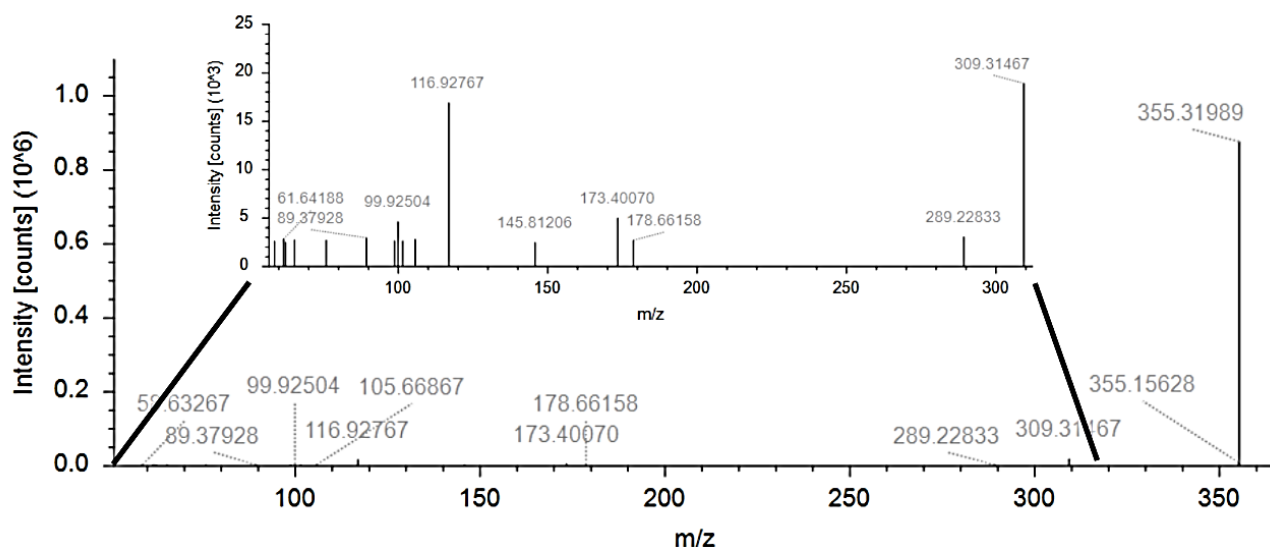
Figure 46: MSMS, fragmentation spectrum for the unknown compound, parent ion had an m/z value of 355.31989, highest
fragment at m/z 116.92767 and 309.31467.

Based on the fragmentation spectra the lipid species glycerophospholipids, phospholipids,
can be excluded from the identification process. This is because the fragmentation spectra do
not contain the fragments corresponding to the head groups related to those lipid species [87].
With a suggested molecular formula of $C_{22}H_{44}O_3$. Suggested lipid based on molecular
formula, was a hydroxy-docosanoic acid, with level of confidence 3 (see Figure 22, part 2.9).
Hydroxy-docosanoic acid is the oxidized form of docosanoic acid, docosanoic acid has been

found to be related to inflammation and obesity [88]. As a postulation, the elevated peak areas of hydroxy-docosanoic acid can be a result of increased levels of docosanoic acid. Hydroxy fatty acids are important components in sphingolipids [89], suggesting that a increase of docosanoic acid is not observed due to oxidation for use in sphingolipid synthesis. It is also possible that the finding is not hydroxy-docosanoic acid, the suggested $[M-H]^-$ adduct can be a different adduct, and the ion observed can also be a result of in-source fragmentation. To confirm if the identification is correct, an analytical standard of hydroxy-docosanoic acid needs to be analyzed using the same method. However, due to little time, this was not possible in this project, but should be done in future work.

To summarize part 4.3: The global lipidomics method was able to detect changes in the lipidome on lipid species level. The observed changes were connected to energy consumption and production through lipolysis. Lipids connected to inflammation were altered as a response to exercise. Multiple lipids were found to be significantly altered, including one unidentified lipid suggested to be a hydroxy-docosanoic acid. It is important to consider that short term post high intensity exercise measurements do not fully reflect the long-term effect that exercise can inflict.

5   Conclusion

The optimized and evaluated global lipidomics LC-MSMS method described in this thesis was able to detect lipid classes covering the whole lipidome. The method was able to conduct separation based on class, intra-class and acyl chain composition. In addition, a linear relation between number of carbon atoms, and double bonds situated on the sidechains, in relation to the retention time, within specific lipid classes. For the optimization process of data acquisition methods, scheduled MSMS was shown to be the best alternative compared to Data-Dependent Acquisition (DDA), making it more suitable for clinical diagnostics than DDA. The method was evaluated as close as possible according to the Lipidomics Standard Initiative (LSI), using analytical standards and biological matrices to evaluate intra-batch and in between batch variations. The method showed high repeatability, with low intra-batch and in-between batch variations.

With the use of scheduled MSMS, alterations in the lipidome induced by high intensity exercise (HIT) was observed. Lipids associated with energy production and consumption, were found to be significantly altered in addition to lipids associated with inflammation response. Among the findings, one unidentified lipid, characterized as hydroxy-docosanoic acid was increased significantly as a result of exercising. From this study it was concluded that the method was able to observe normal variations in the lipidome.

5.1   Future Work

For future work, experiments of exercise-induced changes can be repeated. Utilizing the same method, but with more participants, sampling time points, and also with other types of exercise, to generate better and more diverse data. Lipid identification can be made easier by applying an in-house library, consisting of lipids from multiple lipid classes, were retention time and fragmentation spectra are included.

The method needs to be tested further before implementation in clinical diagnostics, this includes testing other biological matrices such as tissue. Linear dynamic range, limit of detection and stability of the samples must be tested as well. But for now, it can be used as a hypothesis generating method to supplement diagnostics to identify new biomarkers in various diseases. It can also be used for proving or disproving diagnosis were known lipid species are altered.

6   References

[1] Beger, R. D., Dunn, W., Schmidt, M. A., Gross, S. S., Kirwan, J. A., Cascante, M., Brennan, L., Wishart, D. S., Oresic, M., Hankemeier, T., Broadhurst, D. I., Lane, A. N., Suhre, K., Kastenmüller, G., Sumner, S. J., Thiele, I., Fiehn, O., Kaddurah-Daouk, R., for "Precision Medicine and Pharmacometabolomics Task Group"-Metabolomics Society Initiative, Metabolomics enables precision medicine: "A White Paper, Community Perspective." *Metabolomics* 2016, 12, 149.

[2] Personalised medicine, https://health.ec.europa.eu/medicinal-products/personalised-medicine_en (last time accessed: September 1, 2022).

[3] Hasin, Y., Seldin, M., Lusis, A., Multi-omics approaches to disease. *Genome Biol.* 2017, 18, 83.

[4] Han, X., Gross, R. W., The foundations and development of lipidomics. *J. Lipid Res.* 2022, 63, 100164.

[5] Untargeted Metabolomics Strategies—Challenges and Emerging Directions | Journal of the American Society for Mass Spectrometry, https://pubs.acs.org/doi/10.1007/s13361-016-1469-y (last time accessed: December 2, 2022).

[6] Wolrab, D., Jirásko, R., Cífková, E., Höring, M., Mei, D., Chocholoušková, M., Peterka, O., Idkowiak, J., Hrnčiarová, T., Kuchař, L., Ahrends, R., Brumarová, R., Friedecký, D., Vivo-Truyols, G., Škrha, P., Škrha, J., Kučera, R., Melichar, B., Liebisch, G., Burkhardt, R., Wenk, M. R., Cazenave-Gassiot, A., Karásek, P., Novotný, I., Greplová, K., Hrstka, R., Holčapek, M., Lipidomic profiling of human serum enables detection of pancreatic cancer. *Nat. Commun.* 2022, 13, 124.

[7] Hunter, W. G., Kelly, J. P., McGarrah, R. W., Khouri, M. G., Craig, D., Haynes, C., Ilkayeva, O., Stevens, R. D., Bain, J. R., Muehlbauer, M. J., Newgard, C. B., Felker, G. M., Hernandez, A. F., Velazquez, E. J., Kraus, W. E., Shah, S. H., Metabolomic Profiling Identifies Novel Circulating Biomarkers of Mitochondrial Dysfunction Differentially Elevated in Heart Failure With Preserved Versus Reduced Ejection Fraction: Evidence for Shared Metabolic Impairments in Clinical Heart Failure. *J. Am. Heart Assoc.* n.d., 5, e003190.

[8] Anesi, A., Di Minno, A., Calcaterra, I., Cavalca, V., Tripaldella, M., Porro, B., Di Minno, M. N. D., An Untargeted Lipidomic Analysis Reveals Depletion of Several Phospholipid Classes in Patients with Familial Hypercholesterolemia on Treatment with Evolocumab. *Biomedicines* 2021, 9, 1941.

[9] Pan, M., Qin, C., Han, X., Lipid Metabolism and Lipidomics Applications in Cancer Research. *Adv. Exp. Med. Biol.* 2021, 1316, 1–24.

[10] Latino, F., Cataldi, S., Carvutto, R., De Candia, M., D'Elia, F., Patti, A., Bonavolontà, V., Fischetti, F., The Importance of Lipidomic Approach for Mapping and Exploring the Molecular Networks Underlying Physical Exercise: A Systematic Review. *Int. J. Mol. Sci.* 2021, 22, 8734.

[11] Lehmann, R., From bedside to bench—practical considerations to avoid pre-analytical pitfalls and assess sample quality for high-resolution metabolomics and lipidomics analyses of body fluids. *Anal. Bioanal. Chem.* 2021, 413, 5567–5585.

[12] Haugan, H. S., Investigating the Lipid Coverage of the Dried Blood Spot Metabolome using Liquid Chromatography – Mass Spectrometry for Global Metabolomics. 2020.

[13] Wishart, D. S., Tzur, D., Knox, C., Eisner, R., Guo, A. C., Young, N., Cheng, D., Jewell, K., Arndt, D., Sawhney, S., Fung, C., Nikolai, L., Lewis, M., Coutouly, M.-A., Forsythe, I., Tang, P., Shrivastava, S., Jeroncic, K., Stothard, P., Amegbey, G., Block, D., Hau, David. D., Wagner, J., Miniaci, J., Clements, M., Gebremedhin, M., Guo, N., Zhang, Y., Duggan, G. E., MacInnis, G. D., Weljie, A. M., Dowlatabadi, R., Bamforth, F., Clive, D., Greiner, R., Li, L., Marrie, T., Sykes, B. D., Vogel, H. J., Querengesser, L., HMDB: the Human Metabolome Database. *Nucleic Acids Res.* 2007, 35, D521–D526.

[14] Mohamed, S., Recognition and diagnostic approach to acute metabolic disorders in the neonatal period. *Sudan. J. Paediatr.* 2011, 11, 20–28.

[15] Wishart, D. S., Metabolomics for Investigating Physiological and Pathophysiological Processes. *Physiol. Rev.* 2019, 99, 1819–1875.

[16] Roca, M., Alcoriza, M. I., Garcia-Cañaveras, J. C., Lahoz, A., Reviewing the metabolome coverage provided by LC-MS: Focus on sample preparation and chromatography-A tutorial. *Anal. Chim. Acta* 2021, 1147, 38–55.

[17] Lipidome - an overview | ScienceDirect Topics, https://www.sciencedirect.com/topics/pharmacology-toxicology-and-pharmaceutical-science/lipidome (last time accessed: August 22, 2022).

[18] Zhao, H., Gao, X., Cao, X., Zhang, L., Zhou, D., Li, J., Revealing serum lipidomic characteristics and potential lipid biomarkers in patients with POEMS syndrome. *J. Cell. Mol. Med.* 2021, 25, 4307–4315.

[19] Lipid synthesis and transport are coupled to regulate membrane lipid dynamics in the endoplasmic reticulum - ScienceDirect, https://www.sciencedirect.com/science/article/pii/S1388198119300757?via%3Dihub (last time accessed: September 14, 2022).

[20] Balla, T., Sengupta, N., Kim, Y. J., Lipid synthesis and transport are coupled to regulate membrane lipid dynamics in the endoplasmic reticulum. *Biochim. Biophys. Acta BBA - Mol. Cell Biol. Lipids* 2020, 1865, 158461.

[21] Khan, S. R., Glenton, P. A., Backov, R., Talham, D. R., Presence of lipids in urine, crystals and stones: Implications for the formation of kidney stones. *Kidney Int.* 2002, 62, 2062–2072.

[22] 5.3: Functions of Lipids, https://med.libretexts.org/Courses/Metropolitan_State_University_of_Denver/Introduction_to_Nutrition_(Diker)/05%3A_Lipids/5.3%3A_Functions_of_Lipids (last time accessed: August 22, 2022).

[23] Fahy, E., Cotter, D., Sud, M., Subramaniam, S., Lipid classification, structures and tools. *Biochim. Biophys. Acta* 2011, 1811, 637–647.

[24] Fahy, E., Subramaniam, S., Brown, H. A., Glass, C. K., Merrill, A. H., Murphy, R. C., Raetz, C. R. H., Russell, D. W., Seyama, Y., Shaw, W., Shimizu, T., Spener, F., van Meer, G., VanNieuwenhze, M. S., White, S. H., Witztum, J. L., Dennis, E. A., A comprehensive classification system for lipids. *J. Lipid Res.* 2005, 46, 839–861.

[25] Holčapek, M., Liebisch, G., Ekroos, K., Lipidomic Analysis. *Anal. Chem.* 2018, 90, 4249–4257.

[26] LIPID MAPS, https://www.lipidmaps.org/resources/tutorials/lipid_tutorial#ST (last time accessed: September 14, 2022).

[27] Shetty, S. S., Kumari, S., Fatty acids and their role in type-2 diabetes (Review). *Exp. Ther. Med.* 2021, 22, 706.

[28] Liebisch, G., Vizcaíno, J. A., Köfeler, H., Trötzmüller, M., Griffiths, W. J., Schmitz, G., Spener, F., Wakelam, M. J. O., Shorthand notation for lipid structures derived from mass spectrometry. *J. Lipid Res.* 2013, 54, 1523–1530.

[29] Koelmel, J. P., Ulmer, C. Z., Jones, C. M., Yost, R. A., Bowden, J. A., Common cases of improper lipid annotation using high-resolution tandem mass spectrometry data and corresponding limitations in biological interpretation. *Biochim. Biophys. Acta BBA - Mol. Cell Biol. Lipids* 2017, 1862, 766–770.

[30] Okazaki, Y., Saito, K., Roles of lipids as signaling molecules and mitigators during stress response in plants. *Plant J.* 2014, 79, 584–596.

[31] Hilgemann, D. W., Dai, G., Collins, A., Larricia, V., Magi, S., Deisl, C., Fine, M., Lipid signaling to membrane proteins: From second messengers to membrane domains and adapter-free endocytosis. *J. Gen. Physiol.* 2018, 150, 211–224.

[32] Lange, M., Ni, Z., Criscuolo, A., Fedorova, M., Liquid Chromatography Techniques in Lipidomics Research. *Chromatographia* 2019, 82, 77–100.

[33] Bligh, E. G., Dyer, W. J., A RAPID METHOD OF TOTAL LIPID EXTRACTION AND PURIFICATION. *Can. J. Biochem. Physiol.* 1959, 37, 911–917.

[34] Pellegrino, R. M., Di Veroli, A., Valeri, A., Goracci, L., Cruciani, G., LC/MS lipid profiling from human serum: a new method for global lipid extraction. *Anal. Bioanal. Chem.* 2014, 406, 7937–7948.

[35] Iriondo, A., Tainta, M., Saldias, J., Arriba, M., Ochoa, B., Goñi, F. M., Martinez-Lage, P., Abad-García, B., Isopropanol extraction for cerebrospinal fluid lipidomic profiling analysis. *Talanta* 2019, 195, 619–627.

[36] Züllig, T., Trötzmüller, M., Köfeler, H. C., Lipidomics from sample preparation to data analysis: a primer. *Anal. Bioanal. Chem.* 2020, 412, 2191–2209.

[37] Satomi, Y., Hirayama, M., Kobayashi, H., One-step lipid extraction for plasma lipidomics analysis by liquid chromatography mass spectrometry. *J. Chromatogr. B Analyt. Technol. Biomed. Life. Sci.* 2017, 1063, 93–100.

[38] Watson, A. D., Thematic review series: Systems Biology Approaches to Metabolic and Cardiovascular Disorders. Lipidomics: a global approach to lipid analysis in biological systems. *J. Lipid Res.* 2006, 47, 2101–2111.

[39] Ahluwalia, K., Ebright, B., Chow, K., Dave, P., Mead, A., Poblete, R., Louie, S. G., Asante, I., Lipidomics in Understanding Pathophysiology and Pharmacologic Effects in Inflammatory Diseases: Considerations for Drug Development. *Metabolites* 2022, 12, 333.

[40] Quehenberger, O., Armando, A. M., Brown, A. H., Milne, S. B., Myers, D. S., Merrill, A. H., Bandyopadhyay, S., Jones, K. N., Kelly, S., Shaner, R. L., Sullards, C. M., Wang, E., Murphy, R. C., Barkley, R. M., Leiker, T. J., Raetz, C. R. H., Guan, Z., Laird, G. M., Six, D. A., Russell, D. W., McDonald, J. G., Subramaniam, S., Fahy, E., Dennis, E. A., Lipidomics reveals a remarkable diversity of lipids in human plasma1[S]. *J. Lipid Res.* 2010, 51, 3299–3305.

[41] Yang, K., Han, X., Lipidomics: Techniques, applications, and outcomes related to biomedical sciences. *Trends Biochem. Sci.* 2016, 41, 954–969.

[42] Carrasco-Pancorbo, A., Navas-Iglesias, N., Cuadros-Rodríguez, L., From lipid analysis towards lipidomics, a new challenge for the analytical chemistry of the 21st century. Part I: Modern lipid analysis. *TrAC Trends Anal. Chem.* 2009, 28, 263–278.

[43] Li, J., Vosegaard, T., Guo, Z., Applications of nuclear magnetic resonance in lipid analyses: An emerging powerful tool for lipidomics studies. *Prog. Lipid Res.* 2017, 68, 37–56.

[44] Goldansaz, S. A., Guo, A. C., Sajed, T., Steele, M. A., Plastow, G. S., Wishart, D. S., Livestock metabolomics and the livestock metabolome: A systematic review. *PLoS ONE* 2017, 12, e0177675.

[45] Züllig, T., Trötzmüller, M., Köfeler, H. C., in: Hsu, F.-F. (Ed.), Mass Spectrometry-Based Lipidomics: Methods and Protocols. Springer US, New York, NY 2021, pp. 39–51.

[46] Imbert, L., Gaudin, M., Libong, D., Touboul, D., Abreu, S., Loiseau, P. M., Laprévote, O., Chaminade, P., Comparison of electrospray ionization, atmospheric pressure chemical ionization and atmospheric pressure photoionization for a lipidomic analysis of Leishmania donovani. *J. Chromatogr. A* 2012, 1242, 75–83.

[47] Hansen, S. H., Reubsaet, L., Bioanalysis of Pharmaceuticals. John Wiley & Sons, Ltd 2015, pp. 123–172.

[48] Elsa Lundanes, Léon Reubsaet, Tyge Greibrokk, Chromatography : Basic Principles, Sample Preparations and Related Methods. Wiley-VCH, [N.p.] 2013.

[49] Cajka, T., Fiehn, O., Comprehensive analysis of lipids in biological systems by liquid chromatography-mass spectrometry. *Trends Anal. Chem. TRAC* 2014, 61, 192–206.

[50] Criscuolo, A., Zeller, M., Cook, K., Angelidou, G., Fedorova, M., Rational selection of reverse phase columns for high throughput LC–MS lipidomics. *Chem. Phys. Lipids* 2019, 221, 120–127.

[51] Okusa, K., Iwasaki, Y., Kuroda, I., Miwa, S., Ohira, M., Nagai, T., Mizobe, H., Gotoh, N., Ikegami, T., McCalley, D. V., Tanaka, N., Effect of pressure on the selectivity of polymeric C18 and C30 stationary phases in reversed-phase liquid chromatography. Increased separation of isomeric fatty acid methyl esters, triacylglycerols, and tocopherols at high pressure. *J. Chromatogr. A* 2014, 1339, 86–95.

80

[52] Narváez-Rivas, M., Zhang, Q., Comprehensive untargeted lipidomic analysis using core–shell C30 particle column and high field orbitrap mass spectrometer. *J. Chromatogr. A* 2016, 1440, 123–134.

[53] Rampler, E., Criscuolo, A., Zeller, M., Abiead, Y. E., Schoeny, H., Hermann, G., Sokol, E., Cook, K., Peake, D. A., Delanghe, B., Koellensperger, G., A Novel Lipidomics Workflow for Improved Human Plasma Identification and Quantification Using RPLC-MSn Methods and Isotope Dilution Strategies. *Anal. Chem.* 2018, DOI: 10.1021/acs.analchem.7b05382.

[54] Michalski, A., Cox, J., Mann, M., More than 100,000 Detectable Peptide Species Elute in Single Shotgun Proteomics Runs but the Majority is Inaccessible to Data-Dependent LC–MS/MS, DOI: 10.1021/pr101060vhttps://pubs.acs.org/doi/pdf/10.1021/pr101060v (last time accessed: July 6, 2023).

[55] Guo, J., Huan, T., Comparison of Full-Scan, Data-Dependent, and Data-Independent Acquisition Modes in Liquid Chromatography–Mass Spectrometry Based Untargeted Metabolomics. *Anal. Chem.* 2020, 92, 8072–8080.

[56] Fang, N., Yu, S., Ronis, M. J., Badger, T. M., Matrix effects break the LC behavior rule for analytes in LC-MS/MS analysis of biological samples. *Exp. Biol. Med.* 2015, 240, 488–497.

[57] Kupke, I. R., Zeugner, S., Gottschalk, A., Kather, B., Differences in lipid and lipoprotein concentrations of capillary and venous blood samples. *Clin. Chim. Acta* 1979, 97, 279–283.

[58] Wang, D., Xu, P., Mesaros, C., Sphingolipidome Quantification by Liquid Chromatography- High Resolution Mass Spectrometry: Whole Blood vs. Plasma. 2021, DOI: 10.20944/preprints202103.0289.v1.

[59] Chace, D. H., Hannon, W. H., Filter Paper as a Blood Sample Collection Device for Newborn Screening. *Clin. Chem.* 2016, 62, 423–425.

[60] Hoehn, T., Lukacs, Z., Stehn, M., Mayatepek, E., Philavanh, K., Bounnack, S., Establishment of the First Newborn Screening Program in the People's Democratic Republic of Laos. *J. Trop. Pediatr.* 2013, 59, 95–99.

[61] Zakaria, R., Allen, K. J., Koplin, J. J., Roche, P., Greaves, R. F., Advantages and Challenges of Dried Blood Spot Analysis by Mass Spectrometry Across the Total Testing Process. *EJIFCC* 2016, 27, 288–317.

[62] Koulman, A., Prentice, P., Wong, M. C. Y., Matthews, L., Bond, N. J., Eiden, M., Griffin, J. L., Dunger, D. B., The development and validation of a fast and robust dried blood spot based lipid profiling method to study infant metabolism. *Metabolomics* 2014, 10, 1018–1025.

[63] Broadhurst, D., Goodacre, R., Reinke, S. N., Kuligowski, J., Wilson, I. D., Lewis, M. R., Dunn, W. B., Guidelines and considerations for the use of system suitability and quality control samples in mass spectrometry assays applied in untargeted clinical metabolomic studies. *Metabolomics* 2018, 14, 72.

[64] Getting the peaks perfect: System suitability for HPLC, http://pubsapp.acs.org/subscribe/archive/tcaw/10/i09/html/09dong.html? (last time accessed: December 2, 2022).

[65] Schymanski, E. L., Jeon, J., Gulde, R., Fenner, K., Ruff, M., Singer, H. P., Hollender, J., Identifying Small Molecules via High Resolution Mass Spectrometry: Communicating Confidence. *Environ. Sci. Technol.* 2014, 48, 2097–2098.

[66] lipidomicstandards.org. n.d.

[67] Neue, U. D., Theory of peak capacity in gradient elution. *J. Chromatogr. A* 2005, 1079, 153–161.

[68] Hu, A., Noble, W. S., Wolf-Yadlin, A., Technical advances in proteomics: new developments in data-independent acquisition. 2016, DOI: 10.12688/f1000research.7042.1.

[69] Hodge, K., Have, S. T., Hutton, L., Lamond, A. I., Cleaning up the masses: Exclusion lists to reduce contamination with HPLC-MS/MS. *J. Proteomics* 2013, 88, 92–103.

[70] Jankevics, A., Jenkins, A., Dunn, W. B., Najdekr, L., An improved strategy for analysis of lipid molecules utilising a reversed phase C30 UHPLC column and scheduled MS/MS acquisition. *Talanta* 2021, 229, 122262.

[71] Hornemann, T., in: von Eckardstein, A., Binder, C. J. (Eds.), Prevention and Treatment of Atherosclerosis : Improving State-of-the-Art Management and Search for Novel Targets. Springer International Publishing, Cham 2022, pp. 493–510.

[72] Vasku, G., Peltier, C., He, Z., Thuret, G., Gain, P., Gabrielle, P.-H., Acar, N., Berdeaux, O., Comprehensive mass spectrometry lipidomics of human biofluids and ocular tissues. *J. Lipid Res.* 2023, 64, 100343.

[73] Horowitz, J. F., Klein, S., Lipid metabolism during endurance exercise. *Am. J. Clin. Nutr.* 2000, 72, 558S-563S.

[74] Grabner, G. F., Xie, H., Schweiger, M., Zechner, R., Lipolysis: cellular mechanisms for lipid mobilization from fat stores. *Nat. Metab.* 2021, 3, 1445–1465.

[75] Kerner, J., Hoppel, C., Fatty acid import into mitochondria. *Biochim. Biophys. Acta BBA - Mol. Cell Biol. Lipids* 2000, 1486, 1–17.

[76] Cogo, P. E., Giordano, G., Badon, T., Orzali, A., Zimmermann, L. J. I., Zacchello, F., Sauer, P. J. J., Carnielli, V. P., Simultaneous Measurement of the Rates of Appearance of Palmitic and Linoleic Acid in Critically Ill Infants. *Pediatr. Res.* 1997, 41, 178–182.

[77] Foufelle, F., Ferré, P., in: Bastard, J.-P., Fève, B. (Eds.), Physiology and Physiopathology of Adipose Tissue. Springer, Paris 2013, pp. 101–121.

[78] Makrecka-Kuka, M., Sevostjanovs, E., Vilks, K., Volska, K., Antone, U., Kuka, J., Makarova, E., Pugovics, O., Dambrova, M., Liepinsh, E., Plasma acylcarnitine concentrations reflect the acylcarnitine profile in cardiac tissues. *Sci. Rep.* 2017, 7, 17528.

[79] Dolinsky, V. W., Gilham, D., Alam, M., Vance, D. E., Lehner, R., Triacylglycerol hydrolase: role in intracellular lipid metabolism. *Cell. Mol. Life Sci. CMLS* 2004, 61, 1633–1651.

[80] Bergman, B. C., Brozinick, J. T., Strauss, A., Bacon, S., Kerege, A., Bui, H. H., Sanders, P., Siddall, P., Kuo, M. S., Perreault, L., Serum sphingolipids: relationships to insulin sensitivity and changes with exercise in humans. *Am. J. Physiol.-Endocrinol. Metab.* 2015, 309, E398–E408.

[81] Nixon, G. F., Sphingolipids in inflammation: pathological implications and potential therapeutic targets. *Br. J. Pharmacol.* 2009, 158, 982–993.

[82] Cerqueira, É., Marinho, D. A., Neiva, H. P., Lourenço, O., Inflammatory Effects of High and Moderate Intensity Exercise—A Systematic Review. *Front. Physiol.* 2020, 10.

[83] Showing Compound SM(d18:1/16:0) (FDB027352) - FooDB, https://foodb.ca/compounds/FDB027352 (last time accessed: July 24, 2023).

[84] Havulinna, A. S., Sysi-Aho, M., Hilvo, M., Kauhanen, D., Hurme, R., Ekroos, K., Salomaa, V., Laaksonen, R., Circulating Ceramides Predict Cardiovascular Outcomes in the Population-Based FINRISK 2002 Cohort. *Arterioscler. Thromb. Vasc. Biol.* 2016, 36, 2424–2430.

[85] van der Veen, J. N., Kennelly, J. P., Wan, S., Vance, J. E., Vance, D. E., Jacobs, R. L., The critical role of phosphatidylcholine and phosphatidylethanolamine metabolism in health and disease. *Biochim. Biophys. Acta BBA - Biomembr.* 2017, 1859, 1558–1572.

[86] Moretti, A., Paoletta, M., Liguori, S., Bertone, M., Toro, G., Iolascon, G., Choline: An Essential Nutrient for Skeletal Muscle. *Nutrients* 2020, 12, 2144.

[87] Brouwers, J. F. H. M., Vernooij, E. A. A. M., Tielens, A. G. M., van Golde, L. M. G., Rapid separation and identification of phosphatidylethanolamine molecular species. *J. Lipid Res.* 1999, 40, 164–169.

[88] Cho, K., Moon, J. S., Kang, J.-H., Jang, H. B., Lee, H.-J., Park, S. I., Yu, K.-S., Cho, J.-Y., Combined untargeted and targeted metabolomic profiling reveals urinary biomarkers for discriminating obese from normal-weight adolescents. *Pediatr. Obes.* 2017, 12, 93–101.

[89] Hama, H., Fatty acid 2-Hydroxylation in mammalian sphingolipid biology. *Biochim. Biophys. Acta BBA - Mol. Cell Biol. Lipids* 2010, 1801, 405–414.

[90] Evans, K., Mitcheson, J., Laker, M. F., Effect of storage at — 70°C on lipid, lipoprotein and apolipoprotein concentrations. *Clin. Chim. Acta* 1997, 258, 219–229.

[91] Reis, G. B., Rees, J. C., Ivanova, A. A., Kuklenyik, Z., Drew, N. M., Pirkle, J. L., Barr, J. R., Stability of lipids in plasma and serum: Effects of temperature-related storage conditions on the human lipidome. *J. Mass Spectrom. Adv. Clin. Lab* 2021, 22, 34–42.

[92] Hricko, J., Rudl Kulhava, L., Paucova, M., Novakova, M., Kuda, O., Fiehn, O., Cajka, T., Short-Term Stability of Serum and Liver Extracts for Untargeted Metabolomics and Lipidomics. *Antioxidants* 2023, 12, 986.

[93] Wagner-Golbs, A., Neuber, S., Kamlage, B., Christiansen, N., Bethan, B., Rennefahrt, U., Schatz, P., Lind, L., Effects of Long-Term Storage at −80 °C on the Human Plasma Metabolome. *Metabolites* 2019, 9, 99.

[94] Pauling, J. K., Hermansson, M., Hartler, J., Christiansen, K., Gallego, S. F., Peng, B., Ahrends, R., Ejsing, C. S., Proposal for a common nomenclature for fragment ions in mass spectra of lipids. *PLOS ONE* 2017, 12, e0188394.

[95] van Rijt, W. J., Schielen, P. C. J. I., Özer, Y., Bijsterveld, K., van der Sluijs, F. H., Derks, T. G. J., Heiner-Fokkema, M. R., Instability of Acylcarnitines in Stored Dried Blood Spots: The Impact on Retrospective Analysis of Biomarkers for Inborn Errors of Metabolism. *Int. J. Neonatal Screen.* 2020, 6, 83.

7 Appendix

7.1 Supplementary information for optimizing the lipidomics LC-MSMS method

For positive and negative ions used for extracted ion chromatograms (EIC) in part 4.1 Figure 28, see table 18.

Table 18: Adducts and m/z values for each adduct in positive and negative ionization mode for the isotopically labelled EquiSplash lipidomics standards.

Compound	Positive Adduct	*m/z* value	Negative adduct	*m/z* value
PC (15:0/18:1 (d7))	[M+H]+	753.6127	[M+HCOO]-	797.6021
LPC (18:1 (d7))	[M+H]+	529.3998	[M+HCOO]-	573.3893
PE (15:0/18:1 (d7))	[M+H]+	711.5696	[M-H]-	709.5494
LPE (18:1 (d7))	[M+H]+	487.3525	[M-H]-	485.3365
PG (15:0/18:1 (d7))	[M+H]+	764.5428	[M-HCOO]-	808.5309
PI (15:0/18:1 (d7))	[M+H]+	847.6031	[M-H]	845.5947
PS (15:0/18:1 (d7))	[M+NH4]+	799.5197	[M-H]-	775.5211
TG (15:0/18:1 (d7)/15:0)	[M+NH4]+	812.7689	[M-H]-	810.5372
DG (15:0/18:1 (d7))	[M+H]+	588.5552	[M+HCOO]-	632.5477
MG (18:1 (d7))	[M+NH4]+	364.3437	[M+HCOO]-	408.3337
ChE (18:1 (d7))	[M+H]+	658.6514	[M+HCOO]-	702.6401
SM (d18:1/18:1 (d9))	[M+H]+	738.6445	[M-HCOO]-	782.6361
Cer (d18:1 (d7)/15:0)	[M+H]+	531.5497	[M-H]-	529.5314

For average retention time and standard deviation of triacylglycerol used to calculate linearity between number of carbons present on the sidechains and retention time used in part 4.1, Figure 30 see Table 19.

Table 19: Retention time in minutes and standard deviation for triacylglycerols used in figure 32, part 4.1, for finding linearity between number of carbons and retention time. Includes number of carbons and retention time from 4 different batches. For each batch N=3.

linearity TG	Batch	1		2		3		4		combined	
Number of carbons		AVG RT	STD	AVG RT	STD	AVG RT	STD	AVG RT	STD	AVG RT	STD
	34	14.03	0.10	13.92	0.01	13.86	0.03	14.22	0.02	14.02	0.15
	36	14.94	0.03	14.92	0.01	14.86	0.01	14.91	0.02	14.94	0.06
	38	15.42	0.12	15.56	0.00	15.50	0.01	15.77	0.11	15.56	0.15
	40	16.15	0.05	16.11	0.01	16.13	0.09	16.29	0.05	16.17	0.09
	42	17.06	0.04	17.06	0.03	17.04	0.11	17.26	0.06	17.10	0.11
	44	18.05	0.05	18.00	0.01	17.90	0.02	18.28	0.03	17.56	0.15
	46	19.07	0.06	19.03	0.03	18.97	0.03	19.35	0.04	19.11	0.16
	47	19.53	0.11	19.50	0.13	19.49	0.01	19.73	0.21	19.56	0.15
	48	20.17	0.03	20.14	0.01	20.02	0.01	20.40	0.16	20.18	0.16
	49	20.71	0.01	20.67	0.03	20.57	0.00	20.99	0.04	20.75	0.16
	50	21.09	0.09	21.12	0.01	21.03	0.01	21.38	0.13	21.15	0.15
	51	21.48	0.09	21.50	0.01	21.44	0.01	21.79	0.05	21.55	0.15
	52	21.87	0.04	21.83	0.01	21.79	0.01	22.12	0.05	21.90	0.14
	54	22.46	0.05	22.41	0.01	22.38	0.03	22.76	0.05	22.50	0.16

For average retention time and standard deviation for saturated and monounsaturated phosphatidylcholine used to calculate linearity between number of carbons present on the sidechains and retention time used in part 4.1, Figure 33, see Table 20.

Table 20: Retention time in minutes and standard deviation for triacylglycerols used in figure 33, part 4.1, for finding linearity between number of carbons and retention time. Includes number of carbons and retention time from 4 different batches. For each batch N=3.

N	N	Batch 1		Batch 2		Batch 3		Batch 4		Combined	
Double bonds	Carbons	AVG RT [min]	STD	AVG RT [min]	STD	AVG RT [min]	STD	AVG RT [min]	STD	AVG RT [min]	STD
0	30	8.21	0.01	8.19	0.04	8.57	0.06	8.54	0.01	8.36	0.19
0	31	9.26	0.01	9.25	0.01	9.21	0.00	9.26	0.01	9.25	0.02
0	32	10.47	0.02	10.48	0.04	10.63	0.02	10.62	0.03	10.55	0.08
0	33	11.40	0.04	11.38	0.04	11.79	0.05	11.75	0.04	11.60	0.20
0	34	13.37	0.01	13.36	0.02	13.50	0.03	13.48	0.01	13.43	0.07
0	35	13.62	0.02	13.62	0.02	13.77	0.02	13.77	0.00	13.70	0.08

1	30	6.79	0.00	6.80	0.01	6.97	0.04	7.00	0.02	6.90	0.10
1	31	7.53	0.01	7.72	0.03	7.81	0.03	7.79	0.06	7.72	0.14
1	32	8.55	0.02	8.46	0.01	8.78	0.06	8.71	0.07	8.62	0.14
1	33	9.47	0.03	9.44	0.04	9.82	0.03	9.74	0.02	9.62	0.17
1	34	10.71	0.03	10.66	0.07	10.66	0.08	10.96	0.05	10.75	0.14
1	35	12.25	0.02	12.19	0.09	12.11	0.02	12.11	0.03	12.17	0.08

7.2 Supplementary information for evaluation of the lipidomics LC-MSMS method

For positive ions used to test the reproducibility of the Equisplash lipidomics standard mixture see Table 18. For the average retention time in minutes, standard deviation and CV in percentage see Table 21.

Table 21: Average retention time in minutes, standard deviation and CV in percentage for lipids present in the Equisplash lipidomics standard mixture for testing reproducibility. Each batch consisted of 3 injections.

Batch	1	2	3	4	Combined	Combined
Lipid	AVG RT [min]	AVG RT [min]	AVG RT [min]	AVG RT [min]	SD	CV (%)
PC (15:0/18:1 (d7))	9.72	9.72	9.71	9.66	0.03	0.3
LPC (18:1 (d7))	2.91	2.90	2.90	2.89	0.01	0.3
PE (15:0/18:1 (d7))	9.87	9.75	9.87	9.77	0.06	0.7
LPE (18:1 (d7))	2.93	2.94	2.95	2.91	0.02	0.6
PG (15:0/18:1 (d7))	6.30	6.29	6.30	6.29	0.01	0.1
PI (15:0/18:1 (d7))	6.04	6.02	6.04	6.04	0.01	0.2
PS (15:0/18:1 (d7))	6.30	6.34	6.30	6.33	0.02	0.3
TG (15:0/18:1 (d7)/15:0)	18.98	18.97	18.99	18.94	0.02	0.1
DG (15:0/18:1 (d7))	13.47	13.48	13.48	13.42	0.03	0.2
MG (18:1 (d7))	4.20	4.18	4.18	4.19	0.01	0.2

ChE (18:1 (d7))	21.52	21.52	21.52	21.41	0.05	0.3
SM (d18:1/18:1 (d9))	8.35	8.31	8.34	8.32	0.02	0.2
Cer (d18:1 (d7)/15:0)	8.89	8.85	8.91	8.88	0.03	0.3

The triacylglycerol and phosphatidylcholine positive ions used for evaluating the method is listed in Table 22, including molecular formula, adduct and *m/z value*.

Table 22: Abbreviation, molecular formula, adduct and m/z value, for selected lipids used to evaluate the retention time variations between and in-between batches.

Compound	Molecular formula	Adduct	*m/z* value
TG(4:0/16:0/16:0)	C39H74O6	[M+NH$_4$]+	656.5824
TG(6:0/16:0/16:0)	C41H78O6	[M+NH$_4$]+	684.6126
TG(10:0/14:0/16:0)	C43H82O6	[M+NH$_4$]+	712.6446
TG(14:0/12:0/16:0)	C45H86O6	[M+NH$_4$]+	740.6758
TG(14:0/14:0/16:0)	C47H90O6	[M+NH$_4$]+	768.7069
TG(14:0/16:0/16:0)	C49H94O6	[M+NH$_4$]+	796.7372
TG(15:0/16:0/16:0)	C50H96O6	[M+NH$_4$]+	810.7540
TG(14:0/16:0/18:0)	C51H98O6	[M+NH$_4$]+	824.7689
TG(15:0/16:0/18:0)	C52H100O6	[M+NH$_4$]+	838.7842
TG(16:0/16:0/18:0)	C53H102O6	[M+NH$_4$]+	852.8001
TG(16:0/17:0/18:0)	C54H104O6	[M+NH$_4$]+	866.8164
TG(16:0/18:0/18:0)	C55H106O6	[M+NH$_4$]+	880.8308
TG(16:0/18:0/20:0)	C57H110O6	[M+NH$_4$]+	908.8619
PC(28:0)	C36H72NO8P	[M+H]+	678.5067
PC(30:0)	C38H76NO8P	[M+H]+	706.5375
PC(31:0)	C39H78NO8P	[M+H]+	720.5527
PC(32:0)	C40H80NO8P	[M+H]+	734.5696
PC(33:0)	C41H82NO8P	[M+H]+	748.5842
PC(34:0)	C42H84NO8P	[M+H]+	762.6007
PC(30:1)	C38H74NO8P	[M+H]+	704.5224
PC(32:1)	C40H78NO8P	[M+H]+	732.5529
PC(33:1)	C41H80NO8P	[M+H]+	746.5689
PC(34:1)	C42H82NO8P	[M+H]+	760.5846
PC(35:1)	C43H84NO8P	[M+H]+	774.6004
PC(36:1)	C44H86NO8P	[M+H]+	788.6158
PC(37:1)	C45H88NO8P	[M+H]+	802.6319
PC(38:1)	C46H90NO8P	[M+H]+	816.6477

See Table 23 for measured retention times for the different triacylglycerols used to evaluate the reproducibility in retention time. One serum sample with three technical replicates injected three times each per date listed in the table below.

Table 23: Sidechain composition, average retention time (AVG RT), coefficient of variation in percentage, for selected triacylglycerols (TG) used to evaluate the reproducibility of the global lipidomics method.

	Batch 1		Batch 2		Batch 3		Batch 4		Mean
TG	AVG RT [min]	CV (%)	AVG RT [min]	CV (%)	AVG RT [min]	CV (%)	AVG RT [min]	CV (%)	CV (%)
4:0/16:0/16:0	15.023	0.088	14.860	0.054	14.921	0.047	14.942	0.223	0.421
6:0/16:0/16:0	15.767	0.705	15.500	0.046	15.557	0.019	15.417	0.809	0.982
10:0/14:0/16:0	16.294	0.293	16.127	0.577	16.108	0.052	16.155	0.307	0.562
14:0/12:0/16:0	17.260	0.376	17.040	0.653	17.056	0.159	17.062	0.233	0.647
14:0/14:0/16:0	18.276	0.158	17.901	0.107	17.997	0.051	18.046	0.302	0.834
14:0/16:0/16:0	19.350	0.221	18.970	0.169	19.031	0.133	19.069	0.297	0.818
15:0/16:0/16:0	19.729	1.053	19.486	0.053	19.498	0.659	19.529	0.559	0.786
14:0/16:0/18:0	20.400	0.778	20.021	0.065	20.143	0.032	20.175	0.165	0.787
15:0/16:0/18:0	20.986	0.195	20.570	0.019	20.675	0.125	20.706	0.071	0.776
16:0/16:0/18:0	21.377	0.602	21.030	0.057	21.121	0.069	21.088	0.447	0.731
16:0/17:0/18:0	21.792	0.210	21.437	0.056	21.503	0.042	21.478	0.438	0.711
16:0/18:0/18:0	22.120	0.210	21.785	0.030	21.832	0.045	21.873	0.161	0.628
16:0/18:0/20:0	22.759	0.204	22.382	0.123	22.410	0.027	22.460	0.219	0.713

See Table 24 for measured retention times for the different phosphatidylcholines used to evaluate the reproducibility in retention time. One serum sample with three technical replicates injected three times each per date listed in the table below.

Table 24: Sidechain composition for phosphatidylcholine (PC) selected for evaluating the repeatability of the lipidomics method. Average retention time (AVG RT) in minutes and coefficient of variation per batch, and the mean coefficient of variation in percentage.

	Batch 1		Batch 2		Batch 3		Batch 4		Mean
PC	AVG RT [min]	CV (%)	AVG RT [min]	CV (%)	AVG RT [min]	CV (%)	AVG RT [min]	CV (%)	CV (%)
28:0	6.763	0.109	6.783	0.242	6.816	0.308	6.774	0.239	0.336
30:0	8.521	0.114	8.532	0.189	8.571	0.169	8.544	0.103	0.250
31:0	9.264	0.129	9.251	0.090	9.212	0.150	9.259	0.171	0.257
32:0	10.669	0.209	10.677	0.397	10.625	0.148	10.625	0.288	0.262
33:0	11.740	0.314	11.758	0.395	11.787	0.406	11.754	0.322	0.168
34:0	13.367	0.098	13.362	0.117	13.501	0.189	13.478	0.089	0.541
30:1	6.988	0.054	6.980	0.122	6.970	0.542	6.999	0.294	0.172
32:1	8.746	0.217	8.746	0.133	8.784	0.731	8.709	0.849	0.350
33:1	9.724	0.331	9.740	0.421	9.819	0.314	9.739	0.195	0.440
34:1	10.711	0.311	10.665	0.637	10.658	0.763	10.657	0.455	0.240
35:1	12.255	0.203	12.188	0.773	12.115	0.193	12.112	0.240	0.562
36:1	13.436	0.075	13.444	0.077	13.517	0.497	13.552	0.063	0.419
37:1	13.984	0.154	13.984	0.089	14.006	0.119	14.052	0.272	0.229

38:1	6.763	0.109	6.783	0.242	6.816	0.308	6.774	0.439	0.336

See Table 25 for retention time, average retention time, standard deviation and CV for lipid species selected to test the repeatability of the retention times in human serum. 10 injections of the same human serum sample.

Table 25: Repeatability of retention time for selected lipid species found in human serum. Retention time in minutes for 10 injections in a sample sequence of the same serum sample.

Lipid Inj.nr.	1	2	3	4	5	6	7	8	9	10	AVG RT [min]	CV (%)
LPC(16:0)	2.635	2.678	2.614	2.620	2.623	2.607	2.643	2.652	2.638	2.657	2.637	0.8
LPC(18:0)	4.047	4.046	4.030	4.023	4.034	4.038	4.036	4.032	4.057	4.063	4.041	0.3
PC(30:0)	8.492	8.379	8.522	8.542	8.511	8.459	8.419	8.414	8.477	8.387	8.460	0.7
PC(32:0)	10.825	10.829	10.896	10.795	10.721	10.702	10.757	10.753	10.832	10.863	10.797	0.6
PC(33:0)	11.786	11.671	11.699	11.746	11.642	11.689	11.655	11.673	11.646	11.707	11.691	0.4
PC(34:0)	13.485	13.387	13.453	13.488	13.422	13.439	13.391	13.367	13.343	13.399	13.417	0.4
TG(46:0)	18.163	18.207	17.921	18.223	18.258	18.251	18.170	18.283	18.194	18.239	18.194	0.7
TG(48:0)	19.154	19.103	19.205	19.165	19.198	19.130	19.083	19.232	19.143	19.179	19.160	0.3
TG(50:0)	20.163	20.127	20.216	20.193	20.239	20.132	20.084	20.292	20.142	20.192	20.180	0.4
TG(52:0)	21.104	21.095	21.415	21.141	21.162	21.099	21.032	21.200	21.108	21.173	21.158	0.6

7.3 Supplementary information for the observed effect of high intensity training on the lipidome

Participant C did not deliver the DBS sample taken 12 hours after the high intensity exercise session. For lipid species and their corresponding molecular formula, adduct and *m/z* value found to be significantly altered as a result to high intensity exercise, see Table 26.

Table 26: Lipid species, molecular formula, adduct and m/z value for lipids affected by high intensity exercise.

Abbreviation	Moleuclar formula	Adduct	m/z value
FA(16:0)	C16H32O2	[M-H]-	255.2330
FA(18:0)	C18H36O2	[M-H]-	283.2643
PC(16:0/18:1)	C42H82NO8P	[M+H]+	760.5846
TG(16:0/18:1/18:1)	C55H102O6	[M+NH$_4$]+	876.8014
AcCa(18:1)	C25H47NO4	[M+H]+	426.3756
AcCa(16:0)	C23H45NO4	[M+H]+	400.3415
DG(18:1/18:1)	C39H72O5	[M+Na]+	643.5254
DG(16:0/18:1)	C37H70O5	[M+Na]+	617.5101
SM(d18:1/16:0)	C39H79N2O6P	[M+H]+	703.5743
Cer(d18:1/24:0)	C42H83NO3	[M+H-H2O]+	632.6330

| Cer(d18:1/24:1) | C42H81NO3 | [M+H-H2O]+ | 630.6183 |

For measured peak area, average peak area and standard deviation of Cer(d18:1/24:1) in participant A, B, C, D and E right before and certain time points after high intensity exercise session, see Table 27.

Table 27: Peak area for participant, A, B, C, D, E,, standard deviation (SD) and coefficient of variation (CV%) for Cer(d18:1/24:1), before exercise, 1 min, 10 min, 30 min 60 min, 2 hours, 6 hours, and 12 hours after high intensity exercise session.

Cer(d18:1/24:1)	Before Excercise	1 min	10 min	30 min	60 min	2 hours	6 hours	12 hours
A	5.35E+05	7.94E+05	7.77E+05	8.54E+05	6.46E+05	6.03E+05	7.20E+05	7.35E+05
B	7.30E+05	8.19E+05	1.04E+06	7.60E+05	6.73E+05	6.93E+05	1.01E+06	6.43E+05
C	9.19E+05	9.80E+05	1.06E+06	9.97E+05	2.86E+04	7.00E+05	8.42E+05	
D	6.47E+05	7.34E+05	8.45E+05	6.10E+05	5.79E+05	7.44E+05	5.91E+05	6.66E+05
E	6.68E+05	7.62E+05	8.72E+05	8.42E+05	5.17E+05	6.75E+05	6.15E+05	6.40E+05
AVG	7.00E+05	8.18E+05	9.18E+05	8.13E+05	4.89E+05	6.83E+05	7.55E+05	6.71E+05
SD	1.41E+05	9.63E+04	1.24E+05	1.42E+05	2.64E+05	5.13E+04	1.72E+05	4.41E+04

For measured peak area, average peak area and standard deviation of ceramide as a class in participant A, B, C, D and E right before and certain time points after high intensity exercise session, see Table 2728.

Table 28: Peak area for participant, A, B, C, D, E, standard deviation (SD) and coefficient of variation (CV%) for Cer class, before exercise, 1 min, 10 min, 30 min 60 min, 2 hours, 6 hours, and 12 hours after high intensity exercise session.

Cer CLASS	Before Excercise	1 min	10 min	30 min	60 min	2 hours	6 hours	12 hours
A	1.14E+06	1.57E+06	1.56E+06	1.64E+06	1.36E+06	1.39E+06	1.43E+06	1.45E+06
B	1.51E+06	1.71E+06	2.16E+06	1.77E+06	1.52E+06	1.43E+06	2.06E+06	1.33E+06
C	1.95E+06	2.02E+06	2.18E+06	1.98E+06	9.48E+05	1.53E+06	1.80E+06	
D	1.49E+06	1.59E+06	1.91E+06	1.42E+06	1.39E+06	1.67E+06	1.38E+06	1.48E+06
E	1.47E+06	1.62E+06	2.03E+06	1.83E+06	1.17E+06	1.47E+06	1.36E+06	1.40E+06
AVG	1.51E+06	1.70E+06	1.97E+06	1.73E+06	1.28E+06	1.50E+06	1.60E+06	1.41E+06
SD	2.89E+05	1.84E+05	2.53E+05	2.11E+05	2.23E+05	1.09E+05	3.08E+05	6.65E+04

For measured peak area, average peak area and standard deviation of SM(d18:1/16:0) in participant A, B, C, D and E right before and certain time points after high intensity exercise session, see Table 29.

Table 29: Peak area for participant, A, B, C, D, E, standard deviation (SD) and coefficient of variation (CV%) for SM(d18:1/16:0), before exercise, 1 min, 10 min, 30 min 60 min, 2 hours, 6 hours, and 12 hours after high intensity exercise session.

SM(d18:1/16:0)	Before Excercise	1 min	10 min	30 min	60 min	2 hours	6 hours	12 hours
A	1.68E+07	1.92E+07	2.37E+07	2.72E+07	1.81E+07	1.94E+07	1.46E+07	2.15E+07
B	2.46E+07	3.46E+07	3.43E+07	3.04E+07	1.29E+07	7.71E+06	4.36E+07	1.75E+07
C	2.08E+07	3.11E+07	3.80E+07	1.55E+07	2.97E+07	2.14E+07	3.56E+07	

D	1.96E+07	2.28E+07	1.72E+07	1.47E+07	1.60E+07	2.41E+07	1.35E+07	2.03E+07
E	1.42E+07	2.61E+07	2.01E+07	1.82E+07	2.20E+07	3.02E+07	2.32E+07	2.16E+07
AVG	1.92E+07	2.68E+07	2.83E+07	2.12E+07	1.97E+07	2.06E+07	2.61E+07	2.02E+07
SD	3.97E+06	6.21E+06	9.57E+06	7.16E+06	6.49E+06	8.27E+06	1.32E+07	1.94E+06

For measured peak area, average peak area and standard deviation of FA(18:0) in participant A, B, C, D and E right before and certain time points after high intensity exercise session, see Table 30.

Table 30: Peak area for participant A, B, C, D, E, average area, standard deviation (SD) and coefficient of variation (CV%) for FA(18:0), before exercise, 1 min, 10 min, 30 min 60 min, 2 hours,, 6 hours, and 12 hours after high intensity exercise session.

FA(18:0)	Before Exercise	1 min	10 min	30 min	60 min	2 hours	6 hours	12 hours
A	5.95E+05	8.91E+05	1.24E+06	9.89E+05	1.05E+06	1.31E+06	1.23E+06	7.65E+05
B	1.74E+06	1.04E+06	1.32E+06	1.13E+06	1.21E+06	1.13E+06	1.46E+06	9.63E+05
C	8.75E+05	1.45E+06	1.37E+06	1.09E+06	1.19E+06	9.68E+05	7.94E+05	
D	1.26E+06	1.34E+06	1.17E+06	1.54E+06	1.28E+06	1.34E+06	1.34E+06	9.27E+05
E	1.19E+06	1.37E+06	1.31E+06	9.28E+05	1.07E+06	1.36E+06	6.39E+05	8.35E+05
AVG	1.13E+06	1.22E+06	1.28E+06	1.13E+06	1.16E+06	1.22E+06	1.09E+06	8.73E+05
SD	4.31E+05	2.40E+05	8.02E+04	2.39E+05	9.88E+04	1.68E+05	3.56E+05	9.00E+04

For measured peak area, average peak area and standard deviation of FA(16:0) in participant A, B, C, D and E right before and certain time points after high intensity exercise session, see Table 31.

Table 31: Peak area for participant, A, B, C, D, E, average area, standard deviation (SD) and coefficient of variation (CV%) for FA(16:0), before exercise, 1 min, 10 min, 30 min 60 min, 2 hours,, 6 hours, and 12 hours after high intensity exercise session.

FA(16:0)	Before Excercise	1 min	10 min	30 min	60 min	2 hours	6 hours	12 hours
A	6.06E+05	8.97E+05	8.93E+05	8.38E+05	7.78E+05	1.04E+06	9.61E+05	5.80E+05
B	8.46E+05	7.20E+05	8.50E+05	9.34E+05	6.31E+05	8.98E+05	1.18E+06	6.68E+05
C	6.90E+05	1.13E+06	9.51E+05	6.79E+05	6.40E+05	6.10E+05	1.18E+06	
D	1.14E+06	1.30E+06	1.02E+06	9.76E+05	7.79E+05	9.77E+05	1.06E+06	8.83E+05
E	9.02E+05	1.23E+06	1.05E+06	5.65E+05	9.14E+05	9.03E+05	8.32E+05	5.83E+05
AVG	8.36E+05	1.06E+06	9.53E+05	7.98E+05	7.48E+05	8.86E+05	1.04E+06	6.78E+05
SD	2.06E+05	2.44E+05	8.44E+05	1.73E+05	1.17E+05	1.65E+05	1.51E+05	1.43E+05

For measured peak area, average peak area and standard deviation of AcCa(16:0) in participant A, B, C, D and E right before and certain time points after high intensity exercise session, see Table 32.

AcCa (16:0)	Before Exercise	1 min	10 min	30 min	60 min	2 hours	6 hours	12 hours
A	7.71E+04	3.46E+04	4.49E+04	6.11E+04	9.19E+04	7.23E+04	4.78E+04	4.15E+04
B	6.64E+04	6.46E+04	5.11E+04	7.70E+04	1.08E+05	5.70E+04	1.59E+05	5.10E+04
C	5.12E+04	2.64E+04	1.04E+05	1.31E+05	5.17E+04	1.02E+05	6.94E+04	
D	1.01E+05	9.13E+04	6.08E+04	6.09E+04	6.20E+04	8.35E+04	5.93E+04	6.63E+04
E	1.18E+05	5.99E+04	6.18E+04	7.54E+04	6.18E+04	6.96E+04	3.06E+04	6.62E+04
AVG	8.27E+04	5.53E+04	6.52E+04	8.10E+04	7.51E+04	7.68E+04	7.32E+04	5.62E+04
SD	2.67E+04	2.58E+04	2.67E+04	2.88E+04	2.38E+04	1.68E+04	4.99E+04	1.22E+04

For measured peak area, average peak area and standard deviation of AcCa(18:1) in participant A, B, C, D and E right before and certain time points after high intensity exercise session, see Table 33.

AcCA (18:1)	Before Exercise	1 min	10 min	30 min	60 min	2 hours	6 hours	12 hours
A	8.05E+04	4.70E+04	5.50E+04	9.88E+04	1.02E+05	5.67E+04	1.01E+05	4.49E+04
B	1.19E+05	6.78E+04	5.99E+04	1.01E+05	9.53E+04	5.33E+04	1.76E+05	4.91E+04
C	6.62E+04	5.67E+04	8.30E+04	8.10E+04	6.41E+04	9.03E+04	5.15E+04	
D	1.02E+05	1.16E+05	8.33E+04	6.78E+04	2.86E+04	8.88E+04	6.38E+04	8.11E+04
E	8.49E+04	8.08E+04	7.79E+04	1.32E+05	8.96E+03	6.53E+04	7.39E+04	5.36E+04
AVG	9.05E+04	7.36E+04	7.03E+04	9.61E+04	5.98E+04	7.09E+04	9.34E+04	5.72E+04
SD	2.04E+04	2.67E+04	1.50E+04	2.43E+04	4.07E+04	1.76E+04	4.98E+04	1.63E+04

For measured peak area, average peak area and standard deviation of PC(16:0/18:1) in participant A, B, C, D and E right before and certain time points after high intensity exercise session, see Table 34.

PC(16:0_18:1)	Before Exercise	1 min	10 min	30 min	60 min	2 hours	6 hours	12 hours
A	5.27E+06	5.69E+06	9.91E+06	6.02E+06	8.19E+06	5.06E+06	2.28E+06	9.19E+06
B	8.37E+06	5.42E+06	5.42E+06	4.97E+06	5.46E+06	4.88E+06	1.31E+07	5.26E+06

C	1.05E+07	5.02E+06	9.22E+06	7.77E+06	1.56E+07	7.46E+06	1.32E+07	
D	5.79E+06	6.23E+05	1.29E+07	9.98E+06	8.32E+06	8.50E+06	1.12E+07	1.14E+07
E	6.49E+06	8.17E+06	9.76E+07	5.89E+06	1.17E+07	5.88E+06	8.63E+06	6.36E+06
AVG	7.28E+06	4.98E+06	2.70E+07	6.93E+06	9.86E+06	6.36E+06	9.68E+06	8.04E+06
SD	2.13E+06	2.73E+06	3.96E+07	1.99E+06	3.91E+06	1.57E+06	4.53E+06	2.76E+06

For measured peak area, average peak area and standard deviation of DG(16:0/18:1) in participant A, B, C, D and E right before and certain time points after high intensity exercise session, see Table 35.

Table 35: Peak area for participant, A, B, C, D, E, average area, standard deviation (SD) and coefficient of variation (CV%) for DG(16:0/18:1), before exercise, 1 min, 10 min, 30 min 60 min, 2 hours, 6 hours, and 12 hours after high intensity exercise session.

DG(16:0_18:1)	Before Exercise	1 min	10 min	30 min	60 min	2 hours	6 hours	12 hours
A	1.21E+05	1.83E+05	1.73E+05	1.50E+05	1.26E+05	1.06E+05	2.65E+05	1.30E+05
B	1.04E+05	1.28E+05	1.36E+05	9.97E+04	8.44E+04	8.11E+04	2.38E+05	9.88E+04
C	1.59E+05	2.99E+05	2.58E+05	1.63E+05	1.62E+05	1.20E+05	2.67E+05	1.34E+05
D	1.48E+05	2.29E+05	2.34E+05	1.56E+05	1.46E+05	1.38E+05	1.63E+05	
E	1.07E+05	1.39E+05	1.73E+05	9.13E+04	1.06E+05	1.09E+05	1.83E+05	1.10E+05
AVG	1.28E+05	1.95E+05	2.00E+05	1.32E+05	1.25E+05	1.11E+05	2.23E+05	1.18E+05
SD	2.47E+04	7.03E+04	5.57E+04	3.38E+04	3.09E+04	2.07E+04	4.77E+04	1.66E+04

For measured peak area, average peak area and standard deviation of DG(18:1/18:1) in participant A, B, C, D and E right before and certain time points after high intensity exercise session, see Table 36.

Table 36: Peak area for participant, A, B, C, D, E, average area, standard deviation (SD) and coefficient of variation (CV%) for DG(18:1/18:1), before exercise, 1 min, 10 min, 30 min 60 min, 2 hours, 6 hours, and 12 hours after high intensity exercise session.

DG(18:1_18:1)	Before Exercise	1 min	10 min	30 min	60 min	2 hours	6 hours	12 hours
A	1.37E+05	2.00E+05	1.97E+05	1.49E+05	1.11E+05	1.06E+05	3.20E+05	1.30E+05
B	9.55E+04	1.14E+05	1.19E+05	8.05E+04	6.27E+04	5.87E+04	2.94E+05	7.63E+04
C	1.50E+05	3.38E+05	2.58E+05	1.40E+05	1.38E+05	9.76E+04	3.61E+05	
D	1.22E+05	1.97E+05	2.30E+05	1.45E+05	1.09E+05	1.17E+05	1.67E+05	1.14E+05
E	8.73E+04	1.29E+05	1.38E+05	7.65E+04	1.04E+05	9.01E+04	1.94E+05	8.22E+04
AVG	1.18E+05	1.95E+05	2.01E+05	1.18E+05	1.05E+05	9.38E+04	2.67E+05	1.01E+05
SD	2.66E+04	8.88E+04	6.04E+04	3.63E+04	2.69E+04	2.20E+04	8.31E+04	2.57E+04

For measured peak area, average peak area and standard deviation of TG(16:0/18:1/18:1) in participant A, B, C, D and E right before and certain time points after high intensity exercise session, see Table 37.

Table 37: Peak area for participant, A, B, C, D, E, average area, standard deviation (SD) and coefficient of variation (CV%) for TG(16:0/18:1/18:1), before exercise, 1 min, 10 min, 30 min 60 min, 2 hours, 6 hours, and 12 hours after high intensity exercise session.

TG(16:0/18:1/18:1)	Before Exercise	1 min	10 min	30 min	60 min	2 hours	6 hours	12 hours
A	2.99E+06	3.61E+06	3.76E+06	3.63E+06	3.56E+06	3.70E+06	1.38E+07	2.22E+06
B	1.62E+06	9.57E+05	1.35E+06	1.01E+06	1.11E+06	1.11E+06	1.02E+07	1.11E+06
C	3.70E+06	3.70E+06	3.00E+06	2.46E+06	3.27E+06	1.35E+06	1.25E+07	
D	3.19E+06	3.57E+06	4.39E+06	2.93E+06	2.80E+06	3.24E+06	5.23E+06	2.46E+06
E	1.54E+06	1.18E+06	1.42E+06	1.21E+06	1.93E+06	1.65E+06	4.92E+06	6.57E+05
AVG	2.61E+06	2.60E+06	3.13E+06	2.25E+06	2.53E+06	2.21E+06	9.34E+06	1.61E+06
SD	9.74E+05	1.40E+06	1.31E+06	1.12E+06	1.01E+06	1.18E+06	4.10E+06	8.67E+05

For measured peak area, average peak area and standard deviation of hydroxy-docosanoic acid in participant A, B, C, D and E right before and certain time points after high intensity exercise session, see Table 38.

Table 38: Peak area for participant A, B, C, D, E, average area, standard deviation (SD) and coefficient of variation (CV%) for hydroxy-docosanoiz acid, before exercise, 1 min, 10 min, 30 min 60 min, 2 hours, 6 hours, and 12 hours after high intensity exercise session.

Hydroxy decanoic acid	Before Excercise	1 min	10 min	30 min	60 min	2 hours	6 hours	12 hours
A	1.39E+07	1.86E+07	1.69E+07	1.64E+07	1.44E+07	1.72E+07	1.51E+07	9.39E+06
B	1.19E+07	2.08E+07	1.76E+07	1.67E+07	1.65E+07	1.25E+07	1.30E+07	1.21E+07
C	1.48E+07	2.01E+07	1.99E+07	1.70E+07	1.45E+07	1.22E+07	1.34E+07	
D	1.53E+07	2.07E+07	2.17E+07	1.76E+07	1.28E+07	1.44E+07	1.40E+07	1.51E+07
E	1.33E+07	2.02E+07	2.16E+07	1.82E+07	1.50E+07	1.29E+07	1.39E+07	1.18E+07
AVG	1.38E+07	2.01E+07	1.95E+07	1.72E+07	1.46E+07	1.38E+07	1.39E+07	1.21E+07
SD	1.34E+06	1.01E+06	2.24E+06	7.14E+05	1.35E+06	2.05E+06	7.98E+05	2.36E+06

7.3.1 Regional committee for medical and health research ethics informed consent form

To map and investigate the normal metabolome, an application submitted to the Regional Committee of Medical and Health Research Ethics. The consent form below was given to the participants.

Oslo universitetssykehus

KARTLEGGING AV NORMALMETABOLOMET

Delprosjekt: Endringer i metabolomet ved fysisk aktivitet

Dette er et spørsmål til deg om å delta i et forskningsprosjekt som har til hensikt å undersøke sammensetningen av stoffene som kan påvises i kroppsvæsker i en normalbefolkning. Metabolismen er summen av alle kjemiske reaksjoner i kroppen og innebærer nedbrytning og oppbygging av ulike stoffer som inngår i prosessene som skjer i kroppen. Stoffene som deltar i metabolismen kalles metabolitter, og sammensetningen av metabolitter utgjør det som kalles metabolomet. Metabolismen er et dynamisk system, det vil si det er i endring hele tiden, og påvirkes av en rekke naturlige biologiske faktorer slik som alder, kjønn, tid på døgnet, og ytre påvirkninger slik som matinntak/faste, fysisk aktivitet, sykdom, inntak av legemidler m.m.

For å kunne skille variasjoner i metabolomet som skyldes normale prosesser fra avvik som skyldes sykdom er det nødvendig å undersøke metabolomet fra et stort antall friske personer under ulike betingelser (f.eks. tid på døgnet, fødeinntak, fysisk aktivitet).

Forskningsansvarlig er Oslo Universitetssykehus, Avdeling for medisinsk biokjemi ved avdelingsleder. Prosjektleder er Katja B. Prestø Elgstøen ved samme avdeling.

Hva innebærer PROSJEKTET?

Hensikten med dette prosjektet er å studere endringer i metabolomet ved fysisk aktivitet. Derfor ønsker vi å ta prøve av deg før, under og etter trening.

Vi undersøker blod, i form av «dried blood spots», som er tørkede blodflekker på filterpapir. Det vil bli et stikk i fingeren i forbindelse med blodprøvetaking. I noen tilfeller kan det være aktuelt å undersøke andre prøvematerialer (blodprøve i armen, urinprøve, svette el.l.)

I prosjektet vil vi innhente og registrere følgende opplysninger om deg: kjønn og alder. Det er også ønskelig å registrere annen relevant informasjon, for eksempel om du har et spesielt kosthold (vegetarianer e.l.), kjente sykdommer, medisinbruk osv., men du står helt fritt til å oppgi denne informasjonen.

Det kan være aktuelt å gjøre relevante undersøkelser på gennivå for å bidra til forståelsen av variasjoner i metabolomet.

Mulige fordeler og ulemper

Du vil ikke ha noen spesielle fordeler av forsøkene, men erfaringer/resultater fra forsøkene vil øke vår kunnskap om normalmetabolomet og dermed gjøre det lettere å oppdage avvik fra normalen. Dette vil være viktig i forståelsen av helse og sykdom og i framtidens diagnostikk og behandling.

Frivillig deltakelse og mulighet for å trekke sitt samtykke

Det er frivillig å delta i prosjektet. Dersom du ønsker å delta, undertegner du samtykkeerklæringen på siste side. Der vil det bli spurt spesifikt om a) deltakelse i denne studien om endringer i metabolomet ved fysisk aktivitet og b) om det kan utføres relevante analyser på gennivå knyttet til endring av metabolomet ved fysisk aktivitet.

Du kan når som helst og uten å oppgi noen grunn trekke ditt samtykke. Dersom du trekker deg fra prosjektet, kan du kreve å få slettet innsamlede prøver og opplysninger, med unntak av opplysninger som allerede er inngått i analyser eller brukt i vitenskapelige publikasjoner. Dersom du ønsker å trekke deg eller har spørsmål til prosjektet, kan du kontakte Katja B. P. Elgstøen (kelgstoe@ous-hf.no, tlf. 23073079).

96

Hva skjer med informasjonen om deg?

Informasjonen som registreres om deg skal kun brukes slik som beskrevet i hensikten med studien. Du har rett til innsyn i hvilke opplysninger som er registrert om deg og rett til å få korrigert eventuelle feil i de opplysningene som er registrert.

Alle opplysningene vil bli behandlet uten navn og fødselsnummer eller andre direkte gjenkjennbare opplysninger. En kode knytter deg til dine opplysninger gjennom en navneliste. Det er kun autorisert personell knyttet til prosjektet som har adgang til navnelisten og som kan finne tilbake til deg. Det vil ikke være mulig å identifisere deg i resultatene av studien når disse publiseres. Prosjektleder har ansvar for den daglige driften av forskningsprosjektet og at opplysninger om deg blir behandlet på en sikker måte. Informasjon om deg vil bli slettet senest fem år etter prosjektslutt.

Som i alle forskningsstudier som involverer biologisk materiale er det en viss risiko for at det oppdages noe i prøvene som kan være knyttet til sykdom eller risiko for å utvikle sykdom, såkalt utilsiktede funn. Alle prøver er imidlertid avidentifiserte, og ingen (verken forskere eller personer som deltar i prosjektet) informeres om resultater og funn hos enkeltpersoner.

Hva skjer med prøver som blir tatt av deg?

Prøvene som tas av deg skal oppbevares i en generell forskningsbiobank: Kartlegging av normalmetabolomet. Denne er lokalisert ved Avdeling for medisinsk biokjemi, Rikshospitalet, Oslo Universitetssykehus. Katja B Prestø Elgstøen (kelgstoe@ous-hf.no, tlf. 23073079) er ansvarshavende for biobanken. Dette er en prospektiv biobank, og prøvene vil bli lagret til de eventuelt ønskes fjernet av deg. Det kan være aktuelt å sende prøver ut av landet (innad i EU og til USA, data som overføres til USA behandles i henhold til EUs Personverndirektiv) som et ledd i internasjonalt samarbeid. Materialet vil i så fall kun utleveres uten navn, fødselsnummer eller andre personidentifiserbare opplysninger.

Genetiske undersøkelser

Hva slags informasjon kan de genetiske undersøkelsene i PROSJEKTET gi?

Det kan være aktuelt å gjøre genetiske analyser på det materialet som er samlet inn for å se på sammenhengen mellom metabolomet og underliggende gener og genvarianter (sekvensering av enkeltgen, grupper av gener eller hele genomet). Genomsekvensen til hvert enkelt menneske er så unik at ingen prøver som inneholder DNA i teorien kan være anonyme. I praksis blir imidlertid alle prøver avidentifiserte og ingen (verken forskere eller personer som deltar i prosjektet) informeres om resultater og funn hos enkeltpersoner.

Godkjenning

Dine prøver inngår i biobank **2018/787 Kartlegging av normalmetabolomet** som er godkjent av Regional komite for medisinsk og helsefaglig forskningsetikk (REK).

Ingen analyser utføres før dette delprosjektet er godkjent av REK.

OPPLYSNINGER OM DEG

Kode for avidentifisering:_____

Alder:

Kjønn:

Andre opplysninger (frivillig å oppgi):

Faste medisiner:

Andre medisiner tatt siste døgn:

Eventuelle sykdommer:

Eventuelt spesielt kosthold (f.eks. vegetarianer, laktoseintolerant):

Røyker eller snuser du til vanlig?

Annen relevant informasjon:

Samtykke til deltakelse i PROSJEKTET kartlegging av normalmetabolomet – studier av normalmetabolomet ved fysisk aktivitet

Jeg er villig til å delta i prosjektet:

a) Jeg samtykker til deltakelse i denne studien om endringer i metabolomet ved fysisk aktivitet.

Sted og dato   Deltakers signatur

b) Jeg godkjenner at det kan utføres relevante analyser på gennivå knyttet til endring av metabolomet ved fysisk aktivitet.

Sted og dato   Deltakers signatur

                                                Deltakers navn med blokkbokstaver

Jeg bekrefter å ha gitt informasjon om prosjektet.

Sted og dato   Signatur

                                                Rolle i prosjektet

7.3.2 Diet and Dried Blood Spot sampling plan given to participants

See Table 39 for diet plan given to participants, and Table 40 for DBS sampling plan given to the participants.

Table 39: Diet plan given to participants including what type of food and drink the participants was allowed to have.

Måltider:	Mat:	Drikke:
Dagens første måltid	Brødskive(r) med eggerøre (egg og salt), avokado, tomat, majones.	Vann + 1-2 kopper te
Middag	Fjordland torsk. + brødskive(r)	Vann + 1-2 kopper te
Mellommåltid	Byggryn med bringebær + banan.	Vann

	Kveldsmat		Vann + Bendit smoothie i smaken: blåbær og eple 250 ml.
		Tomatsuppe + brødskive(r)	

Table 40: DBS sampling pllan given to participants, includes day, time point, sample ID, comments and actual time points.

DAG	Ca. tidspunkt	Prøve-ID	NB!	Faktisk tidspunkt	Kommentarer
1	08:55	F	Faste over natten		
	11:20	FL	Rett før lunsj		
	15:30	FM	Rett før middag		
	21:00	FK	Rett før kveldsmat		
	08:55	F	Fastende før trening		

2	09:00		Trening fastende		
	09:21	E1	Rett etter trening		
	09:30	E10	10 minutter etter trening		
	09:50	E30	30 minutter etter trening		
	10:20	E60	1 time etter trening		
	11:20	FL	2 timer etter trening Rett før lunsj		
	15:30	FM	Rett før middag		

	21:00	FK	Rett før kveldsmat		
3	08:55	F	Faste over natten		

7.4 Extra study: The effect of a freeze-thaw cycle on the lipidome using DBS samples

A freeze-thaw cycle refers to the process of freezing a sample, and then allowing it to thaw. Dried blood spot (DBS) cards, are used to collect and store blood samples for various applications, including clinical diagnostics and research. Freezing and thawing is hard to avoid for samples to be analyzed in a hospital laboratory, as samples are often stored for some time before analysis and freezing is a well-established procedure for stabilizing biological material. Undergoing freeze-thaw cycles can have several effects including, metabolite degradation due to physical and mechanical effects of freezing and thawing, and moisture condensating on the cold filter card, introducing water for enabling chemical reaction to take place. There is little knowledge about how the whole lipidome is affected on DBS cards by a freeze thaw cycle. In theory lipids undergoing a freeze thaw cycle can be affected in different ways including phase separation, lipid oxidation, lipid degradation and change in lipid extraction efficiency [90].

Lipids are susceptible to oxidation, especially when exposed to oxygen and fluctuating temperatures. The repeated freezing and thawing process can create opportunities for lipid oxidation reactions, leading to the generation of lipid peroxides and other oxidized lipid species. This oxidative damage can alter the lipid profile and potentially affect the stability of lipids [91]. Freeze-thaw cycles can affect the efficiency of lipid extraction [92]. The freeze-thaw process can alter the structure and accessibility of lipids within the dried blood spots,

potentially impacting the extraction efficiency of lipids during subsequent analysis. Some lipids, particularly labile lipid species, may be prone to degradation during freeze-thaw cycles [93]. The physical stress of temperature fluctuations can result in the breakdown or modification of certain lipid molecules. This degradation can lead to changes in lipid composition and loss of lipid integrity, affecting downstream lipidomic analysis.

The small study on the effect of the lipidome upon a freeze-thaw cycle was done on DBS samples obtained from the effect of high intensity exercise lipidome study. From 5 healthy volunteers two full DBS cards (10 spots) with blood from the fingertip each after fasting for 12 hours was collected. The cards were then left to dry in room temperature for 3 hours, before placed in sealed plastic bags with drying agent. From one dried blood spot, two punches were taken close to the center. One was placed in an Eppendorf tube and left in a -80 degrees freezer for 3 hours and one left in an Eppendorf tube for 3 hours in room temperature. The punches were then prepared for analysis using the sample preparation described in chapter 4.3.2. Hematocrit was not determined for the DBS samples included in this study.

7.4.1 Two significant features affected by freezing and thawing in positive ionization
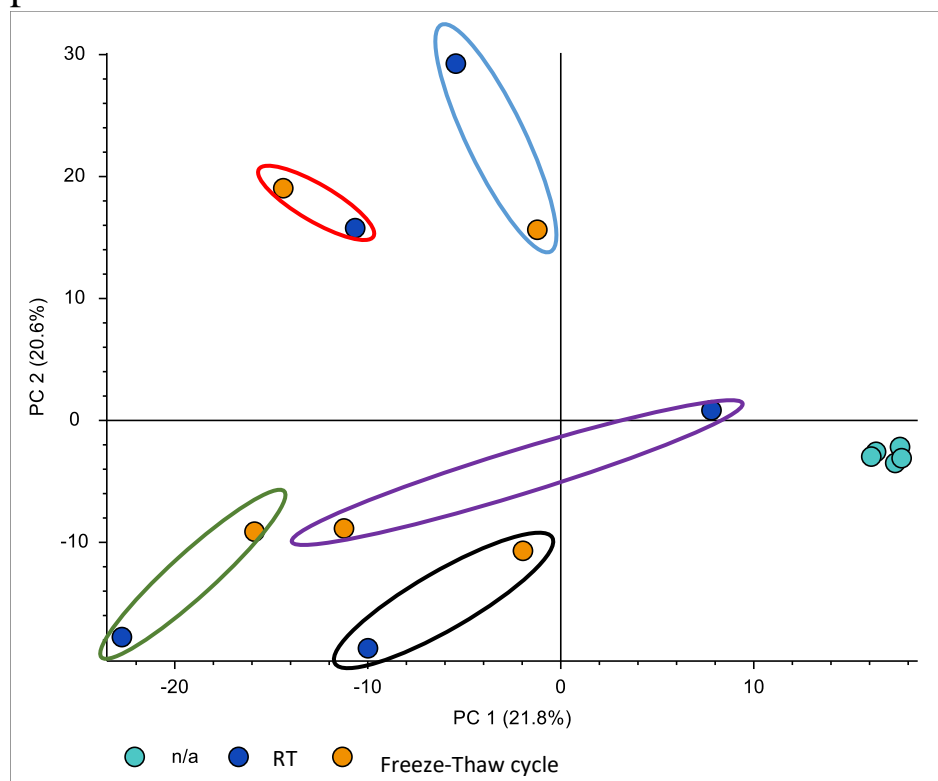
Figure 47: PCA plot in positive ionization mode for DBS samples left in room temperature for 3 hours and punches from the same samples left in a freezer for 3 hours then thawed before analysis. Samples which came from the same DBS are marked together.

As seen in the PCA plot shown in Figure 47, the PQC's are grouped together (dark blue points), demonstrating that there is very little instrumental drift. Points which come from the same DBS spot are marked within the same ellipse. No obvious clustering of the samples can be seen, based on freezing or not were observed. But punches taken from the same dried blood spot (marked with ellipses) that is, from the same individual, show global similarities. Some samples demonstrate bigger differences between unfrozen and freeze/thawed samples than others. For comparing the freeze-thaw cycle samples to the ones left in room temperature, volcano plots where used. See Figure 48 for volcano plot of the two different sample storage conditions.
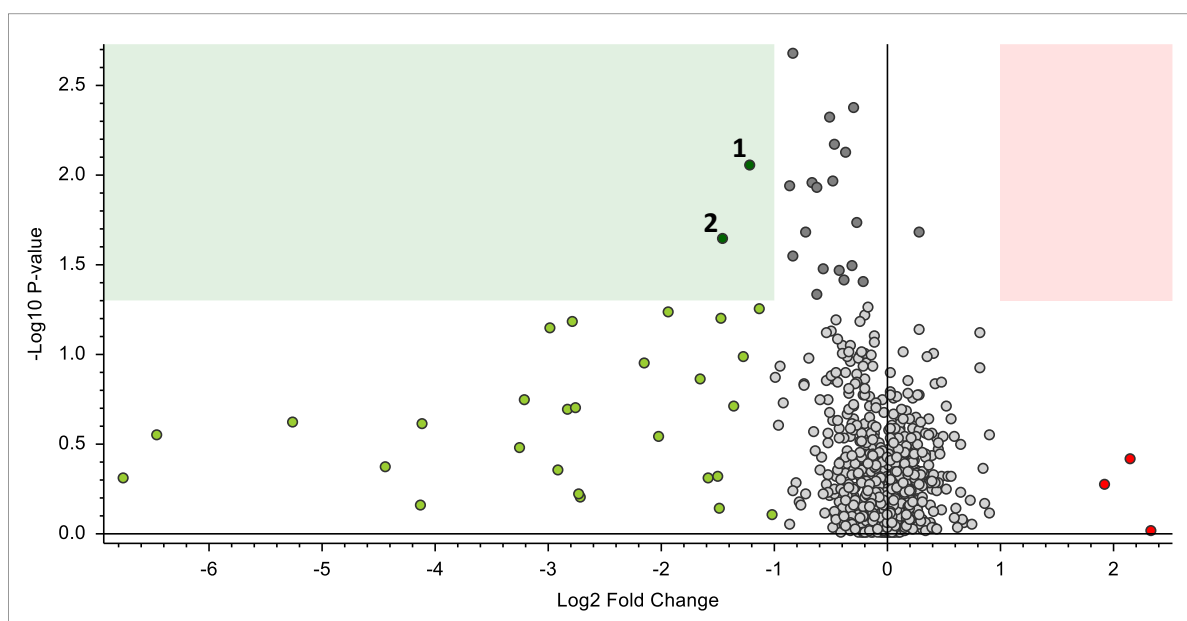
Figure 48: Volcano plot of positive ionization of samples which had a freeze thaw cycle and samples which did not. Each pair of samples consisted of neighbouring punches from the same DBS sample. Features found in green area were higher in the sample group which were stored in room temperature, compared to freezed samples. Features found in the red area is more abundant in the freezed samples.

As seen in Figure 48 two features, marked as 1 and 2, were found to be highly elevated in samples stored in room temperature compared to the samples which were freezed and thawed. Both features had no specific identification except from *m/z* value and retention time (confidence level 1). Feature 1 had *m/z* value 636.42365 and retention time 3.946 min. Feature 2 had *m/z* value 895.77288 and retention time 19.113 min. See Figure 49 for box whisker chart for feature 1, comparing samples which were freezed and thawed with samples which were stored in room temperature.
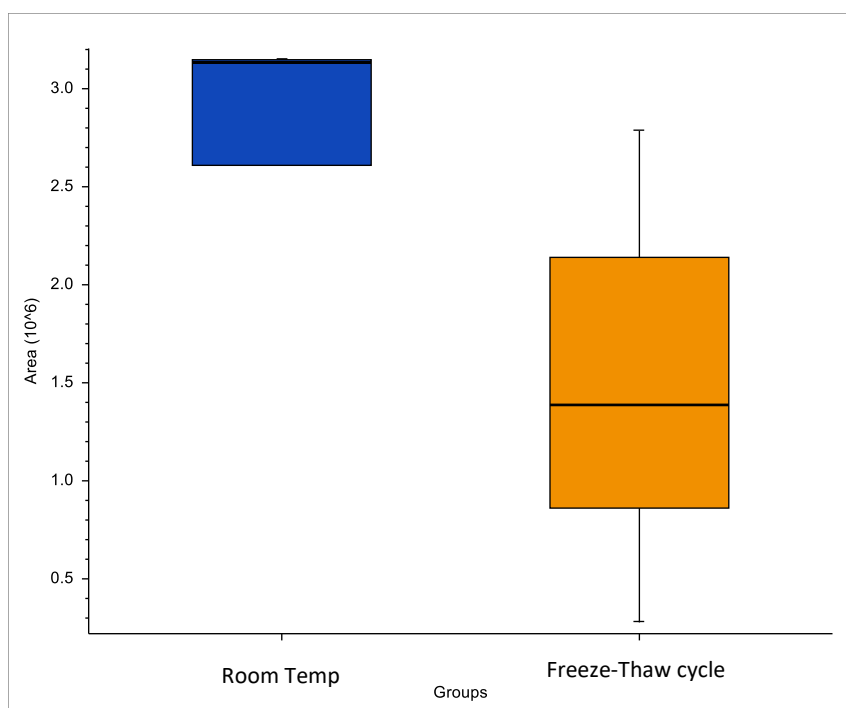
Figure 49: Box whisker chart for feature 1, m/z 636.42365, comparing samples which were freezed-thawed and samples which were stored in room temperature, 10 samples in total.

As seen in Figure 49, there was a big difference between the median of the two boxes. All samples which were freezed had a lower abundance of this lipid, compared to the adversary samples which were stored in room temperature. This means that a degradation of this lipid happened when it was freezed. For fragmentation spectrum of feature 1, see Figure 50.
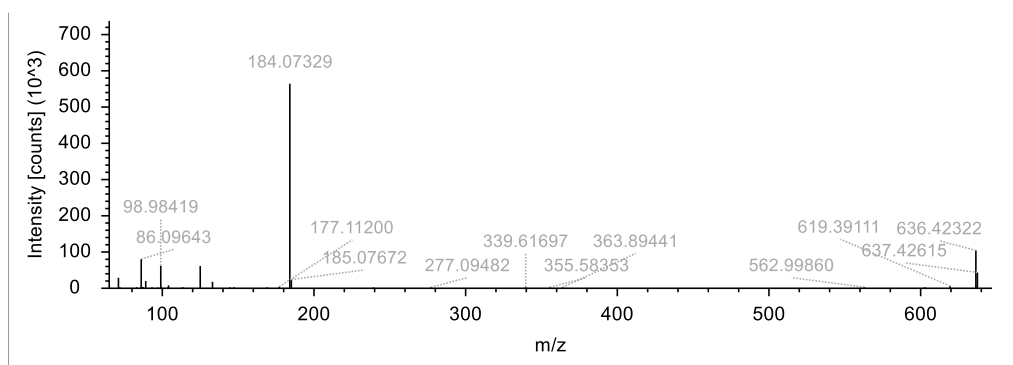
Figure 50: Fragmentation spectrum for feature 1 in positive ionization mode, m/z 636.42365.

As seen from the fragmentation spectrum above, *m/z* 184.07329 stands out. This fragment often represents the phosphate choline head group ($C_5H_{14}O_4PN^+$) [94], suggesting that the unknown feature 1 is from the phosphatidylcholine (PC) class. Suggested molecular formula is $C_{33}H_{66}NO_8P$, exact mass of $[M+H]^+$ was 636.4232 and *m/z* was 635.41622. Suggested that the lipid was PC(25:0) with confidence level 3 (see Figure 22, part 2.9).

For box whisker chart for feature 2, comparing samples which were stored in -80°C freezer for 3 hours then thawed with samples stored for 3 hours in room temperature, see Figure 51. Unfortunately, no fragmentation spectrum was obtained for feature 2. This is because the ion was not in top 5 which the scheduled MSMS method uses, an inclusion list can be used in the future by analysing one of the samples again. Due to limited timeframe this was not done. Based on retention time, m/z value and suggested molecular formula ($C_{58}H_{102}O_6$), feature 2 was most likely a triacylglycerol. More specifically TG(55:5) if the m/z value 895.77288 was an [M+H]$^+$ adduct, or TG(53:2) if it was an [M+Na]$^+$ adduct, confidence level 3 (see Figure 22, part 2.9). The reason for this trend can be that the lipid TG(55:5 or 53:2) degrades when freezed and thawed in a DBS sample.
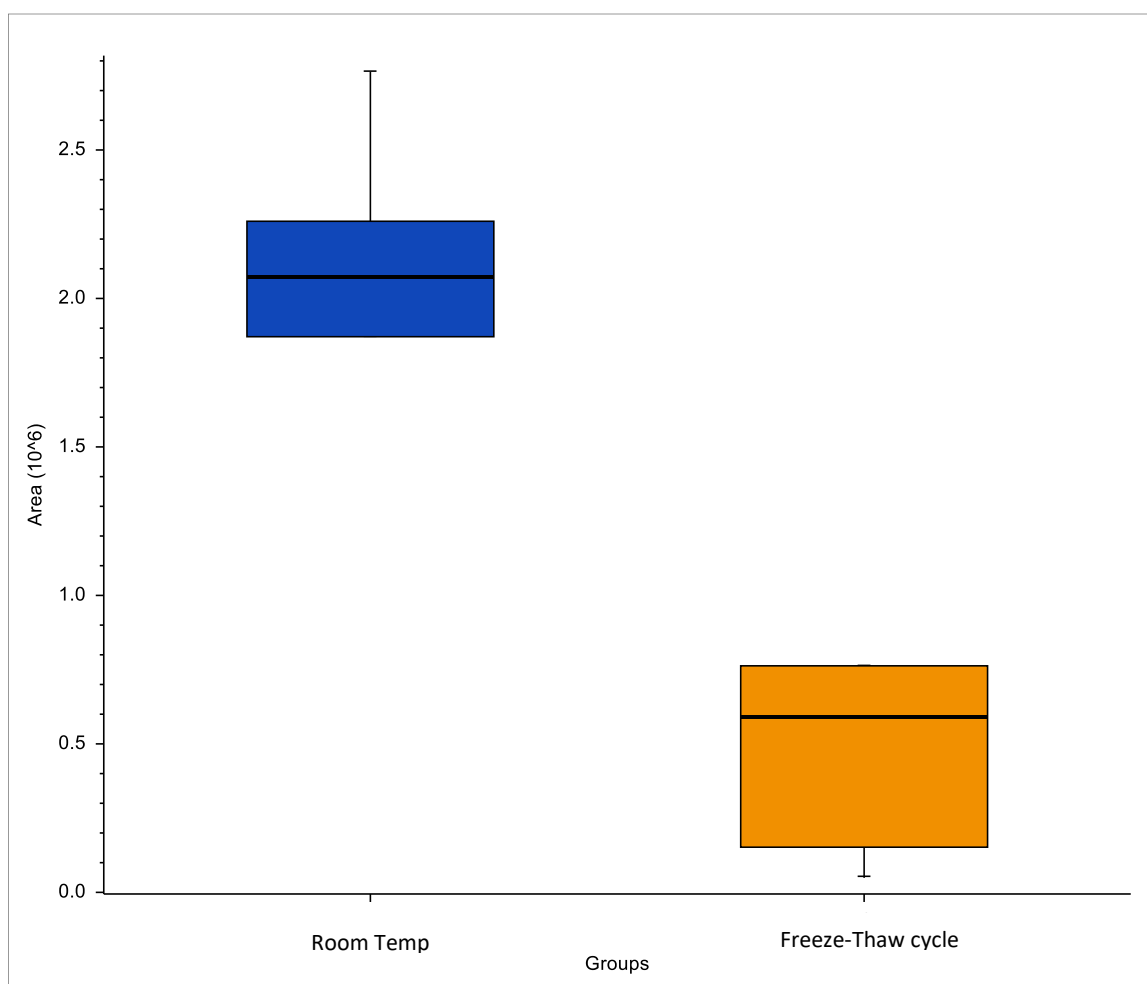
Figure 51: Box whisker chart for feature 2, m/z value 895.77288, retention time 19.113 min. Comparing samples which were stored in -80°C freezer for 3 hours and then thawed and samples stored for 3 hours in room temperature.

7.4.2 One significant feature influenced by freezing and thawing found in negative ionization
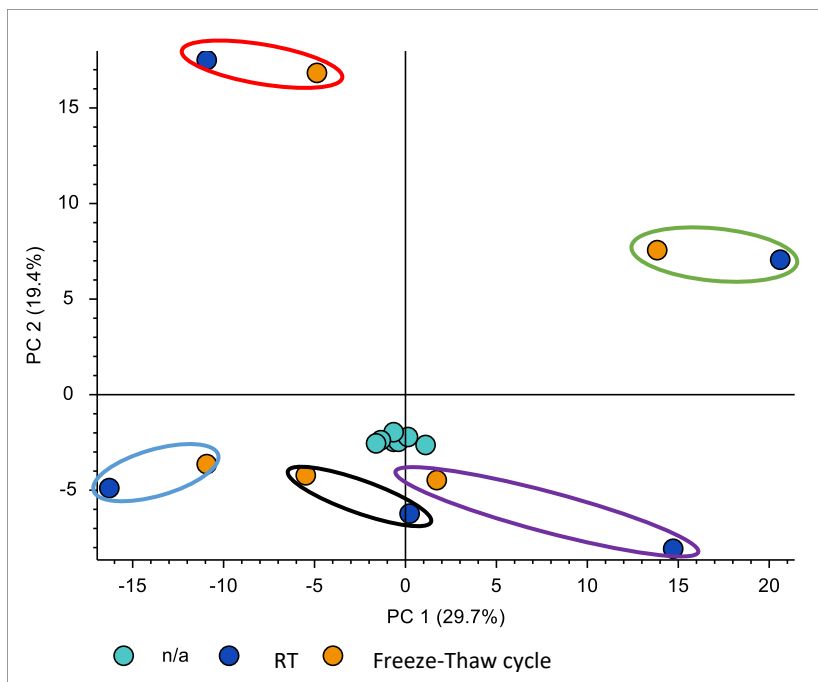

Figure 52: PCA plot in negative ionization mode for DBS samples left in room temperature for 3 hours and punches from the same samples left in a -80ºC freezer for 3 hours and then thawed before analysis. Samples from the same DBS spot are marked within the same ellipse.

As seen in Figure 52, the PQC (dark blue points) were grouped nicely together, demonstrating little instrument drift. Points from the same DBS spot were marked together within an ellipse. No obvious clustering of the samples can be seen, but punches taken from the same dried blood spot that was, from the same individual, show global similarities, as expected. Some samples exhibit bigger differences between frozen and unfrozen samples than others. For comparing the freeze-thaw cycle samples to the ones left in room temperature, volcano plots where used. See Figure 53 for volcano plot of the two different sample situations.
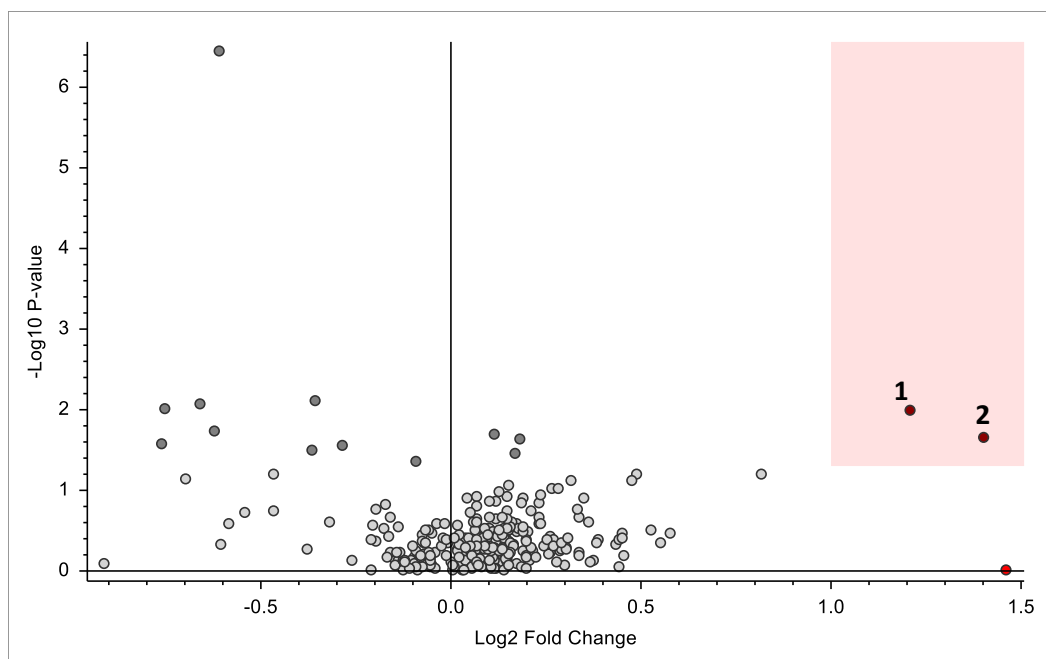
Figure 53: Volcano plot for samples which had a freeze-thaw cycle and samples which did not, in negative ionization mode. Features found in the red area were more abundant in the freezed samples compared to the not freezed samples.

As seen in Figure 53 two features were found to be significantly higher in samples which were stored in the freezer for 3 hours then thawed before analysis compared to samples stored in RT for 3 hours before analysis. These two features had the same *m/z* value and slightly different retention time. Feature 1 with *m/z* 396.21619 and retention time 4.199, and feature 2 with *m/z* is 396.21616 and retention time was 4.309. See Figure 54 for chromatographic peaks of the two features in all samples.
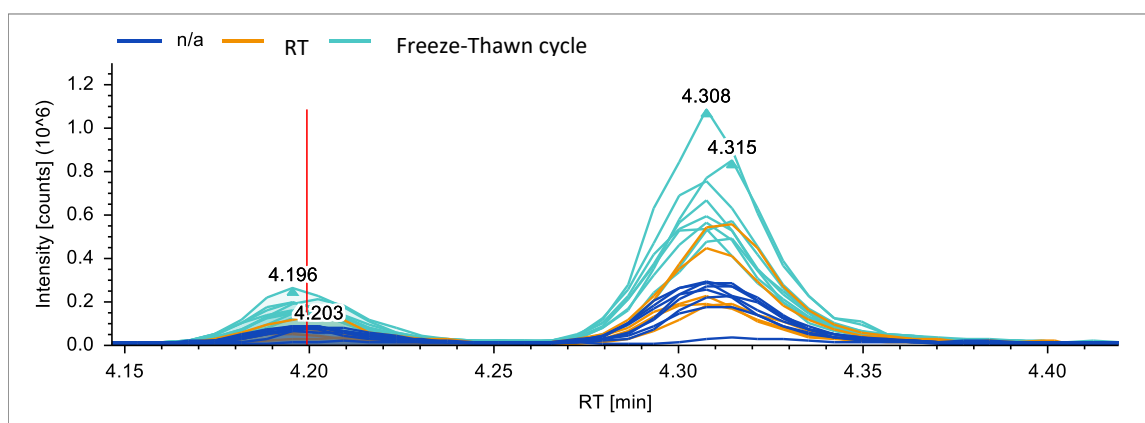
Figure 54: Chromatographic peaks of feature 1 and 2. Retention time [min] along x-axis, intensity [counts] along y-axis. n/a were quality controls, RT were samples stored in room temperature for 3 hours, Freeze-thaw cycle are samples which were stored in -80ºC freezer for 3 hours then thawed before analysis.

As seen in Figure 54 the two features eluted closely, consistent with being two isomers of the same lipid. This trend was usually only found in DG, PC, PE, PA, PG, PS, and SM. No fragmentation spectrum for the unknown feature were obtained, making it almost impossible

to identify without a proper in-house library. In-house libraries contain fragmentation spectrum and retention time for analytes of interest. The samples could have been analyzed again utilizing inclusion lists, but due to limited time available this was not done in the current project. Based on retention time it was more likely to be some sort of lyso- PC, PE, PA, PG, PS, or SM. Based on retention time, *m/z* value, and chromatographic separation, suggested identification was LPE(12:0), confidence level 3. See Figure 22, part 2.9 for description of level of confidence.
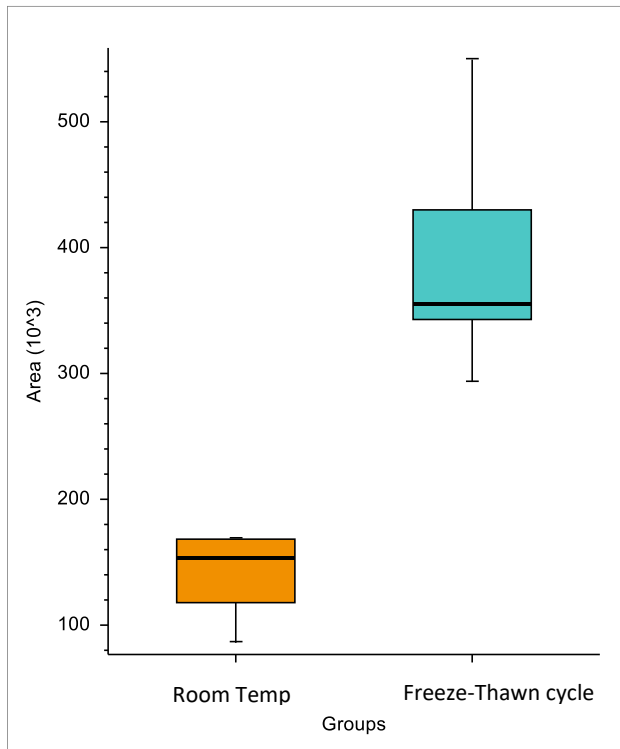
Figure 55: Box Whisker plot of feature 1, m/z 396.21619 retention time 4.199 min, comparing samples which were stored in -80ºC freezer for 3 hours then thawed and samples stored for 3 hours in room temperature.

As seen in Figure 55 there was a significant difference between the median and standard deviations for the two groups. It may be that feature 1 degraded faster in room temperature and therefore a higher amount of it measured in the samples which were frozen. Another possibility is that other lipids degraded to create feature 1 when samples were freezed and thawed. However, the lipid was not fully identified with confidence level 1, making it hard to say if this finding has any clinical value. The methods for analysing DBS cards in clinical

settings are often targeted, meaning that there is a lot of knowledge already about the desired analytes stability and how it is affected by freeze-thaw cycles[95].

To summarize part 7.4: Three lipids were found to be significantly altered as a result of freezing and thawing DBS samples. TG(55:5 or 53:2) and a phospholipid ($C_{32}H_{62}NO_9P$) were found to be significantly lower in samples which were frozen and thawed. LPE(12:0) were significantly lower in samples stored in room temperature compared to frozen samples.

7.5 Poster presented at the Nordic MS Winter meeting 2023

Optimization of Data Collection Parameters in Global Lipidomics for Clinical Diagnostics

Sønder Guttorm[a,b], Helge Rootwelt[b], Elise Mørk Sandås[b], Anja Østeby Vassli[b], Hanne Bendiksen Skogvold[b,c], Hans-Otto Böhm[b], Mazyar Yazdani[b], Steven Ray Wilson[a] and Katja Benedikte Prestø Elgstøen[b]

[a] Department of Chemistry, University of Oslo, Oslo, Norway
[b] Department of Medical Biochemistry, Oslo University Hospital Rikshospitalet, Oslo, Norway
[c] Department of Mechanical, Electronic and Chemical Engineering, Oslo Metropolitan University, Oslo, Norway

INTRODUCTION

Lipidomics has great interest due to the importance of lipids in e.g. development, health/disease, and diagnostics. Lipids pose great analytical challenges due to their diversity in chemical properties. For lipids of clinical relevance, both LogP values and concentration ranges can differ by several orders. Thus, for lipid analysis in a clinical setting, targeted methods for specific lipids have in general been applied. However, to gain new understandings of endogenous lipids and their role in health and disease, a global approach covering the whole "lipidome" are beneficial. Global lipidomics is a system-based study of all lipids and their interactions within a biological system[1].

This study presents a global lipidomics method using liquid chromatography coupled to a high-resolution mass spectrometer, using a separation column featuring a C30 stationary phase for class and intra-class separation of lipid species[2]. The goal in a global lipidomics approach is to maximize the number and diversity of lipids detected. This can be done in two ways, using Data-Dependent Acquisition (DDA) or Scheduled MS/MS[3].

METHODS

Lipidomics platform: LC-MS system used was Vanquish Horizon Binary pump coupled to the Fusion Orbitrap Tribrid Mass Spectrometer (**Figure 1**). An electrospray ionization source was applied, and samples were analysed in both positive and negative mode. The separation column used was an Accucore C30 column (150 mm x 2.1 mm, particle size 2.6 μm, carbon load 5%; Thermo Fisher Scientific).
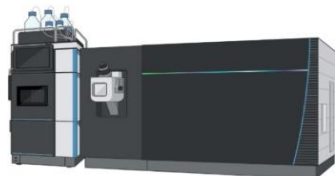
Figure 1: Vanquish Horzon UHPLC coupled to Fusion Orbitrap Tribrid Mass Spectrometer from Thermo Fisher Scientific.

Sample preparation of human serum: Venous blood from a healthy volunteer was collected in a 4 mL tube with gel, and spun down to separate serum (3600 rpm, 10 min). To 50 μL of serum, 150 μL of cold isopropanol (IPA) was added and vortexed for approximately 20 sec. The sample was centrifuged (20 min, 20000 g, 4°C), 150 μL of the supernatant was added to HPLC vials with insert glasses and caps. The samples were analyzed using the lipidomics platform. See **Figure 2** for illustration of the sample preparation.
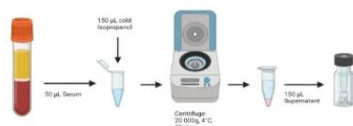
Figure 2: Sample preparation of human serum.

Further Work

In further work the Lipidomics method will be evaluated and validated accordingly or as close as possible to the FDA (Food and Drug Administration), EMA (European Medicin Agency) and LSI (Lipidomics Standards Initiative) claims.

RESULTS

The solvent gradient used is shown in **Figure 3**. Mobile phase A consisted of acetonitrile (60%) + 20mM ammonium formate, mobile phase B consisted of isopropanol (85.5%) + acetonitrile (9.5%) + 20 mM ammonium formate.

With the help of a "gentle" gradient and the use of a C30 colum (in reversed phase lipidomics, lipid class and intra class separation is possible), a correlation between the retention time and lipid class is observed, granting different elution time frames for the different lipid classes. The elution time frames help decide the different m/z windows to be applied in the Scheduled MSMS data collection method. See **Figure 4** for elution time frame of different lipid classes in human serum. The elution time frame widths can shift depending on the length of the lipids nonpolar chain. The calculated peak capacity at baseline was 221 (Pc = 1 + $t_f - t_1/w_{avg}$)[4].
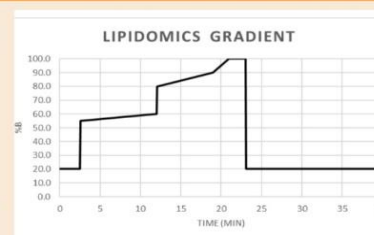
Figure 3: Shows gradient used in the presented lipidomics method. Y-axis is % of mobilephase B, x-axis is time in minutes.
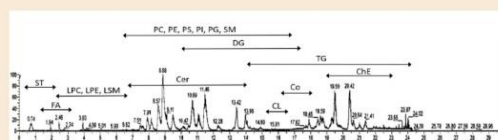
Figure 4: Elution of lipid species in Human Serum based on LipidMAPS annotations (ST=Steroids, FA=fatty acids, LPC=lysophosphocholine, LPE=lysophosphatidylethanolamine, LSM=lysophingomyelin, Cer=Ceramide, PC=phosphatidylcholine, PE=phosphatidylethanolamine, PS=phosphatidylserine, PI=phosphatidylinositol, PG=phosphatidylglycerol, SM=sphingomyelin, DG=diglycerid, TG=triglycerid, Co=Coenzyme, CL=cardiolipin, ChE=cholestrol ester).

A correlation between length of the lipids nonpolar chain and retention time was found. For example, for fully saturated triglycerides (TG), the linearity between the amount of carbons in the saturated side chains and retention time is R^2 = 0.99. This linearity can also be found in other lipid classes, e.g. for saturated sphingomyelin SM: R^2 = 0.99. For unsaturated lipids, the position and amount of double bonds has an effect on the retention time.
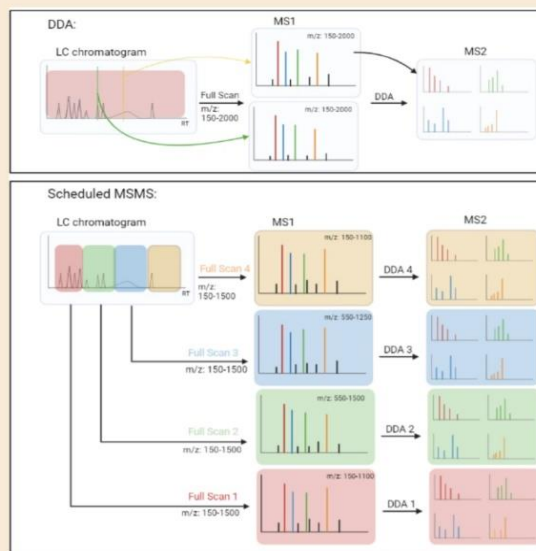
The most used data collection method in metabolomics and lipidomics is Data Dependent Acquisition (DDA). In DDA, a specific m/z range and intensity threshold is chosen, ions with an intensity higher than the given threshold will be sent to fragmentation for identification.

Scheduled MS/MS uses the same principle as DDA, but instead of using one m/z window, multiple m/z windows are applied in a mass dependent retention time profile. That is, the m/z windows are chosen according to when the different lipid categories elute from the column, allowing for more lipids to be detected in one run. By applying a smaller m/z window the cycle time is reduced, resulting in more cycles taking place. Therefore the Scheduled MSMS can obtain more data/lipids compared to DDA. See **Figure 5** for illustration of DDA and Scheduled MSMS.

The disadvantage with Scheduled MS/MS is that drift in retention times can result in lipids "falling out" of its given m/z window and will therefore not be identified.

Figure 5: Illustration of how Data-Dependent Acquisition (DDA) and Scheduled MSMS works.

To identify the different lipid species present in the samples, LipidSearch (Thermo Fisher Scientific, v4.2) was used. LipidSearch uses fragmentation spectra to identify and grade the identification of the different lipid species. The data shown in **Figure 6** is the same sample analyzed with the two data collection methods.

From **Figure 6** it is possible to see that the Scheduled MSMS method is able to identify more lipid species than the regular DDA. This was only the case in positive ionization mode; in negative ionization, mode DDA Top 5 identifies more lipid species than scheduled MSMS. This is again due to the shorter cycle time the Scheduled MSMS can achieve compared to DDA. Why DDA is better than Scheduled MSMS in negative ionization mode is unknown. More testing needs to be done to conclude if scheduled MSMS is a better option than DDA for global lipidomics.

	POS	NEG
Data-Dependent Acquisition Top 5	472	269
Scheduled MSMS Top 5	1091	118

Figure 6: Shows number of lipid species identified with Data-Dependent Acquisition and Scheduled MSMS in both positive and negative ionization.

1. Watson AD. Thematic review series: Systems Biology Approaches to Metabolic and Cardiovascular Disorders. Lipidomics: a global approach to lipid analysis in biological systems. *J Lipid Res*. 2006;47(10):2101-2111. doi:10.1194/jlr.R600022-JLR200
2. LIPID MAPS. Accessed November 30, 2022. https://www.lipidmaps.org/databases/lmsd/browse
3. Jankevics A, Jenkins A, Dunn WB, Najdekr L. An improved strategy for analysis of lipid molecules utilising a reversed phase C30 UHPLC column and scheduled MS/MS acquisition. *Talanta*. 2021;229:122262. doi:10.1016/j.talanta.2021.122262
4. Neue, U. D. Theory of Peak Capacity in Gradient Elution. *J. Chromatogr. A* **2005**, *1079* (1), 153−161. https://doi.org/10.1016/j.chroma.2005.03.008.